This is a repository copy of *Constraints on the cosmic expansion history from GWTC–3*.

White Rose Research Online URL for this paper:
https://eprints.whiterose.ac.uk/200373/

Version: Published Version

CrossMark

Constraints on the Cosmic Expansion History from GWTC–3

R. Abbott[1], H. Abe[2], F. Acernese[3,4], K. Ackley[5], N. Adhikari[6], R. X. Adhikari[1], V. K. Adkins[7], V. B. Adya[8], C. Affeldt[9,10], D. Agarwal[11], M. Agathos[12,13], K. Agatsuma[14], N. Aggarwal[15], O. D. Aguiar[16], L. Aiello[17], A. Ain[18], P. Ajith[19], T. Akutsu[20,21], S. Albanesi[22,23], R. A. Alfaidi[24], A. Allocca[4,25], P. A. Altin[8], A. Amato[26], C. Anand[5], S. Anand[1], A. Ananyeva[1], S. B. Anderson[1], W. G. Anderson[6], M. Ando[27,28], T. Andrade[29], N. Andres[30], M. Andrés-Carcasona[31], T. Andrić[32], S. V. Angelova[33], S. Ansoldi[34,35], J. M. Antelis[36], S. Antier[37,38], T. Apostolatos[39], E. Z. Appavuravther[40,41], S. Appert[1], S. K. Apple[42], K. Arai[1], A. Araya[43], M. C. Araya[1], J. S. Areeda[44], M. Arène[45], N. Aritomi[20], N. Arnaud[46,47], M. Arogeti[48], S. M. Aronson[7], K. G. Arun[49], H. Asada[50], Y. Asali[51], G. Ashton[52], Y. Aso[53,54], M. Assiduo[55,56], S. Assis de Souza Melo[47], S. M. Aston[57], P. Astone[58], F. Aubin[56], K. AultONeal[36], C. Austin[7], S. Babak[45], F. Badaracco[59], M. K. M. Bader[60], C. Badger[61], S. Bae[62], Y. Bae[63], A. M. Baer[64], S. Bagnasco[23], Y. Bai[1], J. Baird[45], R. Bajpai[65], T. Baka[66], M. Ball[67], G. Ballardin[47], S. W. Ballmer[68], A. Balsamo[64], G. Baltus[69], S. Banagiri[15], B. Banerjee[32], D. Bankar[11], J. C. Barayoga[1], C. Barbieri[70,71,72], R. Barbieri[73], B. C. Barish[1], D. Barker[74], P. Barneo[29], F. Barone[4,75], B. Barr[24], L. Barsotti[76], M. Barsuglia[45], D. Barta[77], J. Bartlett[74], M. A. Barton[24], I. Bartos[78], S. Basak[19], R. Bassiri[79], A. Basti[18,80], M. Bawaj[40,81], J. C. Bayley[24], M. Bazzan[82,83], B. R. Becher[84], B. Bécsy[85], V. M. Bedakihale[86], F. Beirnaert[87], M. Bejger[88], I. Belahcene[46], V. Benedetto[89], D. Beniwal[90], M. G. Benjamin[91], T. F. Bennett[92], J. D. Bentley[14], M. BenYaala[33], S. Bera[11], M. Berbel[93], F. Bergamin[9,10], B. K. Berger[79], S. Bernuzzi[13], C. P. L. Berry[24], D. Bersanetti[94], A. Bertolini[60], J. Betzwieser[57], D. Beveridge[95], R. Bhandare[96], A. V. Bhandari[11], U. Bhardwaj[38,60], R. Bhatt[1], D. Bhattacharjee[97], S. Bhaumik[78], A. Bianchi[60,98], I. A. Bilenko[99], G. Billingsley[1], M. Bilicki[100], S. Bini[101,102], R. Birney[103], O. Birnholtz[104], S. Biscans[1,76], M. Bischi[55,56], S. Biscoveanu[76], A. Bisht[9,10], B. Biswas[11], M. Bitossi[18,47], M.-A. Bizouard[37], J. K. Blackburn[1], C. D. Blair[95], D. G. Blair[95], R. M. Blair[74], F. Bobba[105,106], N. Bode[9,10], M. Boër[37], G. Bogaert[37], M. Boldrini[58,107], G. N. Bolingbroke[90], L. D. Bonavena[82], F. Bondu[108], E. Bonilla[79], R. Bonnand[30], P. Booker[9,10], B. A. Boom[60], R. Bork[1], V. Boschi[18], N. Bose[109], S. Bose[11], V. Bossilkov[95], V. Boudart[69], Y. Bouffanais[82,83], A. Bozzi[47], C. Bradaschia[18], P. R. Brady[6], A. Bramley[57], A. Branch[57], M. Branchesi[32,110], J. E. Brau[67], M. Breschi[13], T. Briant[111], J. H. Briggs[24], A. Brillet[37], M. Brinkmann[9,10], P. Brockill[6], A. F. Brooks[1], J. Brooks[47], D. D. Brown[90], S. Brunett[1], G. Bruno[59], R. Bruntz[64], J. Bryant[14], F. Bucci[56], T. Bulik[112], H. J. Bulten[60], A. Buonanno[73,113], K. Burtnyk[74], R. Buscicchio[14], D. Buskulic[30], C. Buy[114], R. L. Byer[79], G. S. Cabourn Davies[52], G. Cabras[34,35], R. Cabrita[59], L. Cadonati[48], M. Caesar[115], G. Cagnoli[26], C. Cahillane[74], J. Calderón Bustillo[116], J. D. Callaghan[24], T. A. Callister[117,118], E. Calloni[4,25], J. Cameron[95], J. B. Camp[119], M. Canepa[94,120], S. Canevarolo[66], M. Cannavacciuolo[105], K. C. Cannon[28], H. Cao[90], Z. Cao[121], E. Capocasa[20,45], E. Capote[68], G. Carapella[105,106], F. Carbognani[47], M. Carlassara[9,10], J. B. Carlin[122], M. F. Carney[15], M. Carpinelli[47,123,124], G. Carrillo[67], G. Carullo[18,80], T. L. Carver[17], J. Casanueva Diaz[47], C. Casentini[125,126], G. Castaldi[127], S. Caudill[60,66], M. Cavaglià[97], F. Cavalier[46], R. Cavalieri[47], G. Cella[18], P. Cerdá-Durán[128], E. Cesarini[126], W. Chaibi[37], S. Chalathadka Subrahmanya[129], E. Champion[130], C.-H. Chan[131], C. Chan[28], C. L. Chan[132], K. Chan[132], M. Chan[133], K. Chandra[109], I. P. Chang[131], P. Chanial[47], S. Chao[131], C. Chapman-Bird[24], P. Charlton[134], E. A. Chase[15], E. Chassande-Mottin[45], C. Chatterjee[95], Debarati Chatterjee[11], Deep Chatterjee[6], M. Chaturvedi[96], S. Chaty[45], K. Chatziioannou[1], C. Chen[135,136], D. Chen[53], H. Y. Chen[76], J. Chen[131], K. Chen[137], X. Chen[95], Y.-B. Chen[138], Y.-R. Chen[139], Z. Chen[17], H. Cheng[78], C. K. Cheong[132], H. Y. Cheung[132], H. Y. Chia[78], F. Chiadini[106,140], C-Y. Chiang[141], G. Chiarini[83], R. Chierici[142], A. Chincarini[94], M. L. Chiofalo[18,80], A. Chiummo[47], R. K. Choudhary[95], S. Choudhary[11], N. Christensen[37], Q. Chu[95], Y-K. Chu[141], S. S. Y. Chua[8], K. W. Chung[61], G. Ciani[82,83], P. Ciecielag[88], M. Cieślar[88], M. Cifaldi[125,126], A. A. Ciobanu[90], R. Ciolfi[83,143], F. Cipriano[37], F. Clara[74], J. A. Clark[1,48], P. Clearwater[144], S. Clesse[145], F. Cleva[37], E. Coccia[32,110], E. Codazzo[32], P.-F. Cohadon[111], D. E. Cohen[46], M. Colleoni[146], C. G. Collette[147], A. Colombo[70,71], M. Colpi[70,71], C. M. Compton[74], M. Constancio, Jr.[16], L. Conti[83], S. J. Cooper[14], P. Corban[57], T. R. Corbitt[7], I. Cordero-Carrión[148], S. Corezzi[40,81], K. R. Corley[51], N. J. Cornish[85], D. Corre[46], A. Corsi[149], S. Cortese[47], C. A. Costa[16], R. Cotesta[73], R. Cottingham[57], M. W. Coughlin[150], J.-P. Coulon[37], S. T. Countryman[51], B. Cousins[151], P. Couvares[1], D. M. Coward[95], M. J. Cowart[57], D. C. Coyne[1], R. Coyne[152], J. D. E. Creighton[6], T. D. Creighton[91], A. W. Criswell[150], M. Croquette[111], S. G. Crowder[153], J. R. Cudell[69], T. J. Cullen[7], A. Cumming[24], R. Cummings[24], L. Cunningham[24], E. Cuoco[18,47,154], M. Curyło[112], P. Dabadie[26], T. Dal Canton[46], S. Dall'Osso[32], G. Dálya[87,155], A. Dana[79], B. D'Angelo[94,120], S. Danilishin[60,156], S. D'Antonio[126], K. Danzmann[9,10], C. Darsow-Fromm[129], A. Dasgupta[86], L. E. H. Datrier[24], Sayak Datta[11], Sayantani Datta[49], V. Dattilo[47], I. Dave[96], M. Davier[46], D. Davis[1], M. C. Davis[115], E. J. Daw[157], P. F. De Alarc'on[158], R. Dean[115], D. DeBra[79], M. Deenadayalan[11], J. Degallaix[159], M. De Laurentis[4,25], S. Deléglise[111], V. Del Favero[130], F. De Lillo[59], N. De Lillo[24], D. Dell'Aquila[123], W. Del Pozzo[18,80], L. M. DeMarchi[15], F. De Matteis[125,126], V. D'Emilio[17], N. Demos[76], T. Dent[116], A. Depasse[59], R. De Pietri[160,161], R. De Rosa[4,25], C. De Rossi[47], R. DeSalvo[127,162], R. De Simone[140], S. Dhurandhar[11], M. C. Díaz[91], N. A. Didio[68], T. Dietrich[73], L. Di Fiore[4], C. Di Fronzo[14], C. Di Giorgio[105,106], F. Di Giovanni[128], M. Di Giovanni[32], T. Di Girolamo[4,25], A. Di Lieto[18,80], A. Di Michele[81], B. Ding[147], S. Di Pace[58,107], I. Di Palma[58,107],

F. Di Renzo[18,80], A. K. Divakarla[78], A. Dmitriev[14], Z. Doctor[15], L. Donahue[163], L. D'Onofrio[4,25], F. Donovan[76], K. L. Dooley[17], S. Doravari[11], M. Drago[58,107], J. C. Driggers[74], Y. Drori[1], J.-G. Ducoin[46], P. Dupej[24], U. Dupletsa[32], O. Durante[105,106], D. D'Urso[123,124], P.-A. Duverne[46], S. E. Dwyer[74], C. Eassa[74], P. J. Easter[5], M. Ebersold[164], T. Eckhardt[129], G. Eddolls[24], B. Edelman[67], T. B. Edo[1], O. Edy[52], A. Effler[57], S. Eguchi[133], J. Eichholz[8], S. S. Eikenberry[78], M. Eisenmann[20,30], R. A. Eisenstein[76], A. Ejlli[17], E. Engelby[44], Y. Enomoto[27], L. Errico[4,25], R. C. Essick[165], H. Estellés[146], D. Estevez[166], Z. Etienne[167], T. Etzel[1], M. Evans[76], T. M. Evans[57], T. Evstafyeva[12], B. E. Ewing[151], F. Fabrizi[55,56], F. Faedi[56], V. Fafone[32,125,126], H. Fair[68], S. Fairhurst[17], P. C. Fan[163], A. M. Farah[168], S. Farinon[94], B. Farr[67], W. M. Farr[117,118], E. J. Fauchon-Jones[17], G. Favaro[82], M. Favata[169], M. Fays[69], M. Fazio[170], J. Feicht[1], M. M. Fejer[79], E. Fenyvesi[77,171], D. L. Ferguson[172], A. Fernandez-Galiana[76], I. Ferrante[18,80], T. A. Ferreira[16], F. Fidecaro[18,80], P. Figura[112], A. Fiori[18,80], I. Fiori[47], M. Fishbach[15], R. P. Fisher[64], R. Fittipaldi[106,173], V. Fiumara[106,174], R. Flaminio[20,30], E. Floden[150], H. K. Fong[28], J. A. Font[128,175], B. Fornal[162], P. W. F. Forsyth[8], A. Franke[129], S. Frasca[58,107], F. Frasconi[18], J. P. Freed[36], Z. Frei[155], A. Freise[60,98], O. Freitas[176], R. Frey[67], P. Fritschel[76], V. V. Frolov[57], G. G. Fronzé[23], Y. Fujii[177], Y. Fujikawa[178], Y. Fujimoto[179], P. Fulda[78], M. Fyffe[57], H. A. Gabbard[24], B. U. Gadre[73], J. R. Gair[73], J. Gais[132], S. Galaudage[5], R. Gamba[13], D. Ganapathy[76], A. Ganguly[11], D. Gao[180], S. G. Gaonkar[11], B. Garaventa[94,120], C. García Núñez[103], C. García-Quirós[146], F. Garufi[4,25], B. Gateley[74], V. Gayathri[78], G.-G. Ge[180], G. Gemme[94], A. Gennai[18], J. George[96], O. Gerberding[129], L. Gergely[181], P. Gewecke[129], S. Ghonge[48], Abhirup Ghosh[73], Archisman Ghosh[87], Shaon Ghosh[169], Shrobana Ghosh[17], Tathagata Ghosh[11], B. Giacomazzo[70,71,72], L. Giacoppo[58,107], J. A. Giaime[7,57], K. D. Giardina[57], D. R. Gibson[103], C. Gier[33], M. Giesler[182], P. Giri[18,80], F. Gissi[89], S. Gkaitatzis[18,80], J. Glanzer[7], A. E. Gleckl[44], P. Godwin[151], E. Goetz[183], R. Goetz[78], N. Gohlke[9,10], J. Golomb[1], B. Goncharov[32], G. González[7], M. Gosselin[47], R. Gouaty[30], D. W. Gould[8], S. Goyal[19], B. Grace[8], A. Grado[4,184], V. Graham[24], M. Granata[159], V. Granata[105], A. Grant[24], S. Gras[76], P. Grassia[1], C. Gray[74], R. Gray[24], G. Greco[40], A. C. Green[78], R. Green[17], A. M. Gretarsson[36], E. M. Gretarsson[36], D. Griffith[1], W. L. Griffiths[17], H. L. Griggs[48], G. Grignani[40,81], A. Grimaldi[101,102], E. Grimes[36], S. J. Grimm[32,110], H. Grote[17], S. Grunewald[73], P. Gruning[46], A. S. Gruson[44], D. Guerra[128], G. M. Guidi[55,56], A. R. Guimaraes[7], G. Guixé[29], H. K. Gulati[86], A. M. Gunny[76], H.-K. Guo[162], Y. Guo[60], Anchal Gupta[1], Anuradha Gupta[185], I. M. Gupta[151], P. Gupta[60,66], S. K. Gupta[109], R. Gustafson[186], F. Guzman[187], S. Ha[188], I. P. W. Hadiputrawan[137], L. Haegel[45], S. Haino[141], O. Halim[35], E. D. Hall[76], E. Z. Hamilton[164], G. Hammond[24], W.-B. Han[189], M. Haney[164], J. Hanks[74], C. Hanna[151], M. D. Hannam[17], O. Hannuksela[60,66], H. Hansen[74], T. J. Hansen[36], J. Hanson[57], T. Harder[37], K. Haris[60,66], J. Harms[32,110], G. M. Harry[42], I. W. Harry[52], D. Hartwig[129], K. Hasegawa[190], B. Haskell[88], C.-J. Haster[76], J. S. Hathaway[130], K. Hattori[191], K. Haughian[24], H. Hayakawa[192], K. Hayama[133], F. J. Hayes[24], J. Healy[130], A. Heidmann[111], A. Heidt[9,10], M. C. Heintze[57], J. Heinze[9,10], J. Heinzel[76], H. Heitmann[37], F. Hellman[193], P. Hello[46], A. F. Helmling-Cornell[67], G. Hemming[47], M. Hendry[24], I. S. Heng[24], E. Hennes[60], J. Hennig[194], M. H. Hennig[194], C. Henshaw[48], A. G. Hernandez[92], F. Hernandez Vivanco[5], M. Heurs[9,10], A. L. Hewitt[195], S. Higginbotham[17], S. Hild[60,156], P. Hill[33], Y. Himemoto[196], A. S. Hines[187], N. Hirata[20], C. Hirose[178], T-C. Ho[137], S. Hochheim[9,10], D. Hofman[159], J. N. Hohmann[129], D. G. Holcomb[115], N. A. Holland[8], I. J. Hollows[157], Z. J. Holmes[90], K. Holt[57], D. E. Holz[168], Q. Hong[131], J. Hough[24], S. Hourihane[1], E. J. Howell[95], C. G. Hoy[17], D. Hoyland[14], A. Hreibi[9,10], B-H. Hsieh[190], H-F. Hsieh[197], C. Hsiung[135], Y. Hsu[131], H-Y. Huang[141], P. Huang[180], Y-C. Huang[139], Y.-J. Huang[141], Yiting Huang[153], Yiwen Huang[76], M. T. Hübner[5], A. D. Huddart[198], B. Hughey[36], D. C. Y. Hui[199], V. Hui[30], S. Husa[146], S. H. Huttner[24], R. Huxford[151], T. Huynh-Dinh[57], S. Ide[200], B. Idzkowski[112], A. Iess[125,126], K. Inayoshi[201], Y. Inoue[137], P. Iosif[202], M. Isi[76], K. Isleif[129], K. Ito[203], Y. Itoh[179,204], B. R. Iyer[19], V. JaberianHamedan[95], T. Jacqmin[111], P.-E. Jacquet[111], S. J. Jadhav[205], S. P. Jadhav[11], T. Jain[12], A. L. James[17], A. Z. Jan[172], K. Jani[206], J. Janquart[60,66], K. Janssens[37,207], N. N. Janthalur[205], P. Jaranowski[208], D. Jariwala[78], R. Jaume[146], A. C. Jenkins[61], K. Jenner[90], C. Jeon[209], W. Jia[76], J. Jiang[78], H.-B. Jin[210,211], G. R. Johns[64], R. Johnston[24], A. W. Jones[95], D. I. Jones[212], P. Jones[14], R. Jones[24], P. Joshi[151], L. Ju[95], A. Jue[162], P. Jung[63], K. Jung[188], J. Junker[9,10], V. Juste[166], K. Kaihotsu[203], T. Kajita[213], M. Kakizaki[191], C. V. Kalaghatgi[17,60,66,214], V. Kalogera[15], B. Kamai[1], M. Kamiizumi[192], N. Kanda[179,204], S. Kandhasamy[11], G. Kang[215], J. B. Kanner[1], Y. Kao[131], S. J. Kapadia[19], D. P. Kapasi[8], C. Karathanasis[31], S. Karki[97], R. Kashyap[151], M. Kasprzack[1], W. Kastaun[9,10], T. Kato[190], S. Katsanevas[47], E. Katsavounidis[76], W. Katzman[57], T. Kaur[95], K. Kawabe[74], K. Kawaguchi[190], F. Kéfélian[37], D. Keitel[146], J. S. Key[216], S. Khadka[79], F. Y. Khalili[99], S. Khan[17], T. Khanam[149], E. A. Khazanov[217], N. Khetan[32,110], M. Khursheed[96], N. Kijbunchoo[8], A. Kim[15], C. Kim[209], J. C. Kim[218], J. Kim[219], K. Kim[209], W. S. Kim[63], Y.-M. Kim[188], C. Kimball[15], N. Kimura[192], M. Kinley-Hanlon[24], R. Kirchhoff[9,10], J. S. Kissel[74], S. Klimenko[78], T. Klinger[12], A. M. Knee[183], T. D. Knowles[167], N. Knust[9,10], E. Knyazev[76], Y. Kobayashi[179], P. Koch[9,10], G. Koekoek[60,156], K. Kohri[220], K. Kokeyama[221], S. Koley[32], P. Kolitsidou[17], M. Kolstein[31], K. Komori[76], V. Kondrashov[1], A. K. H. Kong[197], A. Kontos[84], N. Koper[9,10], M. Korobko[129], M. Kovalam[95], N. Koyama[178], D. B. Kozak[1], C. Kozakai[53], V. Kringel[9,10], A. Królak[222,223], G. Kuehn[9,10], F. Kuei[131], P. Kuijer[60], S. Kulkarni[185], A. Kumar[205], Prayush Kumar[19], Rahul Kumar[74], Rakesh Kumar[86], J. Kume[28], K. Kuns[76], Y. Kuromiya[203], S. Kuroyanagi[224,225], K. Kwak[188], G. Lacaille[24], P. Lagabbe[30], D. Laghi[114], E. Lalande[226], M. Lalleman[207], T. L. Lam[132], A. Lamberts[37,227], M. Landry[74], B. B. Lane[76], R. N. Lang[76], J. Lange[172], B. Lantz[79], I. La Rosa[30], A. Lartaux-Vollard[46], P. D. Lasky[5], M. Laxen[57], A. Lazzarini[1], C. Lazzaro[82,83], P. Leaci[58,107], S. Leavey[9,10], S. LeBohec[162],

Y. K. Lecoeuche[183] , E. Lee[190] , H. M. Lee[228] , H. W. Lee[218] , K. Lee[229] , R. Lee[139], I. N. Legred[1], J. Lehmann[9,10],
A. Lemaître[230], M. Lenti[56,231] , M. Leonardi[20] , E. Leonova[38], N. Leroy[46] , N. Letendre[30], C. Levesque[226], Y. Levin[5],
J. N. Leviton[186], K. Leyde[45], A. K. Y. Li[1], B. Li[131] , J. Li[15], K. L. Li[232] , P. Li[233], T. G. F. Li[132], X. Li[138], C-Y. Lin[234] ,
E. T. Lin[197] , F-K. Lin[141] , F-L. Lin[235] , H. L. Lin[137] , L. C.-C. Lin[232], F. Linde[60,214], S. D. Linker[92,127], J. N. Linley[24],
T. B. Littenberg[236], G. C. Liu[135] , J. Liu[95] , K. Liu[131] , X. Liu[6], F. Llamas[91], R. K. L. Lo[1] , T. Lo[131], L. T. London[38,76],
A. Longo[237] , D. Lopez[164], M. Lopez Portilla[66], M. Lorenzini[125,126] , V. Loriette[238], M. Lormand[57], G. Losurdo[18] ,
T. P. Lott[48], J. D. Lough[9,10] , C. O. Lousto[130] , G. Lovelace[44], J. F. Lucaccioni[239], H. Lück[9,10], D. Lumaca[125,126] ,
A. P. Lundgren[52], L.-W. Luo[141] , J. E. Lynam[64], J. B. Machtinger[15], M. MacInnis[76],
D. M. Macleod[17] , I. A. O. MacMillan[1] , A. Macquet[37], I. Magaña Hernandez[6], C. Magazzù[18], R. M. Magee[1] ,
R. Maggiore[14] , M. Magnozzi[94,120] , S. Mahesh[167], E. Majorana[58,107] , I. Maksimovic[238], S. Maliakal[1], A. Malik[96],
N. Man[37], V. Mandic[150], V. Mangano[58,107] , G. L. Mansell[74,76], M. Manske[6], M. Mantovani[47] , M. Mapelli[82,83] ,
F. Marchesoni[40,41,240], D. Marín Pina[29], F. Marion[30], Z. Mark[138], S. Márka[51] , Z. Márka[51] , C. Markakis[12],
A. S. Markosyan[79], A. Markowitz[1], E. Maros[1], A. Marquina[148], S. Marsat[45], F. Martelli[55,56], I. W. Martin[24] ,
R. M. Martin[169], M. Martinez[31], V. A. Martinez[78], V. Martinez[26], K. Martinovic[61], D. V. Martynov[14], E. J. Marx[76],
H. Masalehdan[129], K. Mason[76], E. Massera[157], A. Masserot[30], M. Masso-Reid[24] , S. Mastrogiovanni[45] , A. Matas[73],
M. Mateu-Lucena[146] , F. Matichard[1,76], M. Matiushechkina[9,10] , N. Mavalvala[76] , J. J. McCann[95], R. McCarthy[74],
D. E. McClelland[8] , P. K. McClincy[151], S. McCormick[57], L. McCuller[76], G. I. McGhee[24], S. C. McGuire[57], C. McIsaac[52],
J. McIver[183] , T. McRae[8], S. T. McWilliams[167], D. Meacher[6] , M. Mehmet[9,10] , A. K. Mehta[73], Q. Meijer[66], A. Melatos[122],
D. A. Melchor[44], G. Mendell[74], A. Menendez-Vazquez[31], C. S. Menoni[170] , R. A. Mercer[6], L. Mereni[159], K. Merfeld[67],
E. L. Merilh[57], J. D. Merritt[67], M. Merzougui[37], S. Meshkov[1,299], C. Messenger[24] , C. Messick[76], P. M. Meyers[122] ,
F. Meylahn[9,10] , A. Mhaske[11], A. Miani[101,102] , H. Miao[14], I. Michaloliakos[78] , C. Michel[159] , Y. Michimura[27] ,
H. Middleton[122] , D. P. Mihaylov[73], L. Milano[25,300], A. L. Miller[59], A. Miller[92], B. Miller[38,60], M. Millhouse[122] ,
J. C. Mills[17], E. Milotti[35,241], Y. Minenkov[126], N. Mio[242], Ll. M. Mir[31], M. Miravet-Tenés[128] , A. Mishkin[78], C. Mishra[243] ,
T. Mishra[78], T. Mistry[157], S. Mitra[11] , V. P. Mitrofanov[99] , G. Mitselmakher[78], R. Mittleman[76], O. Miyakawa[192] ,
K. Miyo[192] , S. Miyoki[192] , Geoffrey Mo[76] , L. M. Modafferi[146] , E. Moguel[239], K. Mogushi[97], S. R. P. Mohapatra[76],
S. R. Mohite[6], I. Molina[44], M. Molina-Ruiz[193], M. Mondin[92], M. Montani[55,56], C. J. Moore[14], J. Moragues[146], D. Moraru[74],
F. Morawski[88], A. More[11] , S. More[11,244], C. Moreno[36], G. Moreno[74], Y. Mori[203], S. Morisaki[6] , N. Morisue[179],
Y. Moriwaki[191], B. Mours[166] , C. M. Mow-Lowry[60,98] , S. Mozzon[52] , F. Muciaccia[58,107], Arunava Mukherjee[245] ,
D. Mukherjee[151] , Soma Mukherjee[91], Subroto Mukherjee[86], Suvodip Mukherjee[38,165], N. Mukund[9,10] , A. Mullavey[57],
J. Munch[90], E. A. Muñiz[68] , P. G. Murray[24] , R. Musenich[94,120] , S. Muusse[90], S. L. Nadji[9,10], K. Nagano[246] ,
A. Nagar[23,247], K. Nakamura[20] , H. Nakano[248] , M. Nakano[190], Y. Nakayama[203], V. Napolano[47], I. Nardecchia[125,126] ,
T. Narikawa[190], H. Narola[66], L. Naticchioni[58] , B. Nayak[92] , R. K. Nayak[249], B. F. Neil[95], J. Neilson[89,106], A. Nelson[187],
T. J. N. Nelson[57], M. Nery[9,10] , P. Neubauer[239], A. Neunzert[216], K. Y. Ng[76], S. W. S. Ng[90], C. Nguyen[45] , P. Nguyen[67],
T. Nguyen[76], L. Nguyen Quynh[250] , J. Ni[150], W.-T. Ni[139,180,210], S. A. Nichols[7], T. Nishimoto[190], A. Nishizawa[28] ,
S. Nissanke[38,60], E. Nitoglia[142] , F. Nocera[47], M. Norman[17], C. North[17], S. Nozaki[191], G. Nurbek[91], L. K. Nuttall[52] ,
Y. Obayashi[190] , J. Oberling[74], B. D. O'Brien[78], J. O'Dell[198], E. Oelker[24] , W. Ogaki[190], G. Oganesyan[32,110] , J. J. Oh[63] ,
K. Oh[199] , S. H. Oh[63] , M. Ohashi[192] , T. Ohashi[179], M. Ohkawa[178] , F. Ohme[9,10] , H. Ohta[28], M. A. Okada[16],
Y. Okutani[200], C. Olivetto[47], K. Oohara[190,251] , R. Oram[57], B. O'Reilly[57] , R. G. Ormiston[150], N. D. Ormsby[64],
R. O'Shaughnessy[130], E. O'Shea[182], S. Oshino[192] , S. Ossokine[73] , C. Osthelder[1], S. Otabe[2], D. J. Ottaway[90] ,
H. Overmier[57], A. E. Pace[151], G. Pagano[18,80], R. Pagano[7], M. A. Page[95], G. Pagliaroli[32,110] , A. Pai[109], S. A. Pai[96], S. Pal[249],
J. R. Palamos[67], O. Palashov[217], C. Palomba[58] , H. Pan[131], K.-C. Pan[139,197], P. K. Panda[205], P. T. H. Pang[60,66],
C. Pankow[15], F. Pannarale[58,107] , B. C. Pant[96], F. H. Panther[95], F. Paoletti[18] , A. Paoli[47], A. Paolone[58,252], G. Pappas[202],
A. Parisi[135] , H. Park[6] , J. Park[253], W. Parker[57] , D. Pascucci[60,87] , A. Pasqualetti[47], R. Passaquieti[18,80] , D. Passuello[18],
M. Patel[64], M. Pathak[90], B. Patricelli[18,47] , A. S. Patron[7], S. Paul[67] , E. Payne[5], M. Pedraza[1], R. Pedurand[106], M. Pegoraro[83],
A. Pele[57], F. E. Peña Arellano[192] , S. Penano[79], S. Penn[254] , A. Perego[101,102], A. Pereira[26], T. Pereira[255], C. J. Perez[74],
C. Périgois[30], C. C. Perkins[78], A. Perreca[101,102] , S. Perriès[142], D. Pesios[202], J. Petermann[129] , D. Petterson[1],
H. P. Pfeiffer[73] , H. Pham[57] , K. A. Pham[150], K. S. Phukon[60,214] , H. Phurailatpam[132], O. J. Piccinni[58] , M. Pichot[37],
M. Piendibene[18,80], F. Piergiovanni[55,56], L. Pierini[58,107] , V. Pierro[89,106], G. Pillant[47], P. Pillas[46], F. Pilo[18], L. Pinard[159],
C. Pineda-Bosque[92], I. M. Pinto[89,106,256], M. Pinto[47], B. J. Piotrzkowski[6], K. Piotrzkowski[59], M. Pirello[74], M. D. Pitkin[195] ,
A. Placidi[40,81] , E. Placidi[58,107], M. L. Planas[146] , W. Plastino[237,257] , C. Pluchar[258], R. Poggiani[18,80] , E. Polini[30] ,
D. Y. T. Pong[132], S. Ponrathnam[11], E. K. Porter[45], R. Poulton[47] , A. Poverman[84], J. Powell[144], M. Pracchia[30], T. Pradier[166],
A. K. Prajapati[86], K. Prasai[79], R. Prasanna[205], G. Pratten[14] , M. Principe[89,106,256], G. A. Prodi[102,259], L. Prokhorov[14],
P. Prosposito[125,126], L. Prudenzi[73], A. Puecher[60,66], M. Punturo[40] , F. Puosi[18,80], P. Puppo[58], M. Pürrer[73] , H. Qi[17] ,
N. Quartey[64], V. Quetschke[91], P. J. Quinonez[36], R. Quitzow-James[97], F. J. Raab[74], G. Raaijmakers[38,60], H. Radkins[74],
N. Radulesco[37], P. Raffai[155] , S. X. Rail[226], S. Raja[96], C. Rajan[96], K. E. Ramirez[57] , T. D. Ramirez[44], A. Ramos-Buades[73] ,
J. Rana[151], P. Rapagnani[58,107], A. Ray[6], V. Raymond[17] , N. Raza[183], M. Razzano[18,80] , J. Read[44], L. A. Rees[42],
T. Regimbau[30], L. Rei[94] , S. Reid[33], S. W. Reid[64], D. H. Reitze[1,78], P. Relton[17] , A. Renzini[1], P. Rettegno[22,23] ,

B. Revenu[260], A. Reza[60], M. Rezac[44], F. Ricci[58,107], D. Richards[198], J. W. Richardson[261], L. Richardson[187], G. Riemenschneider[22,23], K. Riles[186], S. Rinaldi[18,80], K. Rink[183], N. A. Robertson[1], R. Robie[1], F. Robinet[46], A. Rocchi[126], S. Rodriguez[44], L. Rolland[30], J. G. Rollins[1], M. Romanelli[108], R. Romano[3,4], C. L. Romel[74], A. Romero[31], I. M. Romero-Shaw[5], J. H. Romie[57], S. Ronchini[32,110], L. Rosa[4,25], C. A. Rose[6], D. Rosińska[112], M. P. Ross[262], S. Rowan[24], S. J. Rowlinson[14], S. Roy[66], Santosh Roy[11], Soumen Roy[263], D. Rozza[123,124], P. Ruggi[47], K. Ruiz-Rocha[206], K. Ryan[74], S. Sachdev[151], T. Sadecki[74], J. Sadiq[116], S. Saha[197], Y. Saito[192], K. Sakai[264], M. Sakellariadou[61], S. Sakon[151], O. S. Salafia[70,71,72], F. Salces-Carcoba[1], L. Salconi[47], M. Saleem[150], F. Salemi[101,102], A. Samajdar[71], E. J. Sanchez[1], J. H. Sanchez[44], L. E. Sanchez[1], N. Sanchis-Gual[265], J. R. Sanders[266], A. Sanuy[29], T. R. Saravanan[11], N. Sarin[5], B. Sassolas[159], H. Satari[95], B. S. Sathyaprakash[17,151], O. Sauter[78], R. L. Savage[74], V. Savant[11], T. Sawada[179], H. L. Sawant[11], S. Sayah[159], D. Schaetzl[1], M. Scheel[138], J. Scheuer[15], M. G. Schiworski[90], P. Schmidt[14], S. Schmidt[66], R. Schnabel[129], M. Schneewind[9,10], R. M. S. Schofield[67], A. Schönbeck[129], B. W. Schulte[9,10], B. F. Schutz[9,10,17], E. Schwartz[17], J. Scott[24], S. M. Scott[8], M. Seglar-Arroyo[30], Y. Sekiguchi[267], D. Sellers[57], A. S. Sengupta[263], D. Sentenac[47], E. G. Seo[132], V. Sequino[4,25], A. Sergeev[217], Y. Setyawati[9,10,66], T. Shaffer[74], M. S. Shahriar[15], M. A. Shaikh[19], B. Shams[162], L. Shao[201], A. Sharma[32,110], P. Sharma[96], P. Shawhan[113], N. S. Shcheblanov[230], A. Sheela[243], Y. Shikano[268,269], M. Shikauchi[28], H. Shimizu[270], K. Shimode[192], H. Shinkai[271], T. Shishido[54], A. Shoda[20], D. H. Shoemaker[76], D. M. Shoemaker[172], S. ShyamSundar[96], M. Sieniawska[59], D. Sigg[74], L. Silenzi[40,41], L. P. Singer[119], D. Singh[151], M. K. Singh[19], N. Singh[112], A. Singha[60,156], A. M. Sintes[146], V. Sipala[123,124], V. Skliris[17], B. J. J. Slagmolen[8], T. J. Slaven-Blair[95], J. Smetana[14], J. R. Smith[44], L. Smith[24], R. J. E. Smith[5], J. Soldateschi[56,231,272], S. N. Somala[273], K. Somiya[2], I. Song[197], K. Soni[11], V. Sordini[142], F. Sorrentino[94], N. Sorrentino[18,80], R. Soulard[37], T. Souradeep[11,274], E. Sowell[149], V. Spagnuolo[60,156], A. P. Spencer[24], M. Spera[82,83], P. Spinicelli[47], A. K. Srivastava[86], V. Srivastava[68], K. Staats[15], C. Stachie[37], F. Stachurski[24], D. A. Steer[45], J. Steinlechner[60,156], S. Steinlechner[60,156], N. Stergioulas[202], D. J. Stops[14], M. Stover[239], K. A. Strain[24], L. C. Strang[122], G. Stratta[58,275], M. D. Strong[7], A. Strunk[74], R. Sturani[255], A. L. Stuver[115], M. Suchenek[88], S. Sudhagar[11], V. Sudhir[76], R. Sugimoto[246,276], H. G. Suh[6], A. G. Sullivan[51], T. Z. Summerscales[277], L. Sun[8], S. Sunil[86], A. Sur[88], J. Suresh[28], P. J. Sutton[17], Takamasa Suzuki[178], Takanori Suzuki[2], Toshikazu Suzuki[190], B. L. Swinkels[60], M. J. Szczepańczyk[78], P. Szewczyk[112], M. Tacca[60], H. Tagoshi[190], S. C. Tait[24], H. Takahashi[278], R. Takahashi[20], S. Takano[27], H. Takeda[27], M. Takeda[179], C. J. Talbot[33], C. Talbot[1], N. Tamanini[279], K. Tanaka[280], Taiki Tanaka[190], Takahiro Tanaka[281], A. J. Tanasijczuk[59], S. Tanioka[192], D. B. Tanner[78], D. Tao[1], L. Tao[78], R. D. Tapia[151], E. N. Tapia San Martín[60], C. Taranto[125], A. Taruya[282], J. D. Tasson[163], R. Tenorio[146], J. E. S. Terhune[115], L. Terkowski[129], M. P. Thirugnanasambandam[11], M. Thomas[57], P. Thomas[74], E. E. Thompson[48], J. E. Thompson[17], S. R. Thondapu[96], K. A. Thorne[57], E. Thrane[5], Shubhanshu Tiwari[164], Srishti Tiwari[11], V. Tiwari[17], A. M. Toivonen[150], A. E. Tolley[52], T. Tomaru[20], T. Tomura[192], M. Tonelli[18,80], Z. Tornasi[24], A. Torres-Forné[128], C. I. Torrie[1], I. Tosta e Melo[124], D. Töyrä[8], A. Trapananti[40,41], F. Travasso[40,41], G. Traylor[57], M. Trevor[113], M. C. Tringali[47], A. Tripathee[186], L. Troiano[106,283], A. Trovato[45], L. Trozzo[4,192], R. J. Trudeau[1], D. Tsai[131], K. W. Tsang[60,66,284], T. Tsang[285], J-S. Tsao[235], M. Tse[76], R. Tso[138], S. Tsuchida[179], L. Tsukada[151], D. Tsuna[28], T. Tsutsui[28], K. Turbang[207,286], M. Turconi[37], C. Turski[87,100,112], D. Tuyenbayev[179], A. S. Ubhi[14], N. Uchikata[190], T. Uchiyama[192], R. P. Udall[1], A. Ueda[287], T. Uehara[288,289], K. Ueno[28], G. Ueshima[290], C. S. Unnikrishnan[291], A. L. Urban[7], T. Ushiba[192], A. Utina[60,156], G. Vajente[1], A. Vajpeyi[5], G. Valdes[187], M. Valentini[101,102,185], V. Valsan[6], N. van Bakel[60], M. van Beuzekom[60], M. van Dael[60,292], J. F. J. van den Brand[60,98,156], C. Van Den Broeck[60,66], D. C. Vander-Hyde[68], H. van Haevermaet[207], J. V. van Heijningen[59], M. H. P. M. van Putten[293], N. van Remortel[207], M. Vardaro[60,214], A. F. Vargas[122], V. Varma[73], M. Vasúth[77], A. Vecchio[14], G. Vedovato[83], J. Veitch[24], P. J. Veitch[90], J. Venneberg[9,10], G. Venugopalan[1], D. Verkindt[30], P. Verma[223], Y. Verma[96], S. M. Vermeulen[17], D. Veske[51], F. Vetrano[55], A. Viceré[55,56], S. Vidyant[68], A. D. Viets[294], A. Vijaykumar[19], V. Villa-Ortega[116], J.-Y. Vinet[37], A. Virtuoso[35,241], S. Vitale[76], H. Vocca[40,81], E. R. G. von Reis[74], J. S. A. von Wrangel[9,10], C. Vorvick[74], S. P. Vyatchanin[99], L. E. Wade[239], M. Wade[239], K. J. Wagner[130], R. C. Walet[60], M. Walker[64], G. S. Wallace[33], L. Wallace[1], J. Wang[180], J. Z. Wang[186], W. H. Wang[91], R. L. Ward[8], J. Warner[74], M. Was[30], T. Washimi[20], N. Y. Washington[1], J. Watchi[147], B. Weaver[74], C. R. Weaving[52], S. A. Webster[24], M. Weinert[9,10], A. J. Weinstein[1], R. Weiss[76], C. M. Weller[262], R. A. Weller[206], F. Wellmann[9,10], L. Wen[95], P. Weßels[9,10], K. Wette[8], J. T. Whelan[130], D. D. White[44], B. F. Whiting[78], C. Whittle[76], D. Wilken[9,10], D. Williams[24], M. J. Williams[24], A. R. Williamson[52], J. L. Willis[1], B. Willke[9,10], D. J. Wilson[258], C. C. Wipf[1], T. Wlodarczyk[73], G. Woan[24], J. Woehler[9,10], J. K. Wofford[130], D. Wong[183], I. C. F. Wong[132], M. Wright[24], C. Wu[139], D. S. Wu[9,10], H. Wu[139], D. M. Wysocki[6], L. Xiao[1], T. Yamada[270], H. Yamamoto[1], K. Yamamoto[191], T. Yamamoto[192], K. Yamashita[203], R. Yamazaki[200], F. W. Yang[162], K. Z. Yang[150], L. Yang[170], Y.-C. Yang[131], Y. Yang[295], Yang Yang[78], M. J. Yap[8], D. W. Yeeles[17], S.-W. Yeh[139], A. B. Yelikar[130], M. Ying[131], J. Yokoyama[27,28], T. Yokozawa[192], J. Yoo[182], T. Yoshioka[203], Hang Yu[138], Haocun Yu[76], H. Yuzurihara[190], A. Zadrożny[223], M. Zanolin[36], S. Zeidler[296], T. Zelenova[47], J.-P. Zendri[83], M. Zevin[168], M. Zhan[180], H. Zhang[235], J. Zhang[95], L. Zhang[1], R. Zhang[78], T. Zhang[14], Y. Zhang[187], C. Zhao[95], G. Zhao[147], Y. Zhao[20,190], Yue Zhao[162], R. Zhou[193], Z. Zhou[15], X. J. Zhu[5],

Z.-H. Zhu[121,233] , A. B. Zimmerman[172] , M. E. Zucker[1,76], J. Zweizig[1]
The LIGO Scientific Collaboration[297]
and
the Virgo Collaboration, and the KAGRA Collaboration[298]

[1] LIGO Laboratory, California Institute of Technology, Pasadena, CA 91125, USA
[2] Graduate School of Science, Tokyo Institute of Technology, Meguro-ku, Tokyo 152-8551, Japan
[3] Dipartimento di Farmacia, Università di Salerno, I-84084 Fisciano, Salerno, Italy
[4] INFN, Sezione di Napoli, Complesso Universitario di Monte S. Angelo, I-80126 Napoli, Italy
[5] OzGrav, School of Physics & Astronomy, Monash University, Clayton 3800, Victoria, Australia
[6] University of Wisconsin-Milwaukee, Milwaukee, WI 53201, USA
[7] Louisiana State University, Baton Rouge, LA 70803, USA
[8] OzGrav, Australian National University, Canberra, Australian Capital Territory 0200, Australia
[9] Max Planck Institute for Gravitational Physics (Albert Einstein Institute), D-30167 Hannover, Germany
[10] Leibniz Universität Hannover, D-30167 Hannover, Germany
[11] Inter-University Centre for Astronomy and Astrophysics, Pune 411007, India
[12] University of Cambridge, Cambridge CB2 1TN, UK
[13] Theoretisch-Physikalisches Institut, Friedrich-Schiller-Universität Jena, D-07743 Jena, Germany
[14] University of Birmingham, Birmingham B15 2TT, UK
[15] Northwestern University, Evanston, IL 60208, USA
[16] Instituto Nacional de Pesquisas Espaciais, 12227-010 São José dos Campos, São Paulo, Brazil
[17] Cardiff University, Cardiff CF24 3AA, UK
[18] INFN, Sezione di Pisa, I-56127 Pisa, Italy
[19] International Centre for Theoretical Sciences, Tata Institute of Fundamental Research, Bengaluru 560089, India
[20] Gravitational Wave Science Project, National Astronomical Observatory of Japan (NAOJ), Mitaka City, Tokyo 181-8588, Japan
[21] Advanced Technology Center, National Astronomical Observatory of Japan (NAOJ), Mitaka City, Tokyo 181-8588, Japan
[22] Dipartimento di Fisica, Università degli Studi di Torino, I-10125 Torino, Italy
[23] INFN Sezione di Torino, I-10125 Torino, Italy
[24] SUPA, University of Glasgow, Glasgow G12 8QQ, UK
[25] Università di Napoli "Federico II", Complesso Universitario di Monte S. Angelo, I-80126 Napoli, Italy
[26] Université de Lyon, Université Claude Bernard Lyon 1, CNRS, Institut Lumière Matière, F-69622 Villeurbanne, France
[27] Department of Physics, The University of Tokyo, Bunkyo-ku, Tokyo 113-0033, Japan
[28] Research Center for the Early Universe (RESCEU), The University of Tokyo, Bunkyo-ku, Tokyo 113-0033, Japan
[29] Institut de Ciències del Cosmos (ICCUB), Universitat de Barcelona, C/ Martí i Franquès 1, Barcelona, E-08028, Spain
[30] Univ. Savoie Mont Blanc, CNRS, Laboratoire d'Annecy de Physique des Particules—IN2P3, F-74000 Annecy, France
[31] Institut de Física d'Altes Energies (IFAE), Barcelona Institute of Science and Technology, and ICREA, E-08193 Barcelona, Spain
[32] Gran Sasso Science Institute (GSSI), I-67100 L'Aquila, Italy
[33] SUPA, University of Strathclyde, Glasgow G1 1XQ, UK
[34] Dipartimento di Scienze Matematiche, Informatiche e Fisiche, Università di Udine, I-33100 Udine, Italy
[35] INFN, Sezione di Trieste, I-34127 Trieste, Italy
[36] Embry-Riddle Aeronautical University, Prescott, AZ 86301, USA
[37] Artemis, Université Côte d'Azur, Observatoire de la Côte d'Azur, CNRS, F-06304 Nice, France
[38] GRAPPA, Anton Pannekoek Institute for Astronomy and Institute for High-Energy Physics, University of Amsterdam, Science Park 904, 1098 XH Amsterdam, The Netherlands
[39] National and Kapodistrian University of Athens, School of Science Building, 2nd floor, Panepistimiopolis, 15771 Ilissia, Greece
[40] INFN, Sezione di Perugia, I-06123 Perugia, Italy
[41] Università di Camerino, Dipartimento di Fisica, I-62032 Camerino, Italy
[42] American University, Washington, D.C. 20016, USA
[43] Earthquake Research Institute, The University of Tokyo, Bunkyo-ku, Tokyo 113-0032, Japan
[44] California State University Fullerton, Fullerton, CA 92831, USA
[45] Université de Paris, CNRS, Astroparticule et Cosmologie, F-75006 Paris, France
[46] Université Paris-Saclay, CNRS/IN2P3, IJCLab, F-91405 Orsay, France
[47] European Gravitational Observatory (EGO), I-56021 Cascina, Pisa, Italy
[48] Georgia Institute of Technology, Atlanta, GA 30332, USA
[49] Chennai Mathematical Institute, Chennai 603103, India
[50] Department of Mathematics and Physics, Hirosaki University, Aomori 036-8561, Japan
[51] Columbia University, New York, NY 10027, USA
[52] University of Portsmouth, Portsmouth, PO1 3FX, UK
[53] Kamioka Branch, National Astronomical Observatory of Japan (NAOJ), Kamioka-cho, Hida City, Gifu 506-1205, Japan
[54] The Graduate University for Advanced Studies (SOKENDAI), Mitaka City, Tokyo 181-8588, Japan
[55] Università degli Studi di Urbino "Carlo Bo", I-61029 Urbino, Italy
[56] INFN, Sezione di Firenze, I-50019 Sesto Fiorentino, Firenze, Italy
[57] LIGO Livingston Observatory, Livingston, LA 70754, USA
[58] INFN, Sezione di Roma, I-00185 Roma, Italy
[59] Université catholique de Louvain, B-1348 Louvain-la-Neuve, Belgium
[60] Nikhef, Science Park 105, 1098 XG Amsterdam, The Netherlands
[61] King's College London, University of London, London WC2R 2LS, UK
[62] Korea Institute of Science and Technology Information, Daejeon 34141, Republic of Korea
[63] National Institute for Mathematical Sciences, Daejeon 34047, Republic of Korea
[64] Christopher Newport University, Newport News, VA 23606, USA
[65] School of High Energy Accelerator Science, The Graduate University for Advanced Studies (SOKENDAI), Tsukuba City, Ibaraki 305-0801, Japan
[66] Institute for Gravitational and Subatomic Physics (GRASP), Utrecht University, Princetonplein 1, 3584 CC Utrecht, The Netherlands
[67] University of Oregon, Eugene, OR 97403, USA
[68] Syracuse University, Syracuse, NY 13244, USA
[69] Université de Liège, B-4000 Liège, Belgium
[70] Università degli Studi di Milano-Bicocca, I-20126 Milano, Italy

[71] INFN, Sezione di Milano-Bicocca, I-20126 Milano, Italy
[72] INAF, Osservatorio Astronomico di Brera sede di Merate, I-23807 Merate, Lecco, Italy
[73] Max Planck Institute for Gravitational Physics (Albert Einstein Institute), D-14476 Potsdam, Germany
[74] LIGO Hanford Observatory, Richland, WA 99352, USA
[75] Dipartimento di Medicina, Chirurgia e Odontoiatria "Scuola Medica Salernitana", Università di Salerno, I-84081 Baronissi, Salerno, Italy
[76] LIGO Laboratory, Massachusetts Institute of Technology, Cambridge, MA 02139, USA
[77] Wigner RCP, RMKI, H-1121 Budapest, Konkoly Thege Miklós út 29-33, Hungary
[78] University of Florida, Gainesville, FL 32611, USA
[79] Stanford University, Stanford, CA 94305, USA
[80] Università di Pisa, I-56127 Pisa, Italy
[81] Università di Perugia, I-06123 Perugia, Italy
[82] Università di Padova, Dipartimento di Fisica e Astronomia, I-35131 Padova, Italy
[83] INFN, Sezione di Padova, I-35131 Padova, Italy
[84] Bard College, Annandale-On-Hudson, NY 12504, USA
[85] Montana State University, Bozeman, MT 59717, USA
[86] Institute for Plasma Research, Bhat, Gandhinagar 382428, India
[87] Universiteit Gent, B-9000 Gent, Belgium
[88] Nicolaus Copernicus Astronomical Center, Polish Academy of Sciences, 00-716, Warsaw, Poland
[89] Dipartimento di Ingegneria, Università del Sannio, I-82100 Benevento, Italy
[90] OzGrav, University of Adelaide, Adelaide, South Australia 5005, Australia
[91] The University of Texas Rio Grande Valley, Brownsville, TX 78520, USA
[92] California State University, Los Angeles, Los Angeles, CA 90032, USA
[93] Departamento de Matemáticas, Universitat Autònoma de Barcelona, Edificio C Facultad de Ciencias E-08193 Bellaterra (Barcelona), Spain
[94] INFN, Sezione di Genova, I-16146 Genova, Italy
[95] OzGrav, University of Western Australia, Crawley, Western Australia 6009, Australia
[96] RRCAT, Indore, Madhya Pradesh 452013, India
[97] Missouri University of Science and Technology, Rolla, MO 65409, USA
[98] Vrije Universiteit Amsterdam, 1081 HV Amsterdam, The Netherlands
[99] Lomonosov Moscow State University, Moscow 119991, Russia
[100] Center for Theoretical Physics, Polish Academy of Sciences, al. Lotnik'ow 32/46, 02-668 Warsaw, Poland
[101] Università di Trento, Dipartimento di Fisica, I-38123 Povo, Trento, Italy
[102] INFN, Trento Institute for Fundamental Physics and Applications, I-38123 Povo, Trento, Italy
[103] SUPA, University of the West of Scotland, Paisley PA1 2BE, UK
[104] Bar-Ilan University, Ramat Gan, 5290002, Israel
[105] Dipartimento di Fisica "E.R. Caianiello", Università di Salerno, I-84084 Fisciano, Salerno, Italy
[106] INFN, Sezione di Napoli, Gruppo Collegato di Salerno, Complesso Universitario di Monte S. Angelo, I-80126 Napoli, Italy
[107] Università di Roma "La Sapienza", I-00185 Roma, Italy
[108] Univ Rennes, CNRS, Institut FOTON—UMR6082, F-3500 Rennes, France
[109] Indian Institute of Technology Bombay, Powai, Mumbai 400 076, India
[110] INFN, Laboratori Nazionali del Gran Sasso, I-67100 Assergi, Italy
[111] Laboratoire Kastler Brossel, Sorbonne Université, CNRS, ENS-Université PSL, Collège de France, F-75005 Paris, France
[112] Astronomical Observatory Warsaw University, 00-478 Warsaw, Poland
[113] University of Maryland, College Park, MD 20742, USA
[114] L2IT, Laboratoire des 2 Infinis—Toulouse, Université de Toulouse, CNRS/IN2P3, UPS, F-31062 Toulouse Cedex 9, France
[115] Villanova University, Villanova, PA 19085, USA
[116] IGFAE, Universidade de Santiago de Compostela, E-15782 Spain
[117] Stony Brook University, Stony Brook, NY 11794, USA
[118] Center for Computational Astrophysics, Flatiron Institute, New York, NY 10010, USA
[119] NASA Goddard Space Flight Center, Greenbelt, MD 20771, USA
[120] Dipartimento di Fisica, Università degli Studi di Genova, I-16146 Genova, Italy
[121] Department of Astronomy, Beijing Normal University, Beijing 100875, People's Republic of China
[122] OzGrav, University of Melbourne, Parkville, Victoria 3010, Australia
[123] Università degli Studi di Sassari, I-07100 Sassari, Italy
[124] INFN, Laboratori Nazionali del Sud, I-95125 Catania, Italy
[125] Università di Roma Tor Vergata, I-00133 Roma, Italy
[126] INFN, Sezione di Roma Tor Vergata, I-00133 Roma, Italy
[127] University of Sannio at Benevento, I-82100 Benevento, Italy and INFN, Sezione di Napoli, I-80100 Napoli, Italy
[128] Departamento de Astronomía y Astrofísica, Universitat de València, E-46100 Burjassot, València, Spain
[129] Universität Hamburg, D-22761 Hamburg, Germany
[130] Rochester Institute of Technology, Rochester, NY 14623, USA
[131] National Tsing Hua University, Hsinchu City, 30013 Taiwan, People's Republic of China
[132] The Chinese University of Hong Kong, Shatin, NT, Hong Kong, People's Republic of China
[133] Department of Applied Physics, Fukuoka University, Jonan, Fukuoka City, Fukuoka 814-0180, Japan
[134] OzGrav, Charles Sturt University, Wagga Wagga, New South Wales 2678, Australia
[135] Department of Physics, Tamkang University, Danshui Dist., New Taipei City 25137, Taiwan
[136] Department of Physics and Institute of Astronomy, National Tsing Hua University, Hsinchu 30013, Taiwan
[137] Department of Physics, Center for High Energy and High Field Physics, National Central University, Zhongli District, Taoyuan City 32001, Taiwan
[138] CaRT, California Institute of Technology, Pasadena, CA 91125, USA
[139] Department of Physics, National Tsing Hua University, Hsinchu 30013, Taiwan
[140] Dipartimento di Ingegneria Industriale (DIIN), Università di Salerno, I-84084 Fisciano, Salerno, Italy
[141] Institute of Physics, Academia Sinica, Nankang, Taipei 11529, Taiwan
[142] Université Lyon, Université Claude Bernard Lyon 1, CNRS, IP2I Lyon / IN2P3, UMR 5822, F-69622 Villeurbanne, France
[143] INAF, Osservatorio Astronomico di Padova, I-35122 Padova, Italy
[144] OzGrav, Swinburne University of Technology, Hawthorn VIC 3122, Australia
[145] Université libre de Bruxelles, Avenue Franklin Roosevelt B-50-1050 Bruxelles, Belgium
[146] Universitat de les Illes Balears, E-07122 Palma de Mallorca, Spain

[147] Université Libre de Bruxelles, Brussels B-1050, Belgium
[148] Departamento de Matemáticas, Universitat de València, E-46100 Burjassot, València, Spain
[149] Texas Tech University, Lubbock, TX 79409, USA
[150] University of Minnesota, Minneapolis, MN 55455, USA
[151] The Pennsylvania State University, University Park, PA 16802, USA
[152] University of Rhode Island, Kingston, RI 02881, USA
[153] Bellevue College, Bellevue, WA 98007, USA
[154] Scuola Normale Superiore, Piazza dei Cavalieri, I-7-56126 Pisa, Italy
[155] Eötvös University, Budapest 1117, Hungary
[156] Maastricht University, P.O. Box 616, 6200 MD Maastricht, The Netherlands
[157] The University of Sheffield, Sheffield S10 2TN, UK
[158] Universitat de les Illes Balears, IAC3–IEEC, E-07122 Palma de Mallorca, Spain
[159] Université Lyon, Université Claude Bernard Lyon 1, CNRS, Laboratoire des Matériaux Avancés (LMA), IP2I Lyon / IN2P3, UMR 5822, F-69622 Villeurbanne, France
[160] Dipartimento di Scienze Matematiche, Fisiche e Informatiche, Università di Parma, I-43124 Parma, Italy
[161] INFN, Sezione di Milano-Bicocca, Gruppo Collegato di Parma, I-43124 Parma, Italy
[162] The University of Utah, Salt Lake City, UT 84112, USA
[163] Carleton College, Northfield, MN 55057, USA
[164] University of Zurich, Winterthurerstrasse 190, 8057 Zurich, Switzerland
[165] Perimeter Institute, Waterloo, ON N2L 2Y5, Canada
[166] Université de Strasbourg, CNRS, IPHC UMR 7178, F-67000 Strasbourg, France
[167] West Virginia University, Morgantown, WV 26506, USA
[168] University of Chicago, Chicago, IL 60637, USA
[169] Montclair State University, Montclair, NJ 07043, USA
[170] Colorado State University, Fort Collins, CO 80523, USA
[171] Institute for Nuclear Research, Bem t'er 18/c, H-4026 Debrecen, Hungary
[172] University of Texas, Austin, TX 78712, USA
[173] CNR-SPIN, c/o Università di Salerno, I-84084 Fisciano, Salerno, Italy
[174] Scuola di Ingegneria, Università della Basilicata, I-85100 Potenza, Italy
[175] Observatori Astronòmic, Universitat de València, E-46980 Paterna, València, Spain
[176] Centro de Física das Universidades do Minho e do Porto, Universidade do Minho, Campus de Gualtar, PT-4710-057 Braga, Portugal
[177] Department of Astronomy, The University of Tokyo, Mitaka City, Tokyo 181-8588, Japan
[178] Faculty of Engineering, Niigata University, Nishi-ku, Niigata City, Niigata 950-2181, Japan
[179] Department of Physics, Graduate School of Science, Osaka City University, Sumiyoshi-ku, Osaka City, Osaka 558-8585, Japan
[180] State Key Laboratory of Magnetic Resonance and Atomic and Molecular Physics, Innovation Academy for Precision Measurement Science and Technology (APM), Chinese Academy of Sciences, Xiao Hong Shan, Wuhan 430071, People's Republic of China
[181] University of Szeged, Dóm tér 9, Szeged 6720, Hungary
[182] Cornell University, Ithaca, NY 14850, USA
[183] University of British Columbia, Vancouver, BC V6T 1Z4, Canada
[184] INAF, Osservatorio Astronomico di Capodimonte, I-80131 Napoli, Italy
[185] The University of Mississippi, University, MS 38677, USA
[186] University of Michigan, Ann Arbor, MI 48109, USA
[187] Texas A&M University, College Station, TX 77843, USA
[188] Ulsan National Institute of Science and Technology, Ulsan 44919, Republic of Korea
[189] Shanghai Astronomical Observatory, Chinese Academy of Sciences, Shanghai 200030, People's Republic of China
[190] Institute for Cosmic Ray Research (ICRR), KAGRA Observatory, The University of Tokyo, Kashiwa City, Chiba 277-8582, Japan
[191] Faculty of Science, University of Toyama, Toyama City, Toyama 930-8555, Japan
[192] Institute for Cosmic Ray Research (ICRR), KAGRA Observatory, The University of Tokyo, Kamioka-cho, Hida City, Gifu 506-1205, Japan
[193] University of California, Berkeley, CA 94720, USA
[194] Maastricht University, 6200 MD, Maastricht, The Netherlands
[195] Lancaster University, Lancaster LA1 4YW, UK
[196] College of Industrial Technology, Nihon University, Narashino City, Chiba 275-8575, Japan
[197] Institute of Astronomy, National Tsing Hua University, Hsinchu 30013, Taiwan
[198] Rutherford Appleton Laboratory, Didcot OX11 0DE, UK
[199] Department of Astronomy & Space Science, Chungnam National University, Yuseong-gu, Daejeon 34134, Republic of Korea
[200] Department of Physical Sciences, Aoyama Gakuin University, Sagamihara City, Kanagawa 252-5258, Japan
[201] Kavli Institute for Astronomy and Astrophysics, Peking University, Haidian District, Beijing 100871, People's Republic of China
[202] Aristotle University of Thessaloniki, University Campus, 54124 Thessaloniki, Greece
[203] Graduate School of Science and Engineering, University of Toyama, Toyama City, Toyama 930-8555, Japan
[204] Nambu Yoichiro Institute of Theoretical and Experimental Physics (NITEP), Osaka City University, Sumiyoshi-ku, Osaka City, Osaka 558-8585, Japan
[205] Directorate of Construction, Services & Estate Management, Mumbai 400094, India
[206] Vanderbilt University, Nashville, TN 37235, USA
[207] Universiteit Antwerpen, Prinsstraat 13, B-2000 Antwerpen, Belgium
[208] University of Białystok, 15-424 Białystok, Poland
[209] Ewha Womans University, Seoul 03760, Republic of Korea
[210] National Astronomical Observatories, Chinese Academic of Sciences, Chaoyang District, Beijing, People's Republic of China
[211] School of Astronomy and Space Science, University of Chinese Academy of Sciences, Chaoyang District, Beijing, People's Republic of China
[212] University of Southampton, Southampton SO17 1BJ, UK
[213] Institute for Cosmic Ray Research (ICRR), The University of Tokyo, Kashiwa City, Chiba 277-8582, Japan
[214] Institute for High-Energy Physics, University of Amsterdam, Science Park 904, 1098 XH Amsterdam, The Netherlands
[215] Chung-Ang University, Seoul 06974, Republic of Korea
[216] University of Washington Bothell, Bothell, WA 98011, USA
[217] Institute of Applied Physics, Nizhny Novgorod, 603950, Russia
[218] Inje University Gimhae, South Gyeongsang 50834, Republic of Korea
[219] Department of Physics, Myongji University, Yongin 17058, Republic of Korea
[220] Institute of Particle and Nuclear Studies (IPNS), High Energy Accelerator Research Organization (KEK), Tsukuba City, Ibaraki 305-0801, Japan

[221] School of Physics and Astronomy, Cardiff University, Cardiff, CF24 3AA, UK

[222] Institute of Mathematics, Polish Academy of Sciences, 00656 Warsaw, Poland

[223] National Center for Nuclear Research, 05-400 Świerk-Otwock, Poland

[224] Instituto de Física Teorica, E-28049 Madrid, Spain

[225] Department of Physics, Nagoya University, Chikusa-ku, Nagoya, Aichi 464-8602, Japan

[226] Université de Montréal/Polytechnique, Montreal, Quebec H3T 1J4, Canada

[227] Laboratoire Lagrange, Université Côte d'Azur, Observatoire Côte d'Azur, CNRS, F-06304 Nice, France

[228] Seoul National University, Seoul 08826, Republic of Korea

[229] Sungkyunkwan University, Seoul 03063, Republic of Korea

[230] NAVIER, École des Ponts, Univ Gustave Eiffel, CNRS, Marne-la-Vallée, France

[231] Università di Firenze, Sesto Fiorentino I-50019, Italy

[232] Department of Physics, National Cheng Kung University, Tainan City 701, Taiwan

[233] School of Physics and Technology, Wuhan University, Wuhan, Hubei, 430072, People's Republic of China

[234] National Center for High-performance computing, National Applied Research Laboratories, Hsinchu Science Park, Hsinchu City 30076, Taiwan

[235] Department of Physics, National Taiwan Normal University, sec. 4, Taipei 116, Taiwan

[236] NASA Marshall Space Flight Center, Huntsville, AL 35811, USA

[237] INFN, Sezione di Roma Tre, I-00146 Roma, Italy

[238] ESPCI, CNRS, F-75005 Paris, France

[239] Kenyon College, Gambier, OH 43022, USA

[240] School of Physics Science and Engineering, Tongji University, Shanghai 200092, People's Republic of China

[241] Dipartimento di Fisica, Università di Trieste, I-34127 Trieste, Italy

[242] Institute for Photon Science and Technology, The University of Tokyo, Bunkyo-ku, Tokyo 113-8656, Japan

[243] Indian Institute of Technology Madras, Chennai 600036, India

[244] Kavli Institute for the Physics and Mathematics of the Universe, 5-1-5 Kashiwanoha, Chiba 2778583, Japan

[245] Saha Institute of Nuclear Physics, Bidhannagar, West Bengal 700064, India

[246] Institute of Space and Astronautical Science (JAXA), Chuo-ku, Sagamihara City, Kanagawa 252-0222, Japan

[247] Institut des Hautes Etudes Scientifiques, F-91440 Bures-sur-Yvette, France

[248] Faculty of Law, Ryukoku University, Fushimi-ku, Kyoto City, Kyoto 612-8577, Japan

[249] Indian Institute of Science Education and Research, Kolkata, Mohanpur, West Bengal 741252, India

[250] Department of Physics, University of Notre Dame, Notre Dame, IN 46556, USA

[251] Graduate School of Science and Technology, Niigata University, Nishi-ku, Niigata City, Niigata 950-2181, Japan

[252] Consiglio Nazionale delle Ricerche—Istituto dei Sistemi Complessi, Piazzale Aldo Moro 5, I-00185 Roma, Italy

[253] Korea Astronomy and Space Science Institute (KASI), Yuseong-gu, Daejeon 34055, Republic of Korea

[254] Hobart and William Smith Colleges, Geneva, NY 14456, USA

[255] International Institute of Physics, Universidade Federal do Rio Grande do Norte, Natal RN 59078-970, Brazil

[256] Museo Storico della Fisica e Centro Studi e Ricerche "Enrico Fermi", I-00184 Roma, Italy

[257] Dipartimento di Matematica e Fisica, Università degli Studi Roma Tre, I-00146 Roma, Italy

[258] University of Arizona, Tucson, AZ 85721, USA

[259] Università di Trento, Dipartimento di Matematica, I-38123 Povo, Trento, Italy

[260] Subatech, CNRS/IN2P3, IMT Atlantique, Université de Nantes, Nantes, France

[261] University of California, Riverside, Riverside, CA 92521, USA

[262] University of Washington, Seattle, WA 98195, USA

[263] Indian Institute of Technology, Palaj, Gandhinagar, Gujarat 382355, India

[264] Department of Electronic Control Engineering, National Institute of Technology, Nagaoka College, Nagaoka City, Niigata 940-8532, Japan

[265] Departamento de Matemática da Universidade de Aveiro and Centre for Research and Development in Mathematics and Applications, Campus de Santiago, 3810-183 Aveiro, Portugal

[266] Marquette University, Milwaukee, WI 53233, USA

[267] Faculty of Science, Toho University, Funabashi City, Chiba 274-8510, Japan

[268] Graduate School of Science and Technology, Gunma University, Maebashi, Gunma 371-8510, Japan

[269] Institute for Quantum Studies, Chapman University, Orange, CA 92866, USA

[270] Accelerator Laboratory, High Energy Accelerator Research Organization (KEK), Tsukuba City, Ibaraki 305-0801, Japan

[271] Faculty of Information Science and Technology, Osaka Institute of Technology, Hirakata City, Osaka 573-0196, Japan; hisaaki.shinkai@oit.ac.jp

[272] INAF, Osservatorio Astrofisico di Arcetri, Largo E. Fermi 5, I-50125 Firenze, Italy

[273] Indian Institute of Technology Hyderabad, Sangareddy, Khandi, Telangana 502285, India

[274] Indian Institute of Science Education and Research, Pune, Maharashtra 411008, India

[275] Istituto di Astrofisica e Planetologia Spaziali di Roma, Via del Fosso del Cavaliere, 100, I-00133 Roma RM, Italy

[276] Department of Space and Astronautical Science, The Graduate University for Advanced Studies (SOKENDAI), Sagamihara City, Kanagawa 252-5210, Japan

[277] Andrews University, Berrien Springs, MI 49104, USA

[278] Research Center for Space Science, Advanced Research Laboratories, Tokyo City University, Setagaya, Tokyo 158-0082, Japan

[279] Laboratoire des 2 Infinis—Toulouse (L2IT-IN2P3), Université de Toulouse, CNRS, UPS, F-31062 Toulouse Cedex 9, France

[280] Institute for Cosmic Ray Research (ICRR), Research Center for Cosmic Neutrinos (RCCN), The University of Tokyo, Kashiwa City, Chiba 277-8582, Japan

[281] Department of Physics, Kyoto University, Sakyou-ku, Kyoto City, Kyoto 606-8502, Japan

[282] Yukawa Institute for Theoretical Physics (YITP), Kyoto University, Sakyou-ku, Kyoto City, Kyoto 606-8502, Japan

[283] Dipartimento di Scienze Aziendali—Management and Innovation Systems (DISA-MIS), Università di Salerno, I-84084 Fisciano, Salerno, Italy

[284] Van Swinderen Institute for Particle Physics and Gravity, University of Groningen, Nijenborgh 4, 9747 AG Groningen, The Netherlands

[285] Faculty of Science, Department of Physics, The Chinese University of Hong Kong, Shatin, N.T., Hong Kong, People's Republic of China

[286] Vrije Universiteit Brussel, Pleinlaan 2, B-1050 Brussel, Belgium

[287] Applied Research Laboratory, High Energy Accelerator Research Organization (KEK), Tsukuba City, Ibaraki 305-0801, Japan

[288] Department of Communications Engineering, National Defense Academy of Japan, Yokosuka City, Kanagawa 239-8686, Japan

[289] Department of Physics, University of Florida, Gainesville, FL 32611, USA

[290] Department of Information and Management Systems Engineering, Nagaoka University of Technology, Nagaoka City, Niigata 940-2188, Japan

[291] Tata Institute of Fundamental Research, Mumbai 400005, India

[292] Eindhoven University of Technology, Postbus 513, 5600 MB Eindhoven, The Netherlands

[293] Department of Physics and Astronomy, Sejong University, Gwangjin-gu, Seoul 143-747, Republic of Korea

[294] Concordia University Wisconsin, Mequon, WI 53097, USA

[295] Department of Electrophysics, National Yang Ming Chiao Tung University, Hsinchu, Taiwan

[296] Department of Physics, Rikkyo University, Toshima-ku, Tokyo 171-8501, Japan

Abstract

We use 47 gravitational wave sources from the Third LIGO–Virgo–Kamioka Gravitational Wave Detector Gravitational Wave Transient Catalog (GWTC–3) to estimate the Hubble parameter $H(z)$, including its current value, the Hubble constant H_0. Each gravitational wave (GW) signal provides the luminosity distance to the source, and we estimate the corresponding redshift using two methods: the redshifted masses and a galaxy catalog. Using the binary black hole (BBH) redshifted masses, we simultaneously infer the source mass distribution and $H(z)$. The source mass distribution displays a peak around $34\,M_\odot$, followed by a drop-off. Assuming this mass scale does not evolve with the redshift results in a $H(z)$ measurement, yielding $H_0 = 68^{+12}_{-8}$ km s^{-1} Mpc^{-1} (68% credible interval) when combined with the H_0 measurement from GW170817 and its electromagnetic counterpart. This represents an improvement of 17% with respect to the H_0 estimate from GWTC–1. The second method associates each GW event with its probable host galaxy in the catalog GLADE+, statistically marginalizing over the redshifts of each event's potential hosts. Assuming a fixed BBH population, we estimate a value of $H_0 = 68^{+8}_{-6}$ km s^{-1} Mpc^{-1} with the galaxy catalog method, an improvement of 42% with respect to our GWTC–1 result and 20% with respect to recent H_0 studies using GWTC–2 events. However, we show that this result is strongly impacted by assumptions about the BBH source mass distribution; the only event which is not strongly impacted by such assumptions (and is thus informative about H_0) is the well-localized event GW190814.

Key words: Gravitational waves – Gravitational wave astronomy – Gravitational wave sources

1. Introduction

The discovery of a gravitational wave (GW) signal from a binary neutron star (BNS) merger (Abbott et al. 2017a) and the kilonova emission from its remnant (Coulter et al. 2017; Abbott et al. 2017b) provided the first GW standard siren measurement of the cosmic expansion history (Abbott et al. 2017c). As pointed out by Schutz (1986), the GW signal from a compact binary coalescence directly measures the luminosity distance to the source without any additional distance calibrator, earning these sources the name "standard sirens" (Holz & Hughes 2005). Measuring the cosmic expansion as a function of the cosmological redshift is one of the key avenues with which to explore the constituents of the universe, along with the other canonical probes such as the cosmic microwave background (CMB; Spergel et al. 2003, 2007; Komatsu et al. 2011; Ade et al. 2014, 2016; Aghanim et al. 2020), baryon acoustic oscillations (Eisenstein & Hu 1998, 1997; Dawson et al. 2013; Alam et al. 2017), type Ia supernovae (Riess et al. 1996; Perlmutter et al. 1999; Riess et al. 2016; Freedman 2017; Riess et al. 2019), strong gravitational lensing (Suyu et al. 2010; Wong et al. 2020), and cosmic chronometers (Moresco et al. 2016; Jimenez et al. 2019).

Even though GW sources are excellent distance tracers, using them to study the expansion history also requires measurement of their redshift. The redshift information is usually degenerate with the source masses in the GW signal, as the redshifted masses affect the GW frequency evolution. However, several techniques are proposed to infer the redshift of GW sources and break the mass–redshift degeneracy. For sources with confirmed electromagnetic (EM) counterparts, the host galaxy and its redshift can be determined directly

(Holz & Hughes 2005; Dalal et al. 2006; MacLeod & Hogan 2008; Nissanke et al. 2010; Abbott et al. 2017c; Chen et al. 2018; Feeney et al. 2019). For sources without an EM counterpart, alternative techniques to infer the source redshift include comparing the redshifted mass distribution to an astrophysically motivated source mass distribution (Chernoff & Finn 1993; Taylor & Gair 2012; Farr et al. 2019; You et al. 2021; Mastrogiovanni et al. 2021), obtaining statistical redshift information from galaxy catalogs (Schutz 1986; MacLeod & Hogan 2008; Del Pozzo 2012; Nishizawa 2017; Chen et al. 2018; Nair et al. 2018; Fishbach et al. 2019; Soares-Santos et al. 2019; Gray et al. 2020; Yu et al. 2020; Palmese et al. 2020; Borhanian et al. 2020; Finke et al. 2021), comparing the spatial clustering between GW sources and galaxies (Oguri 2016; Bera et al. 2020; Mukherjee et al. 2020, 2021), leveraging external knowledge of the source redshift distribution (Ding et al. 2019; Ye & Fishbach 2021), and exploiting the tidal distortions of neutron stars (Messenger & Read 2012; Chatterjee et al. 2021).

The third LIGO–Virgo–Kamioka Gravitational Wave Detector (KAGRA) GW transient catalog (GWTC–3; Abbott et al. 2021e) contains 90 compact binary coalescence candidate events with at least a 50% probability of being astrophysical in origin. Out of the events from the third observing run, a notable EM counterpart has been claimed only for the high-mass binary black hole (BBH) event GW190521 (Graham et al. 2020). However, the significance of this association has been reassessed by several authors, who found insufficient evidence to claim a confident association (Ashton et al. 2021; De Paolis et al. 2020; Palmese et al. 2021). In this work, we do not include the redshift information from this putative EM counterpart signal. The only standard siren with an EM counterpart in GWTC–3 remains the BNS GW170817.

The remainder of this paper is organized as follows. In Section 2 we discuss the statistical methods used to infer the cosmological parameters with and without galaxy catalog information. In Section 3 we discuss the properties of the GW events and galaxy catalogs used in this paper. In Section 4 we present the results of our analyses, and in Section 5 we discuss

---

[297] lsc-spokesperson@ligo.org
[298] virgo-spokesperson@ego-gw.it
[299] Deceased, August 2020.
[300] Deceased, April 2021.

their implications for the cosmological parameters. Finally, in Section 6 we present our conclusions.

2. Method

We use two analysis methods[301]: (i) jointly fitting the cosmological parameters and the source population properties of BBHs, without using galaxy catalog information (Mastrogiovanni et al. 2021; Section 2.1), and (ii) fixing the source population properties, and inferring the cosmological parameters using statistical galaxy catalog information (Gray et al. 2020; Section 2.2).

2.1. Hierarchical Inference without Galaxy Surveys

The GW event catalog can be described by two sets of parameters: a set of *population hyperparameters* Φ that are common to the entire population of GW sources, and a set of *intrinsic parameters* that are unique for each event. The cosmological population hyperparameters in this work are the cosmological parameters for a flat universe. For the redshift range considered in the analysis, the contribution to the total energy density from radiation and neutrinos is negligible. Hence, we consider the dark energy density today as $\Omega_{\rm DE}(z) = 1 - \Omega_{\rm m}$. The cosmological parameters considered are, therefore, the Hubble constant H_0, the matter density $\Omega_{\rm m}$, and the dark energy equation-of-state (EOS) parameter $w(z) = w_0$. (Chevallier & Polarski 2001). The dark energy EOS is defined by $w = p/\rho$, where for the standard ΛCDM we have $w = -1$. Additionally, the set of hyperparameters Φ includes parameters describing the source mass distribution and the merger rate density as a function of the redshift.

Given a set of $N_{\rm obs}$ GW detections associated with the data $\{x\} = (x_1, \ldots, x_{N_{\rm obs}})$, the posterior on Φ can be expressed as (Mandel et al. 2019; Thrane & Talbot 2019; Vitale et al. 2021)

$$p(\Phi | \{x\}, N_{\rm obs}) = p(\Phi) \prod_{i=1}^{N_{\rm obs}} \frac{\int p(x_i | \Phi, \theta) p_{\rm pop}(\theta | \Phi) d\theta}{\int p_{\rm det}(\theta, \Phi) p_{\rm pop}(\theta | \Phi) d\theta}, \quad (1)$$

where $p(\Phi)$ is a prior on the population parameters including standard cosmological parameters and parameters governing the redshift and mass distributions of GW sources. The variable θ is the set of parameters intrinsic to each GW event, such as spins, masses, redshift etc., $p(x_i | \Phi, \theta)$ is the GW likelihood, $p_{\rm det}(\theta, \Phi)$ is the probability of detecting a GW event with intrinsic parameters θ and for population hyperparameters Φ, and $p_{\rm pop}(\theta | \Phi)$ is a *population modeled* prior. The denominator in Equation (1) correctly normalizes the posterior and takes into account *selection effects* (Mandel et al. 2019). We use the hierarchical statistical framework to infer the population parameters Φ and the prior that they induce on the distributions of the GW parameters.

The intrinsic GW parameters that are interesting for cosmology are those that provide information about the redshift z of the source. For sources that are detected at cosmological distances, GWs provide a measurement of the *redshifted* masses $m_1^{\rm det}$, $m_2^{\rm det}$ and the luminosity distance $D_{\rm L}$,

rather than the redshift and *source* masses m_1, m_2, where

$$m_i = \frac{m_i^{\rm det}}{1 + z(D_{\rm L}; H_0, \Omega_{\rm m}, w_0)}. \quad (2)$$

The relation between the source mass and redshifted mass can then be used to probe cosmology even in the absence of an explicit EM counterpart (Taylor et al. 2012; Taylor & Gair 2012) provided the source mass scale can be well characterized. This approach is more effective if the source mass distribution displays sharp features (Farr et al. 2019; Ezquiaga & Holz 2021; You et al. 2021; Mastrogiovanni et al. 2021).

2.1.1. Population models

We model the BBH population as BBHs represent the majority of the detected sources. We now give a general overview of the source mass and redshift models used in this paper; see Appendix A for a complete description of the population models.

We describe the underlying distribution in the redshift and source masses as

$$p_{\rm pop}(\theta | \Phi_m, H_0, \Omega_{\rm m}, w_0) = C \, p(m_1, m_2 | \Phi_m) \psi(z | \gamma, k, z_{\rm p})$$
$$\times \frac{p(z | H_0, w_0, \Omega_{\rm m})}{1 + z}, \quad (3)$$

where C is a normalization factor, $p(m_1, m_2 | \Phi_m)$ is the source frame mass distribution, Φ_m refers to all the population parameters not related to cosmology, the $(1 + z)$ term encodes the clock difference between the source frame and detector frame, and $p(z | H_0, w_0, \Omega_{\rm m})$ is the redshift prior, which is taken to be uniform in comoving volume. The term $\psi(z | \gamma, k, z_{\rm p})$ describes the redshift evolution of the merger rate with a parameterization similar to that of Madau & Dickinson (2014), characterized by a low-redshift power-law slope γ, a peak at redshift $z_{\rm p}$, and a high-redshift power-law slope k after the peak, or

$$\psi(z | \gamma, k, z_{\rm p})$$
$$= [1 + (1 + z_{\rm p})^{-\gamma - k}] \frac{(1 + z)^\gamma}{1 + [(1 + z)/(1 + z_{\rm p})]^{\gamma + k}}. \quad (4)$$

The above rate evolution model is more complex than that in Fishbach et al. (2018), Abbott et al. (2021b), and Abbott et al. (2021f); this is because when we vary the cosmological parameters, the GW observations may be pushed to higher redshift, $z > 2$, past the peak of the star formation rate (Madau & Dickinson 2014).

The source mass models are factorized as

$$p(m_1, m_2 | \Phi_m) = p(m_1 | \Phi_m) p(m_2 | m_1, \Phi_m), \quad (5)$$

where the secondary mass is modeled by a power-law distribution between a minimum mass $m_{\rm min}$ and maximum mass m_1. For the primary mass, we implement three phenomenological mass models used in Abbott et al. (2019a, 2021b).

The first phenomenological model, the TRUNCATED model, describes the mass distribution as a power law (PL) between a minimum mass $m_{\rm min}$ and a maximum mass $m_{\rm max}$ (Fishbach & Holz 2017). This model was originally proposed in order to characterize the mass spectra of BBHs using two features: a lower hard mass edge representing the gap between NSs and BHs and an upper mass edge representing the imprint of

(pulsational) pair-instability supernovae (Fryer et al. 2001; Heger & Woosley 2002; Farmer et al. 2019; Renzo et al. 2020; Umeda et al. 2020). The BBH mass distribution inferred from GWTC–2 was more complicated than the TRUNCATED, and the second and third models are extensions of the TRUNCATED model that contain more complex structures to better fit the mass distribution (Abbott et al. 2021b). These models were proposed to describe more complex morphologies of the mass spectra such as a possible smooth transition between NSs and BHs and the possibility of having massive BHs formed in channels that are not subject to the (pulsational) pair-instability supernovae, e.g., hierarchical mergers (Mapelli 2021). The second model, the BROKEN POWER LAW, consists of two PLs attached at a break point (Abbott et al. 2021b). The third model is a superposition of a TRUNCATED and a Gaussian component referred to as POWER LAW + PEAK, in which the primary mass distribution is described by a PL with the addition of a Gaussian peak with mean μ_g and variance σ_g^2 (Talbot & Thrane 2018). Using the BROKEN POWER LAW and POWER LAW + PEAK models, GWTC–2 revealed an excess of BBH systems with primary masses in the range ~ 30–$40\,M_\odot$, followed by a drop-off in the merger rate at high masses (Abbott et al. 2021b). This structure in the PL, modeled either as a break or a Gaussian peak, may represent the imprint of (pulsational) pair-instability supernovae.

In a companion paper investigating the GWTC–3 population (Abbott et al. 2021f) we show the evidence for substructures in the BHs primary mass spectrum around $\sim 10 M_\odot$. However we also find that the simpler POWER LAW + PEAK model is still one of the models preferred by the GWTC–3 data. For this reason, and for simplicity in this paper, we only adopt models that are characterized by a single structure (BROKEN POWER LAW and POWER LAW + PEAK) to describe the excess of BHs observed around $35 M_\odot$; this also corresponds to the binaries that we can observe at higher redshifts and for which source mass assumptions could be important.

In order to infer $H(z)$ from the BBH population, a crucial assumption is that the source mass distribution is independent of the redshift (Fishbach et al. 2021). In most BBH formation scenarios, we expect some evolution of the mass distribution with the redshift, due to factors such as the metallicity evolution of the universe (Kudritzki & Puls 2000; Belczynski et al. 2010) and the dependence of the delay time between BBH formation and merger on BBH properties (Kushnir et al. 2016; Gallegos-Garcia et al. 2021; van Son et al. 2022). Nevertheless, if mass features, such as the break in the BROKEN POWER LAW model or the peak in the POWER LAW + PEAK model, are caused by the pair-instability supernova process, their location is thought to stay constant within a few solar masses across cosmic time (Farmer et al. 2019). The presence of these sharp mass features drives our cosmological constraints (Farr et al. 2019; Mastrogiovanni et al. 2021). Moreover, the BBH mass distribution is expected to evolve only weakly over the range of redshift accessible to current observations, at a level below current statistical uncertainties (Fishbach & Kalogera 2021; van Son et al. 2022). Although the BH mass spectrum at *formation* may vary with cosmic time, BBH channels typically predict a wide distribution of delay times between formation and merger, which tends to wash out any dependence of the BBH mass on the merger redshift (Mapelli et al. 2019).

In the following we will neglect the selection effect of spin distribution as the detection probability due to their inclusion

should not vary by more than a factor of 2 (Ng et al. 2018b). This is indeed a negligible term with respect to the statistical uncertainties on our posteriors (see Section 5) and the dependence of the selection bias on other parameters, such as H_0 and γ, for which it nearly follows a power law.

2.2. Statistical Galaxy Catalog Method

We also use the gwcosmo code (Gray et al. 2020) in the pixelated sky scheme (Gray et al. 2022), i.e., using the HEALPix pixelization algorithm (Górski et al. 2005; Zonca et al. 2019), to infer H_0 using information from galaxy surveys. This method assumes a fixed source mass distribution, as well as a fixed-rate evolution for the binaries, and estimates H_0 from the GW data using galaxy catalogs to provide statistical information about the GW source redshifts.

When including galaxy catalog information, the prior on redshift can be replaced by the distribution of galaxies in the survey. However, Equation (1) needs to be modified in order to take into account *completeness corrections*. These extra terms account for the impact of incompleteness, i.e., missing galaxies, due to the limited sensitivity of the catalog, in the GW localization volume. In this case, the posterior is given by

$$p(H_0|x, N_{obs}, \Phi_m) = p(H_0)p(N_{obs}|H_0, \Phi_m)$$
$$\times \prod_{i=1}^{N_{obs}} \sum_{g \in [G, \bar{G}]} p(x_i|\hat{d}, H_0, \Phi_m, g)p(g|H_0, \Phi_m, \hat{d}), \quad (6)$$

where G is the hypothesis that the GW host galaxy is included in the catalog and $\bar{G}$ that it is not, and $p(g|H_0, \Phi_m, \hat{d})$ expresses their probabilities for $g \in [G, \bar{G}]$. The term $p(N_{obs}|H_0, \Phi_m)$ is the probability of having N_{obs} detections. We analytically marginalize over this by assuming a uniform in the log rate prior. The notation $\hat{d}$ indicates the hypothesis that an event has been detected. The likelihoods $p(x_i|\hat{d}, H_0, \Phi_m, g)$ are built from the GW data and corrected for the selection effects in the case that the host galaxy is, and is not, inside the catalog; see Gray et al. (2020).

We implement an improved version of the analysis presented in Abbott et al. (2021a) that can estimate H_0 for any given sky direction covered by the GW localization by dividing the sky into equal-area pixels. In each pixel, the apparent magnitude threshold (m_{thr}) is taken to be the median of the apparent magnitudes of all the galaxies inside that pixel. This assumption is a conservative choice for approximating the impact of catalog completeness: all galaxies with apparent magnitude fainter than the defined threshold are excluded from the analysis. Using this m_{thr} the completeness is assessed, and the H_0 likelihoods are calculated in each pixel. In the end, all the pixel likelihoods are combined using weights proportional to the GW posterior probability in each pixel to give the final H_0 posterior of each GW event. Pixels with no GW support have zero contribution, so only the pixels within the 99.9% sky area are used.

These improvements are necessary to correct for galaxy catalog incompleteness in the case that the galaxy surveys contained within the catalog are less sensitive in particular sky areas, such as the directions of the galactic plane. Moreover, the analysis can take into account the fact that the GW luminosity distance posterior conditioned on the sky position might significantly change between different sky positions. The
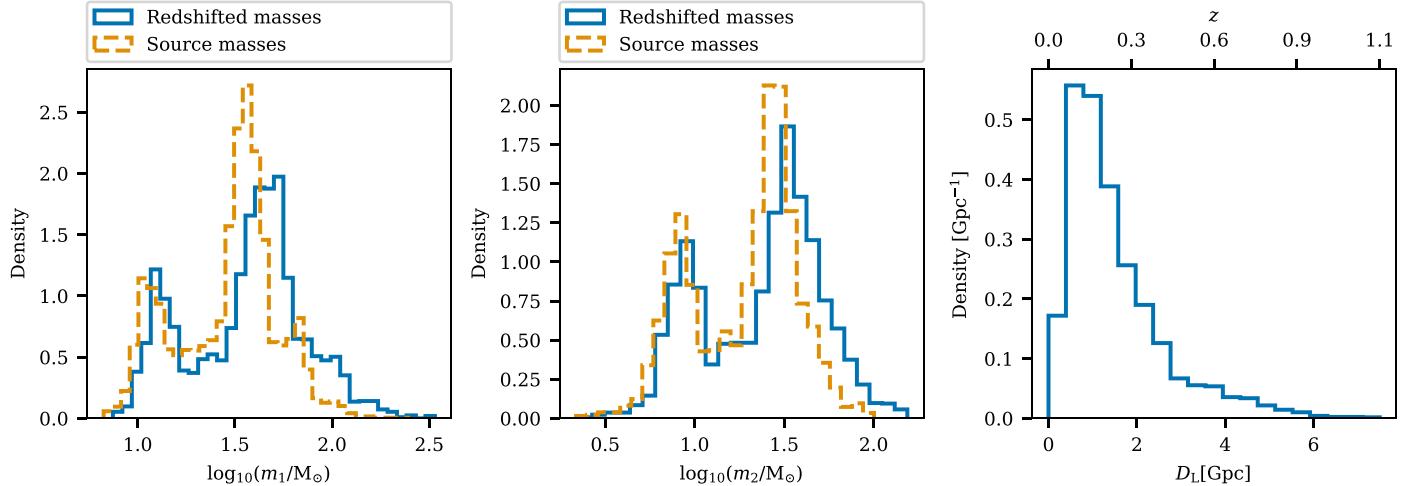
Figure 1. Distribution of the mass and luminosity distance parameters for the 42 BBH events with S/N> 11. The figure is generated using a Planck cosmology with $H_0 = 67.9$ km s^{-1} Mpc^{-1} and $\Omega_m = 0.3065$ with a D_L^2 prior and a uniform prior on the detector frame masses ad stacking posterior samples for each event. This figure is only representative of the events reported in Table 4 and does not indicate the population reconstruction. Left: distribution of the primary detector frame masses (blue solid line) and source frame masses (orange dashed line). Middle: same but for the secondary source mass. Right: distribution of the luminosity distance (bottom axis) and redshift (top axis).

combination of galaxy redshift information and luminosity distance estimation changes from pixel to pixel, leading to a more robust estimation of H_0.

3. Event and Catalog Selection

3.1. GW Events

For our main result, we select 47 GW events with a network matched filter signal-to-noise ratio (S/N) > 11 and an inverse false-alarm rate (IFAR) higher than 4 yr, taking their maximum across the different search pipelines from the data distributions released with GWTC–1 (Abbott et al. 2019c), GWTC–2 (Abbott et al. 2021c), and GWTC–3 (Abbott et al. 2021e), with no plausible instrumental origin. For events released with GWTC–3, we use the first version of the data distribution associated with LIGO Scientific Collaboration et al. (2021). We have verified that the selection of GW events and results of our analysis do not significantly change with the second version of the data release associated with GWTC–3.

We also consider events identified by different S/N choices to explore possible systematics in the computation of selection effects (see Appendix B). In the remainder of the paper we will shortly refer to these different ensembles by quoting the threshold S/N choices. Of the 47 events with S/N > 11, 42 are BBH detections, 2 are the BNS events GW170817 (Abbott et al. 2017a) and GW190425 (Abbott et al. 2020a), 2 are the NSBH events GW200105 and GW200115 (Abbott et al. 2021d), and 1 is the asymmetric mass binary GW190814 (Abbott et al. 2020b). A visual representation of the population of BBHs that we detected is provided in Figure 1, where we show the distribution of detector frame masses and luminosity distance of the BBHs. We have tabulated all the GW sources used in this analysis in Table 1, mentioning their source properties, sky localization error, 3D localization volume, number of galaxies in the catalog within the localization volume, and the probability that the GW host is present in the GLADE+catalog (Dálya et al. 2018, 2022). Note that, unlike in Abbott et al. 2021e, the estimation of masses and distances are reported using a prior $\propto D_L^2$ and not uniform in comoving

volume as we are interested in showing these values using cosmology-agnostic priors. For the events detected during O1, O2, and O3, we use combined posterior samples from the IMRPhenom (Thompson et al. 2020; Pratten et al. 2021) and SEOBNR (Ossokine et al. 2020; Matas et al. 2020) families, while for the two NSBH events GW200105 and GW200115 we use posterior samples generated with low-spin priors (Abbott et al. 2021d).[302]

3.2. Description of the GLADE+ Galaxy Catalog

In one of the analyses that we perform, the redshift information is taken from galaxy surveys for all of the events apart from GW170817, for which we assume the redshift information from its EM counterpart. For the analysis taking into account galaxy surveys we use the GLADE+ (Dálya et al. 2018, 2022) all-sky galaxy catalog, which is a revised version of the first GLADE catalog (Dálya et al. 2018) containing about 22 million galaxies. GLADE+ incorporates six different galaxy catalogs and surveys, namely, the Gravitational Wave Galaxy Catalogue (GWGC; White et al. 2011), HyperLEDA (Makarov et al. 2014), the Two Micron All-Sky Survey Extended Source Catalog (2MASS XSC; Skrutskie et al. 2006), the 2MASS Photometric Redshift Catalog (2MPZ; Bilicki et al. 2014), the WISExSCOS Photometric Redshift Catalogue (WISExS-COSPZ; Bilicki et al. 2016), and the Sloan Digital Sky Survey (SDSS) quasar catalog from the 16th data release (DR16Q; Lyke et al. 2020) and covers the full sky with a completeness of about 20% up to 800 Mpc.[303] Most of the galaxies in the GLADE+ catalog have a redshift measurement obtained

---

[302] Events in the analysis showing differences in posterior samples with different waveforms are GW191109_010717 and GW200129_065458 (Abbott et al. 2021e). These differences are mostly related to the effective and precession spin parameters, which are not considered in this analysis.
[303] Links to the different constituent galaxy catalogs and surveys in GLADE+ are as follows: GWGC- http://vizier.u-strasbg.fr/viz-bin/VizieR?-source=GWGC, HyperLEDA-http://leda.univ-lyon1.fr/, 2MASS XSC-https://wise2.ipac.caltech.edu/staff/jarrett/2mass/XSC/, 2MPZ-http://ssa.roe.ac.uk/TWOMPZ.html, WISExSCOS-http://ssa.roe.ac.uk/WISExSCOS.html, SDSS-DR16Q-https://www.sdss.org/dr16/algorithms/qso_catalog/.

Table 1
GW Events Considered in This Paper and Properties Reported With Their Median Values and 90% Symmetric Credible Intervals

Name	S/N	IFAR [yr]	m_1^{det} [M$_\odot$]	m_2^{det} [M$_\odot$]	D_L [Mpc]	m_1 [M$_\odot$]	m_2 [M$_\odot$]	z	$\Delta\Omega$ [deg^2]	ΔV_c [Gpc^3]	N_{gal}	$p(G\|z, H_0)$
GW150914	24.4	1×10^7	39^{+5}_{-3}	33^{+3}_{-5}	400^{+100}_{-200}	35^{+5}_{-3}	30^{+3}_{-4}	$0.09^{+0.03}_{-0.03}$	200	3×10^{-4}	$3000(3\times10^4)$	50-5(99-72)
GW151012	10.0	100	27^{+16}_{-6}	17^{+4}_{-6}	1100^{+500}_{-500}	23^{+14}_{-5}	14^{+4}_{-5}	$0.21^{+0.09}_{-0.09}$	2000	0.05	$6000(5\times10^5)$	5-0(73-10)
GW151226	13.1	1×10^7	15^{+8}_{-4}	8^{+2}_{-2}	400^{+200}_{-200}	14^{+8}_{-3}	8^{+2}_{-2}	$0.09^{+0.04}_{-0.04}$	1000	0.003	$1\times10^4(1\times10^5)$	58-4(100-70)
GW170104	13.0	1×10^7	37^{+8}_{-6}	24^{+6}_{-6}	1000^{+400}_{-400}	31^{+7}_{-5}	20^{+5}_{-5}	$0.20^{+0.07}_{-0.07}$	900	0.02	$8000(4\times10^5)$	8-0(76-17)
GW170608	15.4	1×10^7	12^{+6}_{-2}	8^{+1}_{-2}	300^{+100}_{-100}	11^{+5}_{-2}	8^{+1}_{-2}	$0.07^{+0.02}_{-0.02}$	400	4×10^{-4}	$4000(2\times10^4)$	69-19(100-87)
GW170729	10.8	6	80^{+20}_{-10}	50^{+10}_{-20}	3000^{+1000}_{-1000}	50^{+20}_{-10}	32^{+10}_{-9}	$0.5^{+0.2}_{-0.2}$	1000	0.3	$60(8\times10^4)$	0-0(12-0)
GW170809	12.4	1×10^7	42^{+10}_{-7}	28^{+6}_{-6}	1000^{+300}_{-400}	35^{+9}_{-6}	24^{+5}_{-5}	$0.20^{+0.05}_{-0.07}$	300	0.004	$2000(1\times10^5)$	4-0(70-21)
GW170814	16.3	1×10^7	34^{+6}_{-3}	29^{+3}_{-5}	600^{+100}_{-200}	30^{+6}_{-3}	25^{+3}_{-4}	$0.12^{+0.03}_{-0.04}$	90	2×10^{-4}	$1000(1\times10^4)$	27-1(91-60)
GW170817	33.0	1×10^7	$1.48^{+0.15}_{-0.09}$	$1.28^{+0.09}_{-0.12}$	40^{+7}_{-15}	$1.47^{+0.15}_{-0.09}$	$1.27^{+0.09}_{-0.11}$	$0.009^{+0.002}_{-0.003}$	20	2×10^{-8}	10(6)	100-100(100-100)
GW170818	11.3	2×10^4	43^{+9}_{-5}	32^{+5}_{-7}	1000^{+400}_{-300}	35^{+7}_{-5}	27^{+4}_{-5}	$0.21^{+0.07}_{-0.06}$	40	6×10^{-4}	$80(1\times10^4)$	2-0(55-9)
GW170823	11.5	1×10^7	53^{+13}_{-8}	39^{+8}_{-10}	1900^{+800}_{-900}	39^{+11}_{-7}	29^{+6}_{-7}	$0.4^{+0.1}_{-0.1}$	2000	0.2	$700(3\times10^5)$	0-0(35-0)
GW190408_181802	14.8	1×10^5	32^{+6}_{-4}	24^{+4}_{-5}	1600^{+400}_{-600}	24^{+5}_{-3}	18^{+3}_{-4}	$0.30^{+0.06}_{-0.10}$	100	0.003	$80(2\times10^4)$	0-0(39-3)
GW190412	19.7	1×10^5	35^{+5}_{-6}	10^{+2}_{-1}	700^{+100}_{-200}	30^{+5}_{-5}	$8.3^{+1.6}_{-0.9}$	$0.15^{+0.03}_{-0.03}$	20	3×10^{-5}	100(4000)	7-0(76-51)
GW190413_134308	10.3	6	80^{+20}_{-10}	60^{+20}_{-20}	5000^{+2000}_{-2000}	45^{+13}_{-10}	31^{+10}_{-10}	$0.8^{+0.3}_{-0.3}$	500	0.2	0(70)	0-0(0-0)
GW190421_213856	10.5	400	62^{+15}_{-9}	48^{+10}_{-13}	3000^{+1000}_{-1000}	41^{+10}_{-7}	31^{+7}_{-8}	$0.5^{+0.2}_{-0.2}$	1000	0.2	$1(2\times10^4)$	0-0(5-0)
GW190425	12.9	30	$2.1^{+0.6}_{-0.4}$	$1.4^{+0.3}_{-0.3}$	160^{+70}_{-70}	$2.0^{+0.6}_{-0.3}$	$1.4^{+0.3}_{-0.3}$	$0.03^{+0.01}_{-0.02}$	8000	0.002	$3\times10^4(6\times10^4)$	95-63(100-100)
GW190503_185404	12.8	1×10^5	55^{+11}_{-10}	40^{+10}_{-10}	1500^{+700}_{-700}	43^{+9}_{-8}	29^{+7}_{-8}	$0.3^{+0.1}_{-0.1}$	90	0.005	$100(4\times10^4)$	0-0(46-1)
GW190512_180714	12.4	1×10^5	29^{+7}_{-7}	16^{+5}_{-3}	1500^{+500}_{-600}	23^{+5}_{-6}	13^{+4}_{-2}	$0.29^{+0.08}_{-0.10}$	200	0.008	$100(3\times10^4)$	0-0(41-2)
GW190513_205428	12.9	8×10^4	50^{+10}_{-10}	25^{+10}_{-6}	2200^{+900}_{-800}	35^{+10}_{-9}	18^{+7}_{-4}	$0.4^{+0.1}_{-0.1}$	500	0.04	$20(3\times10^4)$	0-0(18-0)
GW190517_055101	11.3	3000	51^{+15}_{-8}	35^{+8}_{-10}	2000^{+2000}_{-1000}	36^{+12}_{-8}	25^{+7}_{-7}	$0.4^{+0.3}_{-0.2}$	400	0.1	$90(7\times10^4)$	0-0(28-0)
GW190519_153544	13.9	1×10^5	100^{+20}_{-10}	60^{+20}_{-10}	3000^{+2000}_{-1000}	60^{+10}_{-10}	40^{+10}_{-10}	$0.5^{+0.3}_{-0.2}$	700	0.2	$9(2\times10^4)$	0-0(7-0)
GW190521	14.4	5000	150^{+50}_{-20}	120^{+30}_{-40}	5000^{+2000}_{-2000}	90^{+30}_{-20}	70^{+20}_{-20}	$0.7^{+0.3}_{-0.3}$	900	0.4	4(900)	0-0(0-0)
GW190521_074359	24.7	1×10^5	52^{+7}_{-6}	41^{+6}_{-8}	1300^{+400}_{-600}	42^{+6}_{-5}	33^{+5}_{-6}	$0.25^{+0.06}_{-0.10}$	500	0.01	$700(3\times10^4)$	1-0(59-8)
GW190602_175927	12.6	1×10^5	100^{+20}_{-20}	70^{+20}_{-30}	3000^{+2000}_{-1000}	70^{+20}_{-10}	50^{+10}_{-20}	$0.5^{+0.3}_{-0.2}$	700	0.2	$2(2\times10^4)$	0-0(6-0)
GW190620_030421	10.9	90	80^{+20}_{-20}	50^{+20}_{-20}	3000^{+2000}_{-1000}	60^{+20}_{-10}	30^{+10}_{-10}	$0.5^{+0.2}_{-0.2}$	6000	2	$200(1\times10^5)$	0-0(6-0)
GW190630_185205	15.2	1×10^5	42^{+8}_{-7}	28^{+6}_{-5}	1000^{+500}_{-400}	35^{+7}_{-5}	23^{+5}_{-5}	$0.19^{+0.09}_{-0.08}$	1000	0.03	$9000(5\times10^5)$	8-0(76-12)
GW190701_203306	11.9	200	70^{+20}_{-10}	60^{+10}_{-20}	2200^{+800}_{-700}	54^{+12}_{-8}	41^{+8}_{-11}	$0.4^{+0.1}_{-0.1}$	40	0.003	9(6000)	0-0(17- 0)
GW190706_222641	12.7	2×10^4	110^{+20}_{-20}	70^{+20}_{-30}	5000^{+3000}_{-2000}	60^{+20}_{-20}	40^{+10}_{-10}	$0.8^{+0.3}_{-0.3}$	600	0.3	0(10)	0-0(0-0)
GW190707_093326	13.2	1×10^5	13^{+4}_{-2}	10^{+1}_{-2}	800^{+400}_{-400}	12^{+3}_{-2}	8^{+1}_{-2}	$0.17^{+0.06}_{-0.07}$	1000	0.02	$6000(2\times10^5)$	20-0(86-26)
GW190708_232457	13.1	3000	21^{+6}_{-2}	15^{+2}_{-3}	900^{+300}_{-400}	17^{+5}_{-2}	13^{+2}_{-3}	$0.18^{+0.06}_{-0.07}$	1×10^4	0.2	$1\times10^5(4\times10^6)$	10-0(79-24)
GW190720_000836	11.6	1×10^5	16^{+7}_{-3}	9^{+3}_{-3}	800^{+700}_{-300}	13^{+7}_{-3}	8^{+2}_{-2}	$0.17^{+0.12}_{-0.06}$	500	0.02	$5000(2\times10^5)$	12-0(81-11)
GW190727_060333	12.1	1×10^5	59^{+13}_{-8}	46^{+8}_{-13}	4000^{+2000}_{-1000}	37^{+9}_{-6}	29^{+7}_{-8}	$0.6^{+0.2}_{-0.2}$	700	0.2	0(5000)	0-0(2-0)
GW190728_064510	13.4	1×10^5	14^{+8}_{-2}	9^{+2}_{-3}	900^{+200}_{-400}	12^{+7}_{-2}	8^{+2}_{-3}	$0.18^{+0.04}_{-0.07}$	400	0.004	$2000(1\times10^5)$	10-0(79-30)
GW190814	22.2	1×10^5	24^{+1}_{-1}	$2.72^{+0.08}_{-0.09}$	240^{+40}_{-50}	23^{+1}_{-1}	$2.59^{+0.08}_{-0.09}$	$0.053^{+0.009}_{-0.010}$	20	9×10^{-7}	90(200)	76-57(100-100)
GW190828_063405	16.6	1×10^5	44^{+7}_{-5}	36^{+5}_{-6}	2200^{+600}_{-900}	32^{+4}_{-4}	26^{+4}_{-5}	$0.40^{+0.09}_{-0.15}$	500	0.03	$30(6\times10^4)$	0-0(19-0)
GW190828_065509	11.1	3×10^4	31^{+9}_{-9}	13^{+5}_{-3}	1700^{+600}_{-600}	24^{+7}_{-7}	10^{+4}_{-2}	$0.31^{+0.10}_{-0.10}$	600	0.03	$100(5\times10^4)$	0-0(32-1)
GW190910_112807	13.4	300	57^{+9}_{-6}	46^{+7}_{-9}	1600^{+1100}_{-700}	43^{+8}_{-6}	35^{+6}_{-7}	$0.3^{+0.2}_{-0.1}$	9000	0.9	$6000(1\times10^6)$	0-0(41-0)
GW190915_235702	13.1	1×10^5	46^{+12}_{-8}	32^{+7}_{-6}	1700^{+700}_{-700}	35^{+9}_{-6}	24^{+5}_{-6}	$0.3^{+0.1}_{-0.1}$	300	0.02	$700(1\times10^5)$	0-0(35-1)
GW190924_021846	13.0	1×10^5	10^{+8}_{-2}	6^{+1}_{-2}	600^{+200}_{-200}	9^{+7}_{-2}	5^{+1}_{-2}	$0.12^{+0.04}_{-0.04}$	400	0.002	$5000(6\times10^4)$	34-1(93-55)
GW190929_012149	10.3	6	100^{+30}_{-20}	40^{+30}_{-20}	4000^{+3000}_{-2000}	60^{+20}_{-10}	26^{+14}_{-10}	$0.6^{+0.4}_{-0.2}$	2000	1	$0(1\times10^4)$	0-0(2-0)
GW190930_133541	10.1	80	14^{+14}_{-2}	9^{+2}_{-4}	800^{+400}_{-300}	12^{+12}_{-2}	8^{+2}_{-3}	$0.16^{+0.07}_{-0.06}$	2000	0.02	$7000(2\times10^5)$	18-0(85-31)
GW191105_143521	10.7	80	13^{+5}_{-2}	9^{+2}_{-2}	1200^{+400}_{-500}	11^{+4}_{-2}	7^{+1}_{-2}	$0.23^{+0.07}_{-0.08}$	800	0.02	$3000(3\times10^5)$	1-0(61-10)

Table 1
(Continued)

Name	S/N	IFAR [yr]	$m_1^{\rm det}$ [$M_\odot$]	$m_2^{\rm det}$ [$M_\odot$]	$D_{\rm L}$ [Mpc]	m_1 [$M_\odot$]	m_2 [$M_\odot$]	z	$\Delta\Omega$ [deg^2]	ΔV_c [Gpc^3]	$N_{\rm gal}$	$p(G\vert z, H_0)$
GW191109_010717	15.8	6000	80^{+10}_{-8}	60^{+20}_{-20}	1300^{+1400}_{-700}	60^{+10}_{-10}	50^{+20}_{-10}	$0.3^{+0.2}_{-0.1}$	1000	0.3	$5000(5\times10^5)$	3-0(66-0)
GW191127_050227	10.3	4	100^{+60}_{-30}	40^{+30}_{-30}	5000^{+3000}_{-3000}	50^{+40}_{-10}	20^{+20}_{-10}	$0.7^{+0.4}_{-0.4}$	1000	1	2(10000)	0-0(3-0)
GW191129_134029	13.3	1×10^5	13^{+5}_{-3}	8^{+2}_{-2}	800^{+200}_{-300}	11^{+4}_{-2}	7^{+2}_{-2}	$0.16^{+0.04}_{-0.06}$	800	0.006	$9000(2\times10^5)$	13-0(82-35)
GW191204_171526	17.1	1×10^5	14^{+4}_{-2}	9^{+2}_{-2}	600^{+200}_{-200}	12^{+3}_{-2}	8^{+2}_{-2}	$0.13^{+0.03}_{-0.04}$	300	0.001	$3000(5\times10^4)$	21-0(87-52)
GW191215_223052	10.9	1×10^5	33^{+9}_{-5}	25^{+4}_{-5}	2100^{+900}_{-900}	24^{+7}_{-4}	18^{+4}_{-4}	$0.4^{+0.1}_{-0.2}$	600	0.07	$100(8\times10^4)$	0-0(28-0)
GW191216_213338	18.6	1×10^5	14^{+4}_{-3}	8^{+2}_{-2}	300^{+100}_{-100}	13^{+4}_{-3}	7^{+2}_{-2}	$0.07^{+0.02}_{-0.03}$	500	4×10^{-4}	$4000(3\times10^4)$	67-19(100-86)
GW191222_033537	12.0	1×10^5	70^{+10}_{-10}	50^{+10}_{-20}	3000^{+2000}_{-2000}	44^{+11}_{-8}	33^{+9}_{-10}	$0.6^{+0.2}_{-0.3}$	2000	0.7	$20(8\times10^4)$	0-0(9-0)
GW191230_180458	10.3	20	80^{+20}_{-10}	60^{+10}_{-20}	5000^{+2000}_{-2000}	48^{+13}_{-9}	36^{+10}_{-10}	$0.8^{+0.2}_{-0.3}$	800	0.2	0(40)	0-0(0-0)
GW200105_162426	13.9	5	9^{+3}_{-2}	$2.1^{+0.5}_{-0.4}$	300^{+100}_{-100}	9^{+3}_{-2}	$1.9^{+0.4}_{-0.4}$	$0.06^{+0.02}_{-0.03}$	7000	0.007	$8\times10^4(3\times10^5)$	80-26(100-90)
GW200112_155838	17.6	1×10^5	45^{+6}_{-6}	34^{+6}_{-7}	1300^{+400}_{-500}	36^{+5}_{-5}	27^{+5}_{-6}	$0.25^{+0.07}_{-0.08}$	4000	0.09	$8000(1\times10^6)$	0-0(51-7)
GW200115_042309	11.5	1×10^5	7^{+2}_{-2}	$1.4^{+0.4}_{-0.2}$	300^{+200}_{-100}	7^{+2}_{-2}	$1.3^{+0.4}_{-0.2}$	$0.06^{+0.03}_{-0.03}$	700	0.001	$7000(2\times10^4)$	77-17(100-85)
GW200128_022011	10.1	200	65^{+14}_{-9}	50^{+10}_{-13}	4000^{+2000}_{-2000}	40^{+11}_{-7}	31^{+9}_{-8}	$0.6^{+0.3}_{-0.3}$	2000	1	$7(3\times10^4)$	0-0(4-0)
GW200129_065458	26.5	1×10^5	44^{+10}_{-6}	31^{+6}_{-9}	1000^{+200}_{-300}	37^{+9}_{-5}	26^{+5}_{-7}	$0.19^{+0.04}_{-0.06}$	80	5×10^{-4}	$400(2\times10^4)$	5-0(70-27)
GW200202_154313	11.3	1×10^5	11^{+4}_{-2}	8^{+1}_{-2}	400^{+100}_{-200}	10^{+4}_{-2}	7^{+1}_{-2}	$0.09^{+0.03}_{-0.03}$	200	3×10^{-4}	$2000(1\times10^4)$	57-8(69-17)
GW200208_130117	10.8	3000	53^{+12}_{-8}	39^{+9}_{-11}	2400^{+1000}_{-900}	37^{+9}_{-6}	27^{+6}_{-7}	$0.4^{+0.1}_{-0.1}$	40	0.004	0(2000)	0-0(11-0)
GW200209_085452	10.0	20	56^{+14}_{-10}	40^{+10}_{-10}	4000^{+2000}_{-2000}	34^{+9}_{-6}	26^{+7}_{-7}	$0.6^{+0.3}_{-0.3}$	900	0.4	4(7000)	0-0(3-0)
GW200219_094415	10.8	1000	59^{+13}_{-9}	44^{+9}_{-13}	4000^{+2000}_{-2000}	36^{+10}_{-6}	27^{+7}_{-7}	$0.6^{+0.2}_{-0.2}$	700	0.2	7(3000)	0-0(2-0)
GW200224_222234	19.2	1×10^5	53^{+9}_{-6}	42^{+6}_{-10}	1800^{+500}_{-700}	40^{+7}_{-5}	32^{+5}_{-7}	$0.33^{+0.07}_{-0.11}$	50	0.002	$30(1\times10^4)$	0-0(32-1)
GW200225_060421	13.1	9×10^4	24^{+5}_{-3}	17^{+3}_{-3}	1200^{+500}_{-500}	19^{+5}_{-3}	14^{+3}_{-3}	$0.23^{+0.08}_{-0.09}$	500	0.01	$2000(2\times10^5)$	3-0(68-9)
GW200302_015811	10.6	9	49^{+9}_{-7}	25^{+12}_{-7}	1600^{+1000}_{-700}	38^{+8}_{-5}	19^{+8}_{-5}	$0.3^{+0.2}_{-0.1}$	7000	0.8	$7000(1\times10^6)$	0-0(50-0)
GW200311_115853	17.6	1×10^5	42^{+9}_{-5}	33^{+5}_{-8}	1200^{+300}_{-400}	34^{+7}_{-6}	27^{+4}_{-4}	$0.23^{+0.05}_{-0.07}$	40	3×10^{-4}	$90(1\times10^4)$	0-0(56-16)
GW200316_215756	10.1	1×10^5	17^{+14}_{-4}	9^{+3}_{-3}	1100^{+400}_{-400}	14^{+11}_{-4}	7^{+2}_{-3}	$0.22^{+0.07}_{-0.08}$	200	0.005	$500(2\times10^4)$	2-0(59-8)

Note. First, second, and third columns: GW event label, detected S/N (highest among the different pipelines; see Abbott et al. 2021e), and inverse false-alarm rate. Fourth, fifth, sixth columns: estimated primary and secondary detector frame masses and luminosity distance. Seventh, eighth, and ninth columns: primary and secondary source frame masses and redshift assuming a reference cosmology. Tenth and eleventh columns: sky localization area and 3D localization comoving volume. The twelfth column lists the number of galaxies in GLADE+ inside the localization volume for each event with observed K band (B_J band in parenthesis), while the thirteenth column reports the probability $p(G\vert z, H_0)$ that GLADE+ detected the GW event host galaxy using the K-band (B_J in parenthesis) luminosity function calculated for a fiducial flat ΛCDM cosmology with $H_0 = 67.9$ km s^{-1} Mpc^{-1} and $\Omega_{\rm m} = 0.3065$. The lower and upper bounds on these probabilities are derived from the completeness fractions at the boundaries of the 90% localization volume. We report these values using a distance prior proportional to D_L^2 and a uniform in the detector frame masses prior. The events in bold are the ones with S/N > 11 entering all the analyses, while the others are the ones used only for the systematic studies in Appendix B. For events released with GWTC–3, we use the first data release associated with LIGO Scientific Collaboration et al. (2021).

photometrically using an artificial neural network algorithm (Collister & Lahav 2004) with a relative error $\sigma_{z_{ph}} \sim 0.033(1 + z_{ph})$ (Bilicki et al. 2016). The peculiar velocity corrections are implemented for galaxies up to redshifts $z < 0.05$ using a Bayesian technique (Mukherjee et al. 2021c) that can capture both linear and nonlinear components of the velocity field.

For our main results, we use all galaxies with measured K_s-band (denoted as K band henceforth) luminosity reported in the Vega system, and we assign a probability for each galaxy to be the host of a GW event that is proportional to this luminosity (*luminosity weighting*). We also explore possible systematics in our results by not using luminosity weighting and by using B_J-band observations; see Section 5.2 for more details. We choose these two bands as we have found that there is a good match between the galaxy luminosity functions and the galaxy number density of the GLADE+ catalog, in particular for the K band; see Appendix C for more details. The K-band galaxies in the GLADE+ catalog are the same as the ones in the GLADE catalog. The galaxies in the B_J band are present only in the GLADE+ catalog.

Figure 2 presents a series of sky maps showing the directional dependence of the K-band apparent magnitude threshold for the GLADE+ galaxies, in superposition with the sky localizations of the GW events included in our analysis. Outside of the galactic plane, $m_{thr} \sim 13.5$ on average for the K band, while within the galactic plane region the apparent magnitude threshold is significantly lower (i.e., brighter).

We assume that the K-band absolute magnitude distribution for GLADE+ galaxies is well described by a Schechter function with parameters (reported for $H_0 = 100$ km s^{-1} Mpc^{-1}) $M_{*,K} = -23.39$ and $\alpha_K = -1.09$ (Kochanek et al. 2001), while for the B_J band we use $M_{*,B_J} = -19.66$ and $\alpha_{B_J} = -1.21$ (Norberg et al. 2002). We set a bright cutoff high enough to include all the bright galaxies supported by the Schechter function: $M_{min,K} = -27.00$ and $M_{min,B_J} = -22.00$. Further, we consider all the galaxies no fainter than $M_{max,K} = -19.0$, $M_{max,B_J} = -16.5$. These choices correspond to all galaxies with luminosity $L > 0.017 L_{*,K}$ and $L > 0.054 L_{*,B_J}$, where L_* is the characteristic galaxy luminosity of the Schechter luminosity function. To calculate the rest-frame absolute magnitudes of the galaxies, for a given cosmology, we apply color and evolution corrections as reported in Kochanek et al. (2001) for the K band and Norberg et al. (2002) for the B_J band.

For all events, apart from GW190814, we carry out the analysis using a pixel size of 3.35 deg^2, while for GW190814 we use a pixel size of 0.2 deg^2 as the sky localization for this event was 10 times smaller than most of the others. These values have been chosen taking into account the average number of galaxies per square degree reported in GLADE+. Considering the bright and faint limits of the Schechter function assumed with a median apparent magnitude threshold $m_{thr,K} = 13.5$ for the K band and $m_{thr,B_J} = 19.7$ for the B_J band, we find that there are ~ 25 galaxies per square degree in GLADE+ reported in the K band and 500 galaxies per square degree reported in the B_J band considered in the analysis. Note that the actual galaxy density per square degree is higher outside the galactic plane and in the region of GW190814.

For any given redshift, the *completeness fraction*, which is the probability that the galaxy catalog contains the host galaxy of the GW event, $P(G|z, H_0)$, is defined as the fraction of galaxies with absolute magnitudes brighter than the absolute magnitude threshold (calculated from m_{thr}), namely,

$$P(G|z, H_0) = \frac{\int_{L_{thr}(m_{thr}, z, H_0)}^{L_{max}} \phi(L) L dL}{\int_{L_{min}}^{L_{max}} \phi(L) L dL}. \tag{7}$$

Here $\phi(L)$ is the assumed galaxy luminosity function, L_{min} and L_{max} are the minimum and maximum luminosity corresponding to M_{max} and M_{min}, and L_{thr} is the threshold luminosity for detection, calculated from m_{thr}.

Figure 3 shows the completeness fraction of the GLADE+ catalog, in the K band and B_J band, respectively, as a function of the redshift and for different values of m_{thr}, assuming a fiducial cosmology with $H_0 = 67.9$ km s^{-1} Mpc^{-1} and $\Omega_m = 0.3065$ (Ade et al. 2016). As can be seen from the figure, the GLADE+ catalog is less complete in the K band than in the B_J band, but we decide to use the K-band data for our main results as they are better described by the Schechter function assumed in our analysis; see Appendix C.

For GLADE+, the systematic uncertainties of the photometric redshift reconstruction are inside the statistical errors associated to each galaxy (Bilicki et al. 2014) with a very small percentage of outliers. We do not consider deeper galaxy surveys with a restricted sky area footprint, such as the DES Y1 survey (Drlica-Wagner et al. 2018) or DESI Legacy Imaging Survey (Zou et al. 2019) that are supposed to be complete up to redshift $z \sim 1$, as we decide to employ the same all-sky galaxy catalog for all of our events. Moreover, color corrections and photometric redshift reconstruction might need particular attention with deeper galaxy surveys.

4. Results

The first analysis that we present in Section 4.1 will focus on the impact of the BBH population source masses on inference of the cosmological parameters, using the formalism discussed in Section 2.1. This analysis uses no galaxy catalog information; instead constraints on the cosmological parameters will be inferred from the mass scale set by the source mass distribution. We use only the BBHs detections as they are the majority of the sources entering in our cosmological analysis and because a joint description of NSBH, BNS, and BBHs is uncertain.

The second analysis in Section 4.2 fixes the source mass distribution and uses redshift information derived from galaxy catalogs, based on the formalism discussed in Section 2.2. Unless stated otherwise, all the figures are generated with a uniform prior on H_0, credible intervals are reported as maximum posterior and 68.3% highest density intervals. We use a flat-in-log prior on H_0 only when quoting results combined with GW170817 and its EM counterpart.

4.1. Implications of Population Assumptions for Cosmology

We jointly estimate population-related GW parameters and cosmological parameters using BBH events, as these are the majority of the GW events observed to date. We use the 42 BBH detected events with S/N > 11. We exclude from this analysis GW190814 (Abbott et al. 2021b) given the current uncertainty on the nature of the secondary object in this system.

We consider two cosmological models: *(i)* a flat w_0CDM model with *wide priors* on the Hubble constant H_0, matter density Ω_m and dark energy EoS w_0 parameter, and *(ii)* a flat
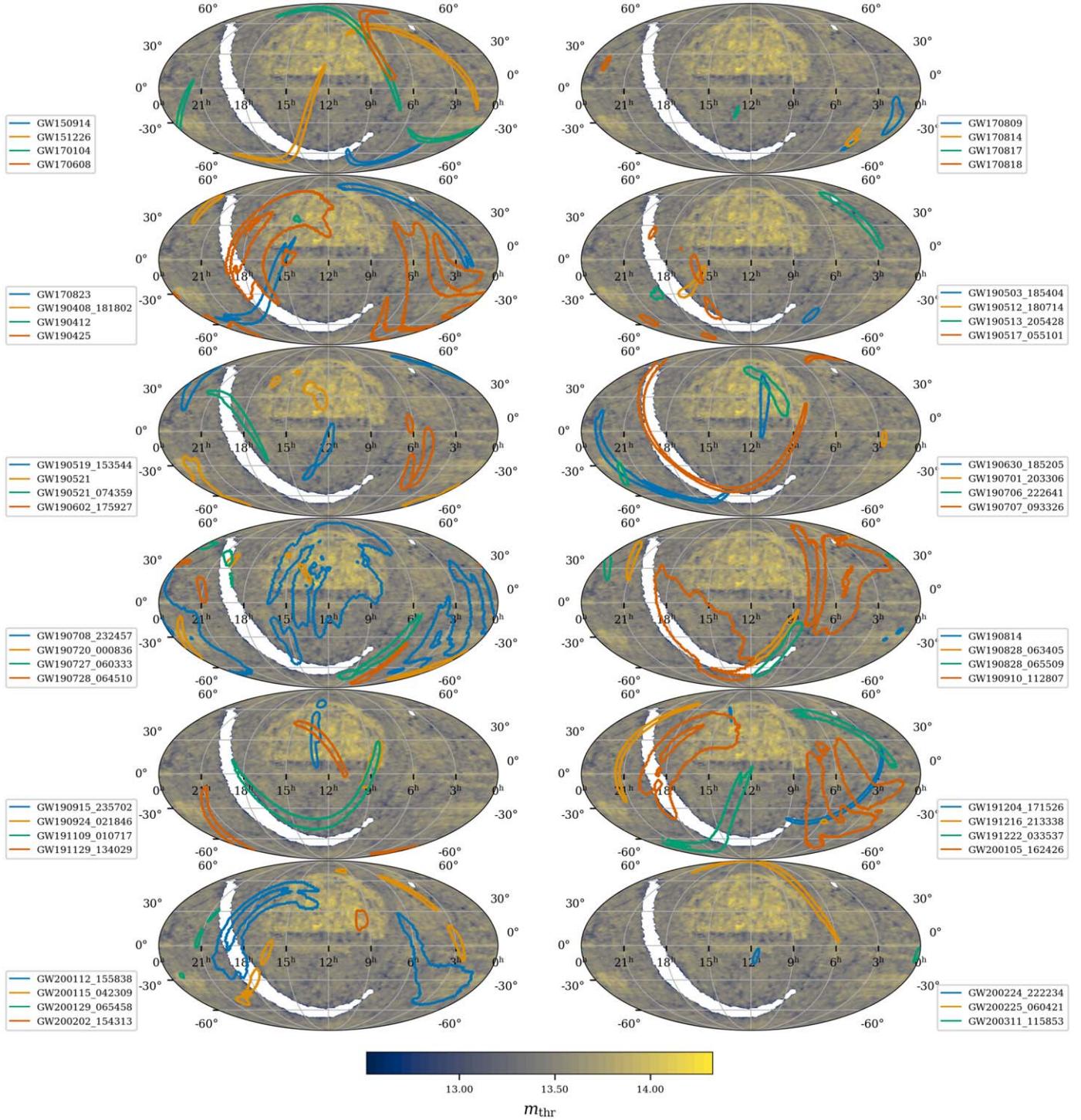
Figure 2. Sky maps showing the GLADE+ K-band apparent magnitude threshold, m_{thr}, generated by dividing the sky into 3.35 deg² pixels; this is the resolution used for all the events but GW190814. A mask is applied that removes from the figures all pixels with $m_{thr} < 12.5$ in order to improve the figure readability. Also shown are the 90% CL sky localizations for the GW events considered in this paper.

ΛCDM universe with a fixed value of $\Omega_m = 0.3065$ (Ade et al. 2016) and dark energy EoS parameter $w_0 = -1$ and with a *restricted prior* in the H_0-tension region ($H_0 \in [65, 77]$ km s⁻¹ Mpc⁻¹). We refer to model *(i)* as the w_0CDM model and to model *(ii)* as the H_0-tension model. We also adopt wide priors on the hyperparameters of the GW source mass distribution and its merger rate evolution as described in Appendix A. For all the phenomenological mass models assumed we obtain posteriors on the source mass distribution

and merger rate parameters, which are compatible with previous population studies (Abbott et al. 2021b, 2021f) and the latest studies with O3b data (Abbott et al. 2021e). See Appendix B for more details.

As evident from values of Bayes factor reported in Table 2, we do not find any preference of the data in supporting any one of the cosmological models (w_0CDM model or the H_0-tension model) considered in the analysis. As we will see later, this is because the posteriors on Ω_m and w_0 are not constrained by the

K-band

B_J-band
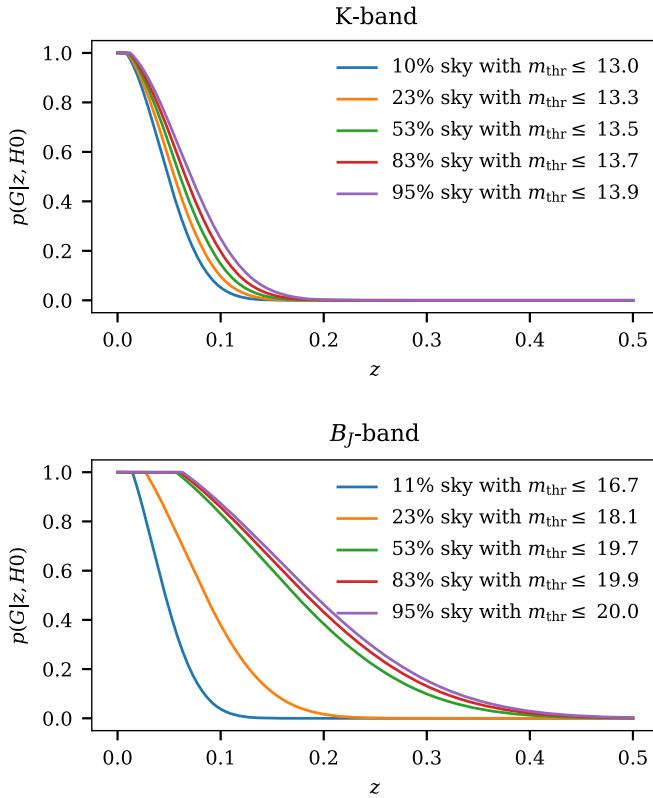
Figure 3. Top: completeness fraction of GLADE+ in the K band, indicating the probability that the catalog contains the host galaxy of a GW event, as a function of the redshift for $H_0 = 67.9$ km s^{-1} Mpc^{-1} and $\Omega_m = 0.3065$. The different lines are calculated for a given K-band apparent magnitude m_{thr} threshold indicated in the legend. The legend also indicates the fraction of the sky, computed by dividing the sky in equally sized pixels of 3.35 deg^2, for which the apparent magnitude threshold is brighter than the one reported in the legend. The fraction of pixels with no galaxies is $\sim 5\%$ for the B_j and K bands. Bottom: same as the top panel but for the B_J band.

Table 2
Logarithm of the Bayes Factor Comparing Runs That Adopt the Same Source Mass Model but Different Cosmologies: Wide Priors (For a General w_0CDM Cosmology) vs. Restricted Priors (in the H_0-tension Region)

Mass model	$\log_{10} \mathcal{B}$
TRUNCATED	0.2
POWER LAW + PEAK	-0.3
BROKEN POWER LAW	-0.4

GW observations, and the error on the H_0 estimation extends beyond the H_0-tension region.

In Table 3 we report the Bayes factors computed between different mass models, for the case of wide priors on the w_0CDM cosmological parameters. Consistent with Abbott et al. (2021b, 2021f), we find that, even if we allow the cosmological parameters to vary with wide priors, the TRUNCATED model is still strongly disfavored with respect to the POWER LAW + PEAK and BROKEN POWER LAW models by a factor ~ 100. This result is consistent with the fact that, as indicated in Figure 1, the source mass distribution contains more structure than a simple TRUNCATED model. As motivated in Abbott et al. (2021b), this comparatively poor fit for the TRUNCATED model is due to the inability of this model to capture a moderate fraction of detected events with high masses, while predicting a large fraction of detected events with lower masses. Using the reduced set of signals with S/N > 11, we do not find any

Table 3
Logarithm of the Bayes Factor Between the Different Mass Models and the POWER LAW + PEAK Model Preferred by the Data, for the Case of a w_0CDM Cosmology with Wide Priors

Mass model	$\log_{10} \mathcal{B}$
TRUNCATED	-1.9
POWER LAW + PEAK	0.0
BROKEN POWER LAW	-0.5

compelling evidence to prefer the POWER LAW + PEAK model over the BROKEN POWER LAW model.

The marginal posterior distributions that we obtain for the cosmological parameters H_0, Ω_m, and w_0 are shown in Figure 4 for each phenomenological mass model. As anticipated by our Bayes factor results, we find that with the current BBH GW events we cannot constrain the values of these three cosmological parameters, as we obtain broad and uninformative posteriors.

With the POWER LAW + PEAK we estimate $H_0 = 50^{+37}_{-30}$ km s^{-1} Mpc^{-1}, while for the BROKEN POWER LAW model we estimate $H_0 = 44^{+52}_{-24}$ km s^{-1} Mpc^{-1}. These constraints on H_0, as we will see later, arise from the ability of these models to fit an excess of BBHs with masses around $35 M_\odot$, which sets a scale for the redshift distribution of BBHs.

We discuss this effect further using the POWER LAW + PEAK model. Figure 5 shows the joint posterior distribution between the cosmological parameters and the parameters μ_g and m_{max} defined in Equation (A11), which govern the position of the BBH Gaussian excess and the upper end of the source primary mass distribution, respectively.

The presence of a peak in the BBH source mass distribution allows us to set a characteristic source mass scale, which informs $H(z)$ and allows us to exclude higher values of H_0. Marginalizing over the cosmological parameters, we obtain a central value of $\mu_g = 32^{+6}_{-8} M_\odot$ for the peak position of the Gaussian BBH excess.

We also find that the estimation of population parameters related to the mass and merger rates of BBHs is not strongly dependent on the choice of cosmological priors between the w_0CDM model and the H_0-tension model. The only parameter showing a nonnegligible impact is μ_g, which is more precisely measured when using the H_0-tension prior, with a posterior standard deviation that is 65% of the value when using the w_0CDM model. This is due to the degeneracy observable between μ_g and H_0 in Figure 5.

On the other hand, the disfavored TRUNCATED model shows support at higher H_0. This result is due to the fact that the TRUNCATED model is not able to adequately fit the presence of massive binaries while producing an excess of BBHs with masses $\sim 40 M_\odot$ in the detector frame. For this reason, higher H_0 values are more supported as those values place events at higher redshifts, thus reducing their source masses.

When we combine the H_0 posteriors from the three mass models with the H_0 inferred from the bright standard siren GW170817 (see Figure 6), we find a value of $H_0 = 68^{+12}_{-8}$ km s^{-1} Mpc^{-1} for the POWER LAW + PEAK model and $H_0 = 68^{+13}_{-8}$ km s^{-1} Mpc^{-1} for the BROKEN POWER LAW model. These results represent an improvement of 17% and 12%, respectively, compared with the H_0 value reported in Abbott et al. (2021a) that made use of GW170817 and six BBH detections from O2, with redshift information
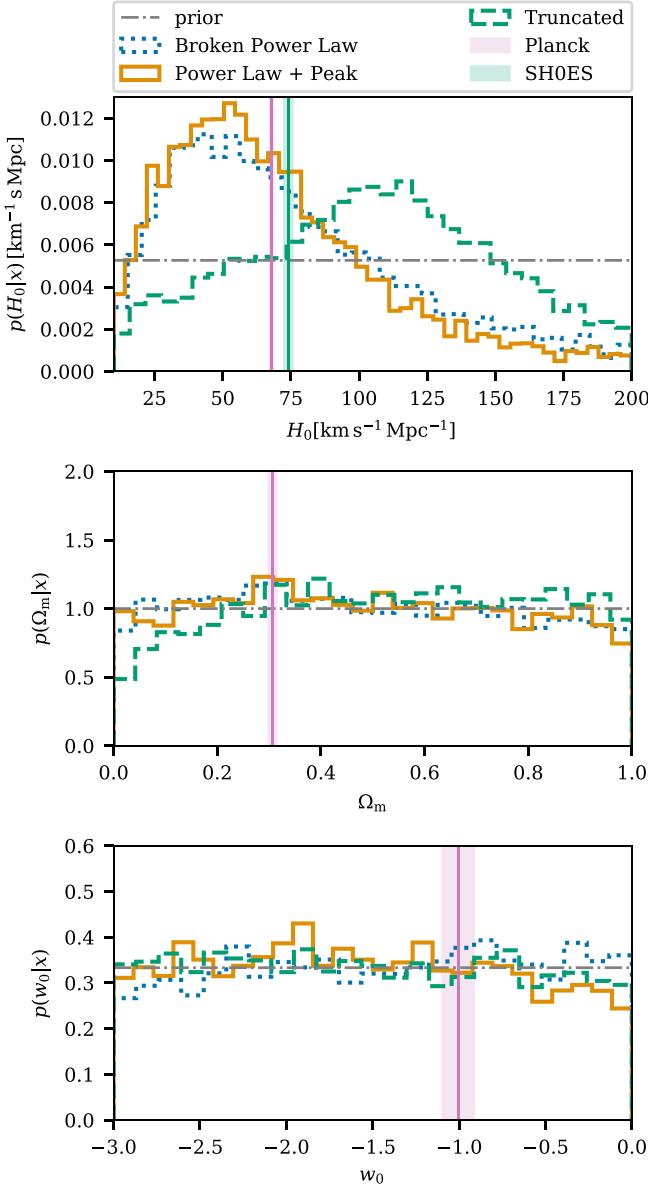
Figure 4. Top panel: marginal posterior distribution for H_0. Middle panel: marginal posterior distribution for Ω_m. Bottom panel: marginal posterior distribution for w_0. In each panel the different lines indicate the three phenomenological mass models. The solid orange line identifies the preferred POWER LAW + PEAK model. The pink shaded areas identify the 68% CI of the cosmological parameters inferred from measurements from the CMB (Ade et al. 2016; apart for w_0 that is reported at 95% CI), and the green shaded area in the top panel shows the value of the Hubble constant measured in the local universe (Riess et al. 2019).

inferred from galaxy catalogs. For the TRUNCATED model, we obtain $H_0 = 69^{+21}_{-8}$ km s^{-1} Mpc^{-1}. These results are obtained assuming a redshift-independent mass distribution. Considering a redshift dependence of the mass distribution can degrade the constraints.

4.2. Results Using Galaxy Catalog Information

We now discuss constraints on H_0 when we fix the source population model but employ galaxy surveys to infer statistical redshift information using the pixelated gwcosmo code (Gray et al. 2020). Our analysis incorporates 47 GW events,

comprising 42 BBH detections, GW190814, the 2 BNS events GW170817 and GW190425, and the 2 NSBH events GW200105 and GW200115. We include all galaxies of the GLADE+ catalog that lie inside the 99.9% estimated sky area of each event. We use the GLADE+ K-band data in this analysis, adopting luminosity weights for each galaxy. For a more in-depth discussion about the impact of our BH population assumptions and choice of photometric bands, see Section 5.2.

To describe the distribution of BH primary masses, we use a POWER LAW + PEAK source mass model where we fix the population parameters to the median values obtained in the joint cosmological and population analysis described in Section 4.1. For the rate evolution we adopt $\gamma = 4.59$, $k = 2.86$, and $z_p = 2.47$, while for the POWER LAW + PEAK model we use $\alpha = 3.78$, $\beta = 0.81$, $m_{max} = 112.5\ M_\odot$, $m_{min} = 4.98\ M_\odot$, $\delta_m = 4.8\ M_\odot$ $\mu_g = 32.27\ M_\odot$, $\sigma_g = 3.88\ M_\odot$, and $\lambda_g = 0.03$. For the NS source mass model we consider a uniform distribution between $m_{min}\ 1 M_\odot$ and $m_{max} = 3 M_\odot$, consistent with (Abbott et al. 2021f). We evaluate the GW selection effects using LIGO and Virgo sensitivities during the O1, O2, and O3 runs.

In Figure 7 we show the posteriors for all of the GW events considered in this analysis for the K band. For many of the O3 events, the H_0 inference is dominated by the likelihood based on the hypothesis that the host galaxy is *not* in the catalog (referred to as out-of-catalog). The out-of-catalog term dominates for sources that are localized at redshifts at which the GLADE+ galaxy catalog has a low completeness fraction (see Figure 3). This is the case for most of the GW sources that are BBHs observed at large luminosity distances. Another interesting trend observed in Figure 7 is that, for lower values of H_0, the in-catalog likelihood terms tend to dominate because for low H_0 values the GW events are placed at smaller redshifts where the galaxy catalog is more complete, as shown in Figure 3.

For most of these events, the number of galaxies present in the sky localization volume is large enough that the redshift information is still dominated by population assumptions (Section 5.2). GW190814 is the only event for which there is a sufficiently small number of galaxies in its sky localization area of about 18 deg^2. Its small area makes this event partially more informative on the value of H_0 in comparison to the other GW events. We can see in Figure 7 that, out of all the GW events, the most informative posterior on H_0 (compared to the zero galaxy catalog completeness posterior) is from GW190814, provided that the luminosity weighting scheme is applied. We have verified that the H_0 posterior with the K band and using luminosity weights does not depend on the faint end magnitude limit used for the analysis. For this event, we infer an H_0 constraint of 67^{+46}_{-28} km s^{-1} Mpc^{-1} (MAP and HDI). We quote the maximum a posteriori probability (MAP) and the corresponding highest density interval (HDI) values in the analysis.

Figure 8 shows the redshift distribution of galaxies in the 90% CI sky area of GW190814 (top panel) and the galaxy catalog completeness (bottom panel), compared to the predicted distribution for a prior that is uniform in the comoving volume. We observe that for the K band the H_0 support results from an excess of galaxies, with respect to the uniform in the comoving volume prior, around $z \sim 0.051$. Switching off the luminosity weighting assumption decreases the contribution of this excess of galaxies as the completeness
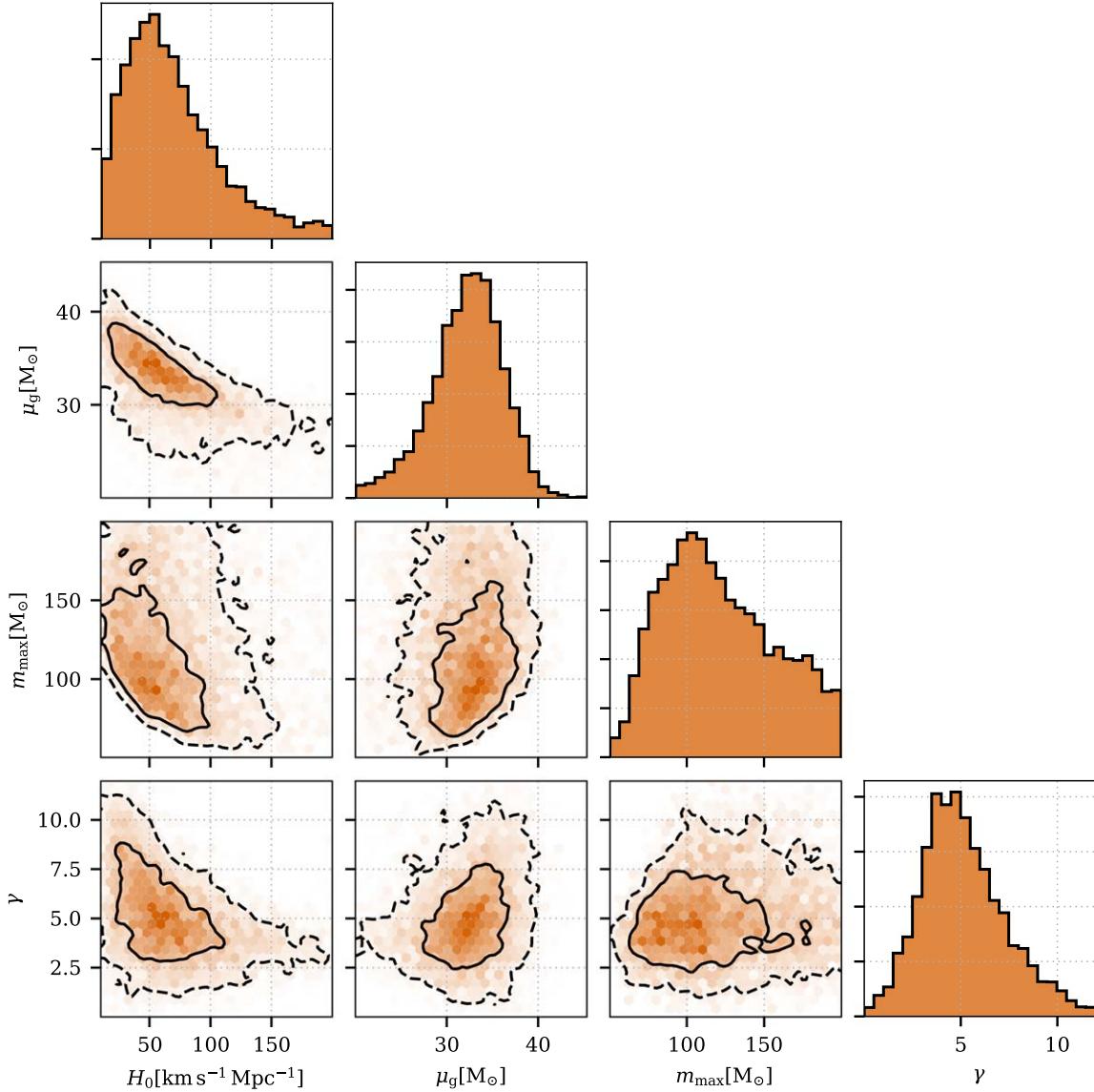
Figure 5. Posterior probability density for H_0 and population parameters μ_g, m_{max} and γ, governing the position of the Gaussian peak, the upper end of the mass distribution, and the merger rate evolution in the POWER LAW + PEAK mass model. The solid and dashed black lines indicate the 50% and 90% CL contours.

is estimated to be lower. The same excess is not visible in the B_J band as more galaxies are reported in this band and some luminous galaxies with measured K-band apparent magnitudes do not have measured apparent magnitudes for the B_J band.

Despite the cases where there is a significant in-catalog contribution, the final H_0 result is nevertheless dominated by the BBHs population assumptions that are contributing to the out-of-catalog likelihood terms (when the galaxy catalog is not complete) and in the in-catalog terms when a large number of galaxies is present in the GW sky localization volume.

In Figure 9 we show the combined H_0 posterior inferred from all of the GW events and for several different scenarios. By using all of the dark sirens, together with K-band galaxy information from GLADE+, we obtain a value of $H_0 = 67^{+13}_{-12}$ km s^{-1} Mpc^{-1}. This value is strongly dominated by the BH population assumptions, as can be seen in Figure 9. The H_0 value obtained from population assumptions alone (empty catalog case in Figure 9) is $H_0 = 67^{+14}_{-13}$ km s^{-1} Mpc^{-1}. When we combine the galaxy catalog measurement with the result from the bright standard siren GW170817, we obtain

$H_0 = 68^{+8}_{-6}$ km s^{-1} Mpc^{-1}. This value represents an improvement of 42% with respect to the corresponding result obtained with GWTC–1 (Abbott et al. 2021a), and an improvement of 44% with respect to the result of $H_0 = 69^{+17}_{-8}$ km s^{-1} Mpc^{-1} obtained using only the GW170817 event (Abbott et al. 2021a).

5. Discussion

5.1. Considerations for The BBH-based Population Analysis

We have shown how population assumptions on BBH formation dominate the inference on cosmological parameters and, in particular, we have seen how the presence of an excess of BBHs with primary masses between $30 M_\odot$ and $40 M_\odot$ (Farr et al. 2019) sets a scale for the BBH redshifts, thus allowing for a weak constraint on H_0.

In the BBH-based population analysis without GW170817, the (H_0, Ω_m, w_0) parameters are not constrained. In Figure 10 we portray these constraints on the expansion rate of the universe, $H(z)$. The best constraint that we obtain on the expansion rate of the universe has a value, and uncertainty
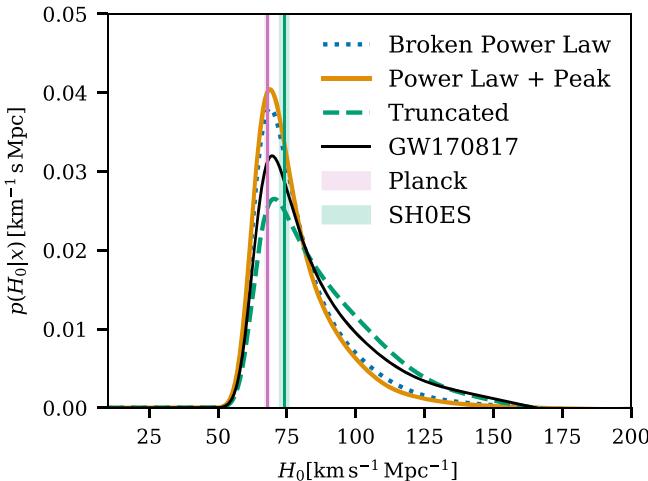
Figure 6. Posterior distributions for H_0 obtained by combining the H_0 posteriors from the 42 BBH detections and the H_0 posterior inferred from the bright standard siren GW170817. The pink and green shaded areas identify the 68% CI constraints on H_0 inferred from the CMB anisotropies (Ade et al. 2016) and in the local universe from SH0ES (Riess et al. 2019), respectively.

(median and symmetric 90% CI), of 74^{+34}_{-13} km s^{-1} Mpc^{-1} at redshift $z = 0$ if we include the bright siren GW170817, and 62^{+87}_{-41} km s^{-1} Mpc^{-1} at redshift $z \sim 0.01$ without it.

5.2. Considerations on The Catalog Analysis

As already discussed in Section 4.2, the H_0 inference is dominated by the population assumptions of the underlying BH mass distribution. In particular, as shown in Figure 5, the population parameter that is most strongly correlated with the value of H_0 is the position of the BHs excess μ_g.

In Figure 11 we show the H_0 posterior computed with different choices of μ_g and fixing the remaining parameters. The values of μ_g are spaced by $\sim 2.5 M_\odot$, which is roughly the uncertainty identified in Section 2.1. It can be seen that the value of μ_g has a strong impact on the inference of H_0. For values of μ_g higher than the median value of $32.55 M_\odot$, the posterior supports low H_0 values as we need GW events to be at a lower redshift to explain the excess of BHs at higher masses. On the other hand, for $\mu_g < 32.55 M_\odot$, the posterior supports higher H_0 value in order to place events at higher redshift compatible with an excess of BHs at lower masses.

We also explored the effect of raising the maximum mass of the black holes to $m_{max} = 150 M_\odot$. As can be seen in Figure 11, raising m_{max} does not have a significant effect on the H_0 posterior as only few events are present at these masses. One more parameter for which we explored the effect of its variation is the γ parameter in the rate evolution model. In the same plot one can see the H_0 posterior for $\gamma = 2.59$. This parameter has a stronger effect on the H_0 posterior, making the posterior less informative and at the same time moving its peak to higher values.

The galaxy catalog brings additional information only for GW190814, due to the much better sky localization (~ 18 deg^2) for this event; this has the effect of providing more support for the H_0-tension region.

In Figure 12, we show how population assumptions impact the hierarchical likelihood calculation as a function of H_0, for the hypotheses that the host galaxy is (or *is not*) *inside* the catalog. Population assumptions strongly impact the out-of-catalog term of the likelihood, which is the dominant

contribution to the H_0 posterior when the event is localized in an area where the galaxy catalog has a low completeness fraction, which happens for most of the GW events that we consider in this analysis. On the other hand, population assumptions are less important for events with a small localization in a region of the galaxy catalog that is complete. In these cases (for example GW190814), the posterior is dominated by the in-catalog likelihood terms and hence exhibits a weak dependence on the population assumptions.

The aforementioned discussion also explains the difference between our results and those found in Finke et al. (2021) using GWTC–2 events. In that work the authors found a weak dependence of their posterior on the source population parameters. However, in their case only a few events, above a given completeness threshold of 70% for the main result, were used to explore systematic effects due to the source population. Moreover, in exploring these systematics they varied the population assumptions only within the range of uncertainties reported in Abbott et al. (2021b), which already assumes a fixed cosmological model with a value of H_0 consistent with the Planck results (Ade et al. 2016). Consequently, the results obtained by them are primarily driven by the Planck cosmological parameters.

Finally, we also explore the systematics introduced by choices related to the galaxy catalog data. In Figure 11 we also show the H_0 posteriors obtained with the GLADE+ catalog, but using K-band galaxies without luminosity weighting and B_J-band galaxies with luminosity weighting. In both cases, the H_0 posterior is not significantly affected by this choice, and it is, again, dominated by the population assumptions.

However, the impact of using luminosity weights is not negligible. For instance, in the case of GW190814 (see Figure 12), removing the extra luminosity weight suppresses the H_0 posterior peak around 70 km s^{-1} Mpc^{-1}. This arises because the luminous galaxies shown in Figure 8, observed in the K band, are now contributing to the GW event redshift localization with the same probability as the other 200+ galaxies included in the GW localization volume. We have verified that the H_0 posterior with the K band and using luminosity weights do not depend on the faint end magnitude limit used for the analysis.

5.3. Additional Systematic Uncertainties

As we have seen, the presence of a known source mass scale can be used to measure cosmological parameters (Farr et al. 2019; Mastrogiovanni et al. 2021). However, if the source mass distribution is mismodeled, then the cosmological inference will be biased. With the current set of events, this effect contributes the dominant source of systematic uncertainty in the measurement of $H(z)$. In the population-based method, a key assumption is that the source mass distribution does not evolve with the redshift (Fishbach et al. 2021); any evolution is degenerate with the cosmological inference. Many BBH formation scenarios predict mild evolution in the mass distribution (Mapelli et al. 2019; Weatherford et al. 2021; Gallegos-Garcia et al. 2021; Mapelli et al. 2022; van Son et al. 2022), but given our broad statistical uncertainties, we expect this evolution to only weakly affect our results, and we do not attempt to calibrate the mass models to theory. In the galaxy-catalog-based method, we fix the source mass distribution. In this case, the choice of the peak location μ_g, associated with excess BHs in the distribution of source masses, is a main
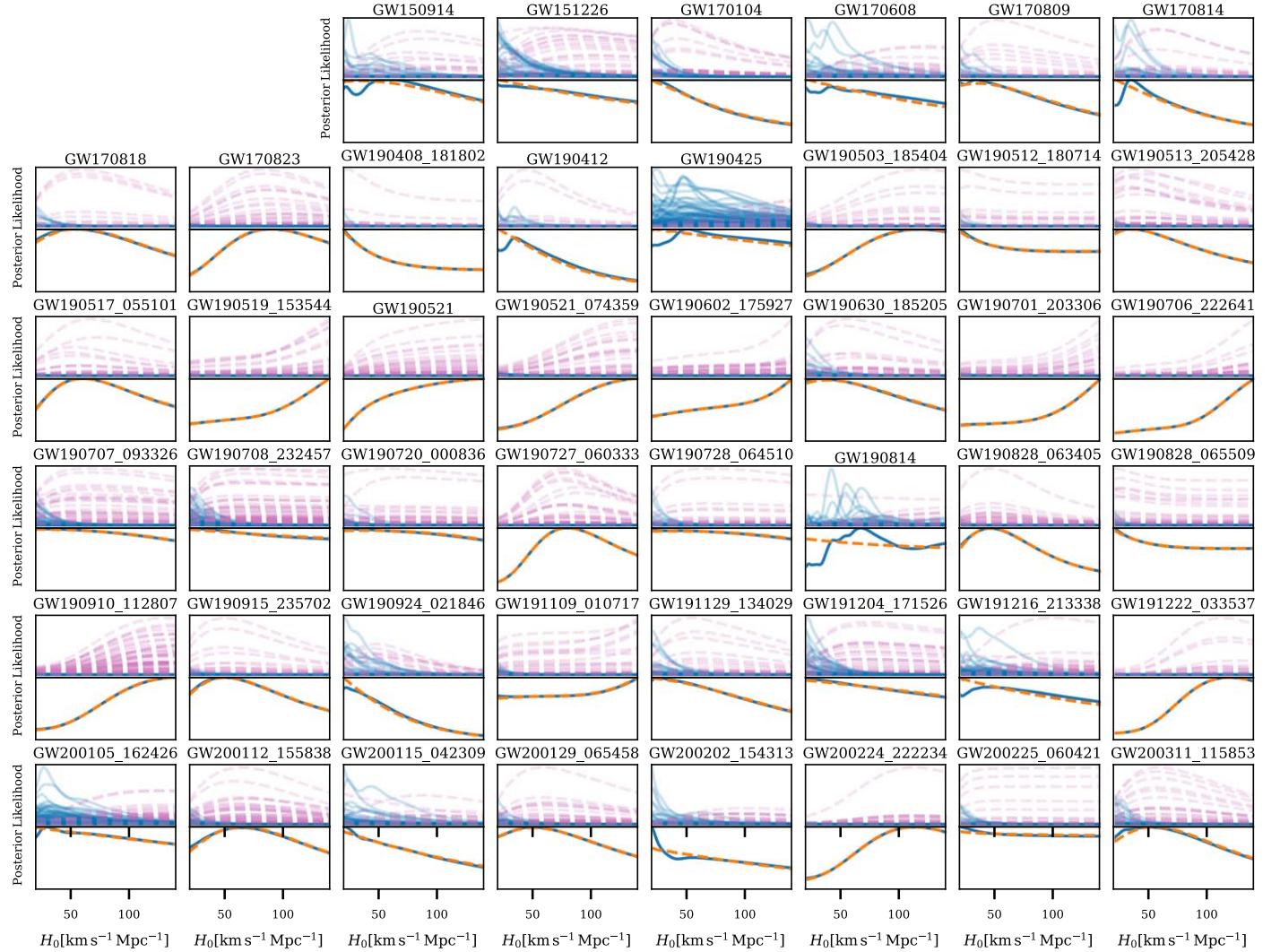
Figure 7. Plots reporting the results on the H_0 inference for each event using the GLADE+ K band and luminosity weighting. Two panels are shown for each event. Top panels: hierarchical likelihood under the hypothesis, G, that the host galaxy is in the catalog (blue solid lines) and under the hypothesis, $\bar{G}$, that the host galaxy is *not* in the catalog (pink dashed lines). The different lines shown in each panel correspond to the different pixels within the sky localization area for each event. Bottom panels: the blue solid line shows the posterior obtained by summing the terms corresponding to the in-catalog and out-of-catalog hypotheses. The orange dashed line shows the posterior obtained by assuming a galaxy catalog with null completeness. In this case the H_0 inference comes entirely from the population assumptions. This plot is intended to show which event is informative on the H_0 value and whether the information is coming from population assumptions or galaxy catalog contribution.

source of systematic uncertainty. If the μ_g parameter is assumed to be lower (or higher) than its true value, this can lead to a higher (or lower) inferred value of H_0. The impact of this bias can be reduced if the support from the in-catalog part of the *statistical galaxy catalog method* is informative, which is mainly possible for sources with better three-dimensional localization error and with a more complete galaxy catalog. In the future, as more GW detectors join the network, resulting in more events with better sky localizations and galaxy catalogs that are more complete at high redshift, the impact of the source population on the galaxy catalog method can be mitigated.

One of the additional sources of contamination, when seeking to infer the true luminosity distance D_L (and hence the true source masses) of a GW source in the absence of an EM counterpart, is the possible lensing of the GW signal due to the intervening matter distribution (Schneider et al. 1992; Bartelmann 2010; Nakamura 1998; Wang et al. 1996; Takahashi & Nakamura 2003; Dai et al. 2017; Broadhurst et al. 2018; Diego 2019). In the geometric optics limit, lensing

modifies the GW signal by a magnification factor μ that only changes the amplitude of the GW strain, leading to a measured luminosity distance given by $\tilde{D}_L = D_L/\mu$. In the strong lensing limit, when the value of μ is large, the inferred luminosity distance to the source $\tilde{d}_L$ may be substantially lower than the true luminosity distance, i.e., introducing a bias in the measurement of the luminosity distance. However, for the GW detections considered here, the probability of observing such a strongly lensed event is less than one percent (Ng et al. 2018a; Oguri 2018; Mukherjee et al. 2021a), even for a broad range of astrophysical time-delay scenarios (Mukherjee et al. 2021b). Moreover, searches from O1+O2 (Hannuksela et al. 2019) and more recent LIGO–Virgo analysis of the O3a data did not reveal any signs of strong lensing (Abbott et al. 2021f). Furthermore, searches for a stochastic GW background also provide a model-independent bound on the lensing event rate of BBHs (Mukherjee et al. 2021a; Buscicchio et al. 2020; Abbott et al. 2021f), which is again consistent with a low probability of contamination due to strong lensing in the GW
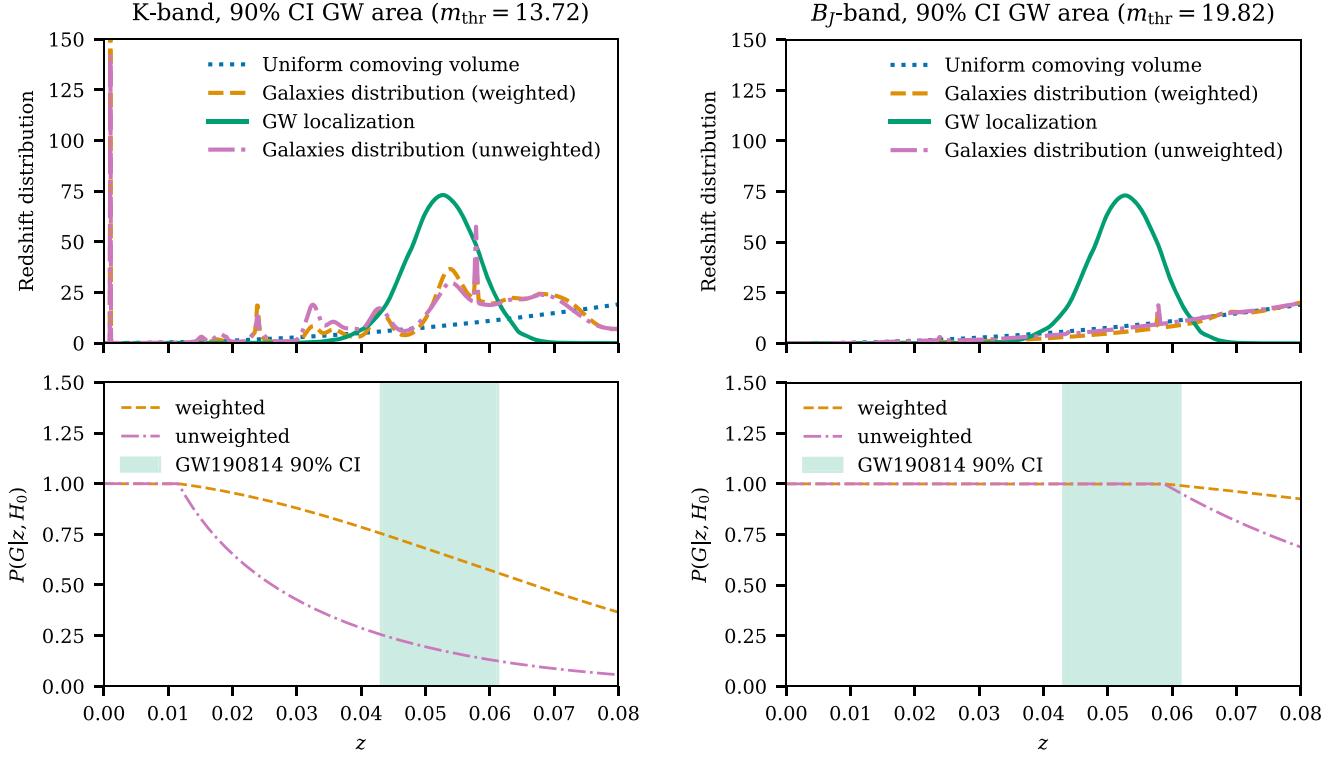
Figure 8. Top panels: distribution of galaxies observed in the GLADE+ K (left panels) and B_J (right panels) bands as a function of the redshift z with and without galaxy luminosity weights, compared with the GW190814 redshift localization in its 90% CI sky area, assuming a cosmology with $H_0 = 67.9$ km s^{-1} Mpc^{-1} and $\Omega_m = 0.3065$ (green line) and the predicted redshift distribution for a prior that is uniform in the comoving volume (blue dashed line). The redshift distribution is not intended as representative of the reconstructed galaxy distribution as it is calculated by stacking each galaxy redshift localization assumed as a normal distribution. This procedure only serves to give a rough idea where the H_0 contribution is coming from. Bottom panels: completeness calculated using the K and B_J band with and without application of the luminosity weighing scheme.
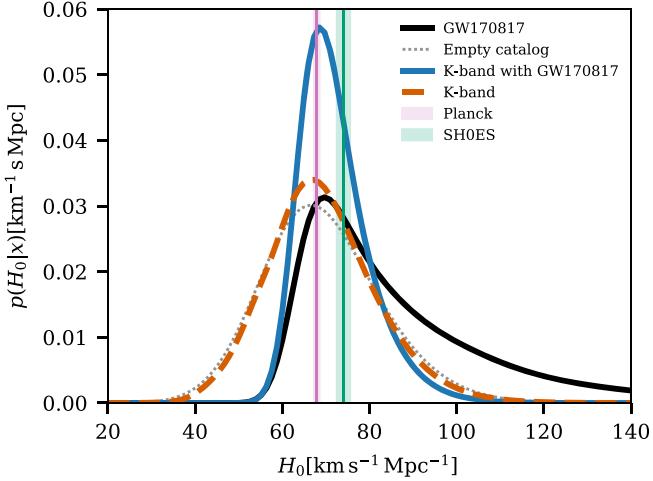
Figure 9. Hubble constant posterior for several cases. Gray dotted line: posterior obtained using all dark standard sirens without any galaxy catalog information and fixing the BBH population model. Orange dashed line: posterior using all dark standard sirens with GLADE+ K-band galaxy catalog information and fixed population assumptions. Black solid line: posterior from GW170817 and its EM counterpart. Blue solid line: posterior combining dark standard sirens and GLADE+ K-band catalog information (orange dashed line) with GW170817 and its EM counterpart (black solid line). The pink and green shaded areas identify the 68% CI constraints on H_0 inferred from the CMB anisotropies (Ade et al. 2016) and in the local universe from SH0ES (Riess et al. 2019), respectively.

Figure 10. Evolution of the Hubble parameter predicted from the most preferred mass model POWER LAW + PEAK (blue lines). The yellow shaded area indicates the 90% CL contours identified by the uniform priors on H_0, Ω_m, and w_0 while the blue shaded area indicates the 90% CL contours from the posterior of the preferred mass model. The dashed lines indicate the median of the prior and posterior for $H(z)$.

sources considered here. In this paper we, therefore, ignore any possible impact of strong lensing on our cosmological parameter estimates.

Apart from strong lensing, weak lensing of GW sources can also be a potential source of contamination. However, due to the effects of sky averaging, weak lensing should not produce a bias in the inferred values of the cosmological parameters, but will introduce additional variance on the luminosity distance of individual sirens at the level of a few percent (Holz & Wald 1998; Hirata et al. 2010) and it is subdominant in comparison to the intrinsic measurement error (of about 20%)
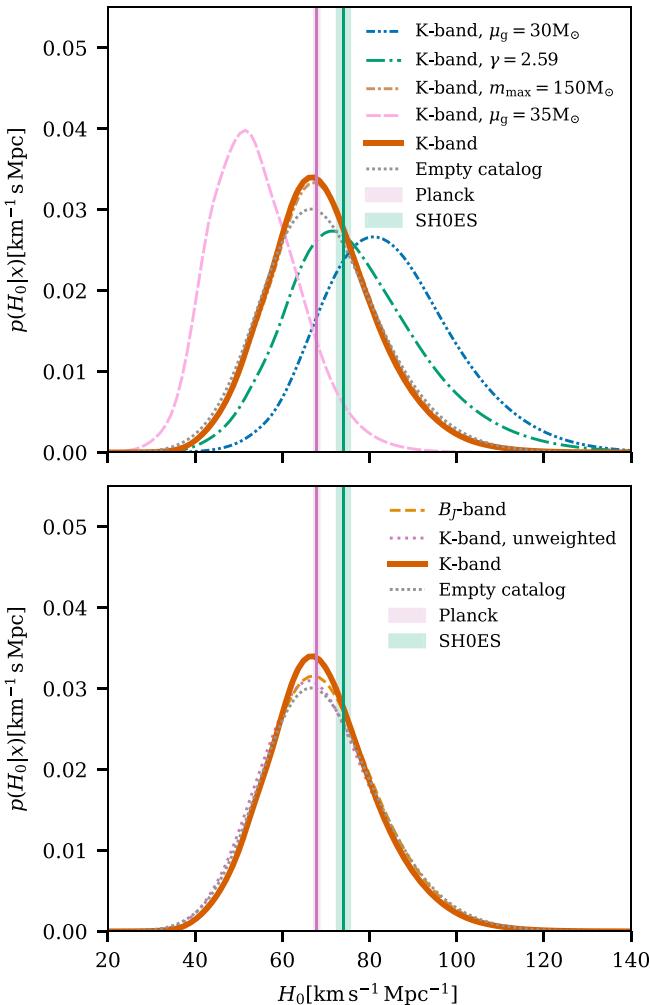
Figure 11. Systematic effects on the inference of the Hubble constant due to the choice of different values for the mean μ_g of the Gaussian component in the source mass model, and other population model parameters (upper panel) and different choices for the luminosity band and weighting scheme adopted for the GLADE+ galaxy catalog (lower panel). The pink and green shaded areas identify the 68% CI constraints on H_0 inferred from the CMB anisotropies (Ade et al. 2016) and in the local universe from SH0ES (Riess et al. 2019), respectively.

on the luminosity distance even for the best source in our current GW catalog. Hence, we also ignore the uncertainty due to weak lensing in this paper. However, in a future analysis, we could include the contribution from weak lensing and its impact on the distance measurement (Holz & Wald 1998; Cutler & Holz 2009; Hirata et al. 2010; Namikawa et al. 2016; Mukherjee et al. 2020).

6. Conclusions

Using the 47 GW events with detected S/N > 11 reported in the third LIGO–Virgo–KAGRA Gravitational Wave Transient Catalog (Abbott et al. 2021e), we have inferred constraints on the cosmological parameters adopting two different approaches: hierarchical inference without galaxy surveys and the statistical galaxy catalog method. We present for the first time analysis that constrains jointly the properties of the population of BBHs and the parameters of the cosmological

model, and we have shown the crucial correlation that exists between the two sectors.

We have shown that an excess population of BHs in the mass range 30–40 $M_\odot$, pointed out by Abbott et al. (2021b), is robust to the choice of assumed cosmological model parameters. While our constraints on the present-day matter density, Ω_m, and dark energy EoS, w_0, parameters are weak, we have measured the Hubble constant to be $H_0 = 68^{+12}_{-8}$ km s^{-1} Mpc^{-1} at 68% CL from combining dark sirens with information from the bright siren GW170817 and its EM counterpart (Abbott et al. 2019b). This result represents an improvement of 17% with respect to the H_0 value reported from analysis of O1 and O2 data (Abbott et al. 2021a) that made use of galaxy catalogs alone to infer statistical redshift information. In our analysis we also obtain weak constraints on the expansion history as a function of the redshift.

In addition we provide a constraint on the value of H_0 adopting a fixed POWER LAW + PEAK population model of BBHs and using statistical redshift information inferred from the GLADE+ galaxy catalog. This analysis obtained, for the K band, $H_0 = 67^{+13}_{-12}$ km s^{-1} Mpc^{-1}, which represents an improvement of 42% with respect to Abbott et al. (2021a) alone, and an improvement of 20% with respect to recent H_0 studies using GWTC–2 events (Finke et al. 2021). Most of the constraining power in our H_0 inference comes from the event GW170817 using its EM counterpart. Combining the above result with information from GW170817 we obtain 68^{+8}_{-6} km s^{-1} Mpc^{-1}. The most informative dark siren in the GWTC–3 catalog is GW190814, which alone provides an estimate of $H_0 = 67^{+46}_{-28}$ km s^{-1} Mpc^{-1}, provided that the luminosity weighting scheme is applied.

A summary of the different H_0 values obtained using different data sets and model assumptions can be seen in Table 4. The table is divided into two parts. The first part summarizes the values that we infer for H_0 when fixing the population model to the most favorable one and then varying the luminosity band from GLADE+ used in our analysis. We used both the B_J band and the K band, and the results are very similar (see also Figure 11). The second part of the table summarizes the results obtained by marginalizing over the population parameters and using no galaxy catalog information.

Although we have improved our previously reported constraints on the value of H_0 using these 47 GW events, our results are still dominated by the systematic effects induced by the assumptions made about the GW source population. The choice of mass scale set by μ_g, the mass at which the excess of BHs is centered, plays a crucial role in constraining the value of H_0.

In the future, with significantly more both bright and dark sirens it will be possible to make robust measurements of H_0 and other cosmological parameters. On the one hand, measurement of bright sirens will greatly help with inferring the redshift from direct observations of EM counterparts (Holz & Hughes 2005; Dalal et al. 2006; Nissanke et al. 2010; Chen et al. 2018; Feeney et al. 2019). On the other hand, for dark sirens, the application of cross-correlation techniques to infer the clustering redshift of GW sources (Mukherjee et al. 2021; Bera et al. 2020) using spectroscopic galaxy surveys (Diaz & Mukherjee 2022), the pair-instability supernovae mass scale of black holes (Farr et al. 2019; Mastrogiovanni et al. 2021), the redshift distribution of the GW sources (Ding et al. 2019;
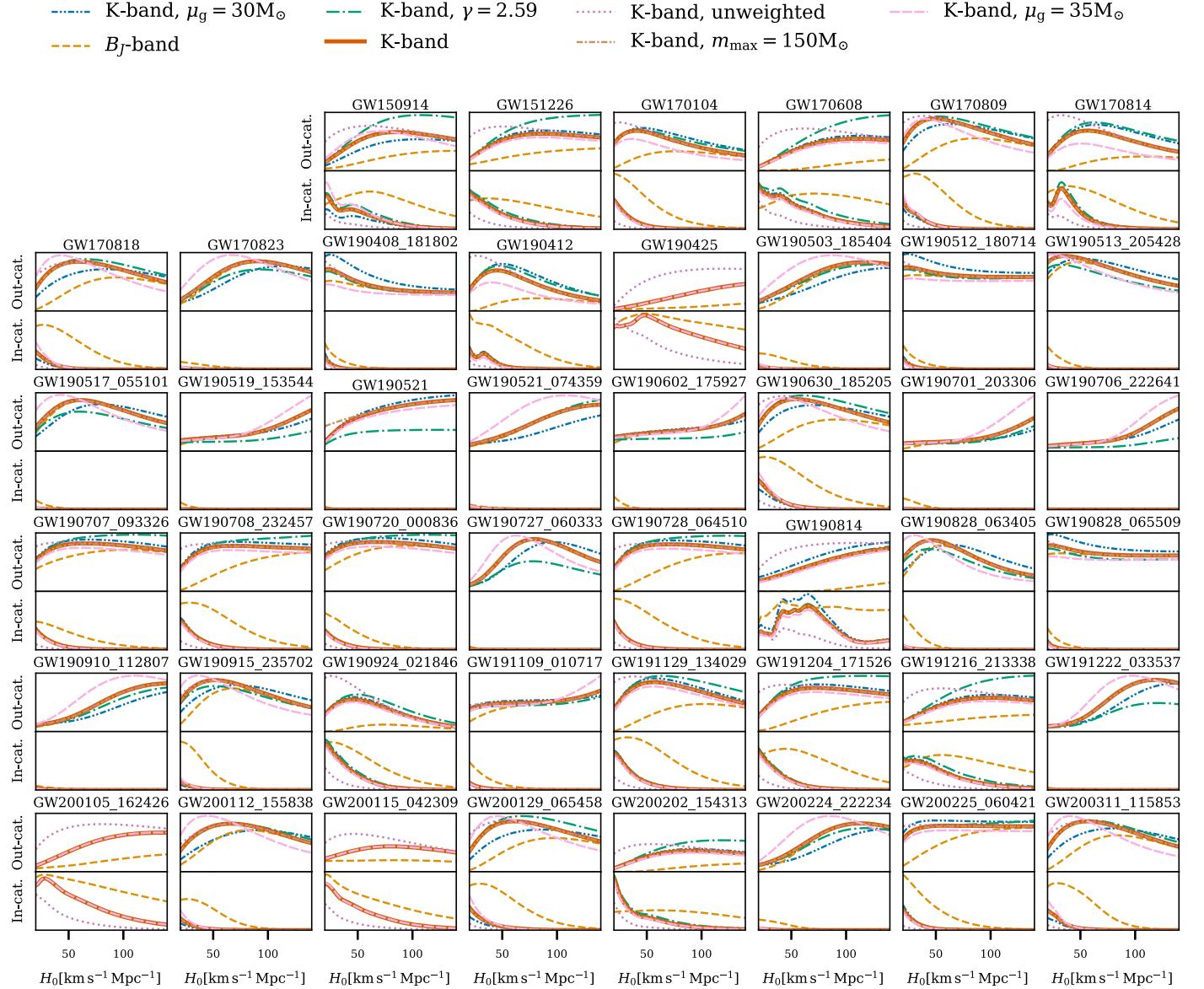
Figure 12. Plots showing, for each event, the hierarchical likelihood as a function of H_0 marginalized over sky localization as a function of different population assumptions and using the GLADE+ K band. The y-axes of each panel start from zero and have the same normalization. Two panels are shown for each event. Top panels: hierarchical likelihood under the hypothesis that the host galaxy is *not* in the catalog, for several different population assumptions. Bottom panels: hierarchical likelihood under the hypothesis that the host galaxy *is* in the catalog, again for several different population assumptions. This shows how population and galaxy catalog treatment affect the information on the H_0 value for each event.

Table 4
Values of the Hubble Constant Obtained in this Study Using Different Data Sets and Analysis Methods

Description	Galaxy catalog	BBH mass model	H_0^{HDI} [km s^{-1} Mpc^{-1}]	H_0^{sym} [km s^{-1} Mpc^{-1}]
No galaxy catalog, marginalizing over population model, 42 events	-	TRUNCATED	109^{+43}_{-54} (69^{+21}_{-8})	104^{+74}_{-77} (79^{+44}_{-19})
	-	POWER LAW + PEAK	50^{+37}_{-30} (68^{+12}_{-8})	62^{+90}_{-42} (72^{+30}_{-13})
	-	BROKEN POWER LAW	44^{+52}_{-24} (68^{+13}_{-8})	66^{+98}_{-47} (73^{+34}_{-14})
Using galaxy catalog, fixed population model, 47 events	GLADE+ K band	POWER LAW + PEAK	67^{+13}_{-12} (68^{+8}_{-6})	68^{+25}_{-21} (70^{+17}_{-13})
	GLADE+ B_J band	POWER LAW + PEAK	67^{+14}_{-12} (68^{+9}_{-6})	69^{+25}_{-23} (71^{+18}_{-12})

Note. The columns are in order: short description of the sources used in the study with S/N > 11, galaxy catalog used (where appropriate), BBH mass model used, and the 68.3% CL H_0 value. The last two columns report the median and symmetric 90% CI H_0 values. The values in the parentheses are those obtained after combining with the GW170817 EM counterpart posterior.

Ye & Fishbach 2021), and the tidal distortion of neutron stars (Messenger & Read 2012; Chatterjee et al. 2021) will enable robust measurement of the cosmic expansion history. With the aid of more observations and further development of analysis techniques, we will be able to reduce the current systematics and proceed toward accurate and precision gravitational wave cosmology.

Appendix A
Population Prior Models

A.1. Models for Background Cosmologies

We use a flat ΛCDM cosmological model with dark energy density as a function of the redshift z described by Linder (2003)

$$\rho_\Lambda(z) = \rho_{\Lambda,0}(1 + z)^{3(1+w_0)}, \tag{A1}$$

where ρ_Λ is the dark energy density, and w_0 is a phenomenological parameter. If the dark energy density is constant during the cosmic expansion, as it is in the standard cosmological model, then $w_0 = -1$. The luminosity distance is calculated as

$$D_L(z) = \frac{c(1 + z)}{H_0} \int_0^z \frac{dz'}{\sqrt{\Omega_m(1 + z')^3 + \Omega_{\Lambda,0}(1 + z')^{3(1+w_0)}}}, \tag{A2}$$

where Ω_m and $\Omega_{\Lambda,0}$ are the present-day dimensionless matter and dark energy densities, respectively, and $\Omega_{\Lambda,0} = 1 - \Omega_m$.

We consider two sets of priors for the cosmological background model, which are indicated in Table 5. For the first set of priors, we adopt a flat ΛCDM cosmology that restricts the Hubble constant to only the range compatible with the H_0 tension, while for the second set we adopt more general, wide priors.

A.2. Merger Rate and Redshift Distribution Priors

We model the binary merger rate using a phenomenological model introduced with the form of Madau & Dickinson (2014), motivated by the fact that the binary formation rate might follow the star formation rate. The parameterization that we use Callister et al. (2020) for the merger rate in the detector frame is

$$\frac{dN}{dt_d dz} = R_0[1 + (1 + z_p)^{-\gamma-k}]\frac{\partial V_c}{\partial z}(\Lambda_c)$$
$$\times \frac{1}{1 + z} \frac{(1 + z)^\gamma}{1 + [(1 + z)/(1 + z_p)]^{\gamma+k}}, \tag{A3}$$

where R_0 is the binary merger rate today, V_c is the comoving volume, γ and k are the slopes of the two power-law regimes before and after a turning point z_p, and Λ_c are a set of parameters describing the cosmological expansion. The extra

Table 5
Summary of the Priors on the Cosmological Parameters for the Two Sets of Priors Considered

Parameter	Description	Prior
Restricted priors (H_0 tension)		
H_0	Hubble constant expressed in km s^{-1} Mpc^{-1} in the H_0-tension region	$\mathcal{U}(65, 77)$
Ω_m	Present-day matter density of the universe fixed to the mean value inferred from measurements of the CMB in Ade et al. (2016)	0.3065
w_0	Dark energy equation-of-state parameter fixed to the value that corresponds to constant density	-1
Wide priors		
Parameter	Description	Prior
H_0	Hubble constant expressed in km s^{-1} Mpc^{-1}	$\mathcal{U}(10.0, 200.0)$
Ω_m	Present-day matter density of the universe	$\mathcal{U}(0.0, 1.0)$
w_0	Dark energy equation-of-state parameter	$\mathcal{U}(-3.0, 0.0)$

Table 6
Summary of the Prior Hyperparameters Used for the Merger Rate Evolution Models Adopted in This Paper

Parameter	Description	Prior
R_0	BBH merger rate today in Gpc^{-3} yr^{-1}	$\mathcal{U}(0.0, 100.0)$
γ	Slope of the power-law regime for the rate evolution before the point z_p	$\mathcal{U}(0.0, 12.0)$
k	Slope of the power-law regime for the rate evolution after the point z_p	$\mathcal{U}(0.0, 6.0)$
z_p	Redshift turning point between the power-law regimes with γ and k	$\mathcal{U}(0.0, 4.0)$

$1/(1 + z)$ factor encodes the clock difference in the source and detector, while the factor $(1 + z_\mathrm{p})$ ensures that today the merger rate is $R(z = 0) = R_0$. The redshift prior, normalized over the redshift, can be expressed as

$$\pi(z|\gamma, \kappa, z_\mathrm{p}, \Lambda_\mathrm{c}) = \frac{1}{C}\frac{dN}{dt_\mathrm{d}dz}, \tag{A4}$$

where C is the normalization factor calculated from Equation (A3).

The priors that we use on the merger rate hyperparameters are indicated in Table 6. The prior ranges that we model are wide enough to include the effect of a possible time delay between the formation and the merger of the binary.

A.3. Phenomenological Mass Priors

The three phenomenological mass models that we implement are a superposition of two probability density distributions and are compatible with the phenomenological priors used for BBHs in Abbott et al. (2021b, 2021f), although the prior ranges on the population parameters are different. The first is a truncated power law $\mathcal{P}(x|x_\mathrm{min}, x_\mathrm{max}, \alpha)$ described by slope α, and lower and upper bounds $x_\mathrm{min}, x_\mathrm{max}$ at which there is a hard cutoff

$$\mathcal{P}(x|x_\mathrm{min}, x_\mathrm{max}, \alpha) \propto \begin{cases} x^\alpha & (x_\mathrm{min} \leqslant x \leqslant x_\mathrm{max}) \\ 0 & \text{Otherwise.} \end{cases} \tag{A5}$$

The second is a Gaussian distribution with mean μ and standard deviation σ,

$$\mathcal{G}(x|\mu, \sigma, a, b) = \frac{1}{\sigma\sqrt{2\pi}}\exp\left[-\frac{(x - \mu)^2}{2\sigma^2}\right]. \tag{A6}$$

The source mass priors for the BBHs population that we consider are factorized as

$$\pi(m_1, m_2|\Phi_m) = \pi(m_1|\Phi_m)\pi(m_2|m_1, \Phi_m), \tag{A7}$$

where $\pi(m_1|\Phi_m)$ is the distribution of the primary mass component while $\pi(m_2|m_1, \Phi_m)$ is the distribution of the secondary mass component given the primary. For all of the

mass models, the secondary mass component m_2 is described with a truncated power law with slope β between a minimum mass m_min and a maximum mass m_1

$$\pi(m_2|m_1, m_\mathrm{min}, \alpha) = \mathcal{P}(m_2|m_\mathrm{min}, m_1, \beta), \tag{A8}$$

while the primary mass is described with several models discussed in the following paragraphs.

For some of the phenomenological models, we also apply a smoothing factor to the lower end of the mass distribution

$$\pi(m_1, m_2|\Phi_m) = [\pi(m_1|\Phi_m)\pi(m_2|m_1, \Phi_m)]S(m_1|\delta_m, m_\mathrm{min})S(m_2|\delta_m, m_\mathrm{min}), \tag{A9}$$

where S is a sigmoid-like window function that adds a tapering of the lower end of the mass distribution. See Equations (B6) and (B7) of Abbott et al. (2021b) for the explicit expression for the window function.

The three phenomenological mass models are highlighted in the following list. In Table 7, we report the prior ranges used for the population hyperparameters.

1. **Truncated model**: It describes the distribution of the primary mass m_1 with a truncated power law with slope $-\alpha$ between a minimum mass m_min and a maximum mass m_max.

$$\pi(m_1|m_\mathrm{min}, m_\mathrm{max}, \alpha) = \mathcal{P}(m_1|m_\mathrm{min}, m_\mathrm{max}, -\alpha). \tag{A10}$$

2. **Power Law + Peak model**: It describes the primary mass component as a superposition of a truncated PL, with slope $-\alpha$ between a minimum mass m_min and a maximum mass m_max, plus a Gaussian component with mean μ_g and standard deviation σ_g,

$$\pi(m_1|m_\mathrm{min}, m_\mathrm{max}, \alpha, \lambda_\mathrm{g}, \mu_\mathrm{g}, \sigma_\mathrm{g})$$
$$= [(1 - \lambda_\mathrm{g})\mathcal{P}(m_1|m_\mathrm{min}, m_\mathrm{max}, -\alpha) + \lambda_\mathrm{g}\mathcal{G}(m_1|\mu_\mathrm{g}, \sigma_\mathrm{g})]. \tag{A11}$$

3. **Broken Power Law model**: It describes the distribution of m_1 as a PL between a minimum mass m_min and a maximum mass m_max. The BROKEN POWER LAW model is characterized by two PL slopes, α_1 and α_2, and by a

Table 7
Summary of the Priors Used for the Population Hyperparameters for the Three Phenomenological Mass Models

	TRUNCATED	
Parameter	**Description**	**Prior**
α	Spectral index for the PL of the primary mass distribution	$\mathcal{U}(1.5, 12.0)$
β	Spectral index for the PL of the mass ratio distribution	$\mathcal{U}(-4.0, 12.0)$
$m_{\min}$	Minimum mass of the PL component of the primary mass distribution	$\mathcal{U}(2.0\,M_\odot, 10.0\,M_\odot)$
$m_{\max}$	Maximum mass of the PL component of the primary mass distribution	$\mathcal{U}(50.0\,M_\odot, 200.0\,M_\odot)$
	POWER LAW + PEAK	
Parameter	**Description**	**Prior**
α	Spectral index for the PL of the primary mass distribution	$\mathcal{U}(1.5, 12.0)$
β	Spectral index for the PL of the mass ratio distribution	$\mathcal{U}(-4.0, 12.0)$
$m_{\min}$	Minimum mass of the PL component of the primary mass distribution	$\mathcal{U}(2.0\,M_\odot, 10.0\,M_\odot)$
$m_{\max}$	Maximum mass of the PL component of the primary mass distribution	$\mathcal{U}(50.0\,M_\odot, 200.0\,M_\odot)$
λ_{g}	Fraction of the model in the Gaussian component	$\mathcal{U}(0.0, 1.0)$
μ_{g}	Mean of the Gaussian component in the primary mass distribution	$\mathcal{U}(20.0\,M_\odot, 50.0\,M_\odot)$
σ_{g}	Width of the Gaussian component in the primary mass distribution	$\mathcal{U}(0.4\,M_\odot, 10.0\,M_\odot)$
δ_m	Range of mass tapering at the lower end of the mass distribution	$\mathcal{U}(0.0\,M_\odot, 10.0\,M_\odot)$
	BROKEN POWER LAW	
Parameter	**Description**	**Prior**
α_1	PL slope of the primary mass distribution for masses below m_{break}	$\mathcal{U}(1.5, 12.0)$
α_2	PL slope for the primary mass distribution for masses above m_{break}	$\mathcal{U}(1.5, 12.0)$
β	Spectral index for the PL of the mass ratio distribution	$\mathcal{U}(-4.0, 12.0)$
$m_{\min}$	Minimum mass of the PL component of the primary mass distribution	$\mathcal{U}(2.0\,M_\odot, 50.0\,M_\odot)$
$m_{\max}$	Maximum mass of the primary mass distribution	$\mathcal{U}(50.0\,M_\odot, 200.0\,M_\odot)$
b	Fraction of the way between $m_{\min}$ and $m_{\max}$ at which the primary mass distribution breaks	$\mathcal{U}(0.0, 1.0)$
δ_m	Range of mass tapering on the lower end of the mass distribution	$\mathcal{U}(0.0\,M_\odot, 10.0\,M_\odot)$

break point between the two regimes at $m_{\mathrm{break}} = b(m_{\max} - m_{\min})$, where b is a number $\in [0, 1]$. The broken PL model is

$$\pi(m_1|m_{\min}, m_{\max}, \alpha_1, \alpha_2) = \mathcal{P}(m_1|m_{\min}, m_{\mathrm{break}}, -\alpha_1)$$
$$+ \frac{\mathcal{P}(m_{\mathrm{break}}|m_{\min}, m_{\mathrm{break}}, -\alpha_1)}{\mathcal{P}(m_{\mathrm{break}}|m_{\mathrm{break}}, m_{\max}, -\alpha_2)} \mathcal{P}(m_1|b, m_{\max}, -\alpha_2).$$

$$(A12)$$

Appendix B
Full Results of the Population Analysis and Effect of Different S/N Cuts

We provide extra details on the joint inference of cosmological and population parameters using BBHs.

In Figure 13 we show the corner plots for the posterior associated with the POWER LAW + PEAK model (the one implemented for the galaxy catalog analysis) adopting wide priors on the cosmological parameters and for the population of BBHs. As was also shown in Figure 5, the main mass-related population parameters correlating with the cosmological parameters, and in particular H_0, are the position of the

Gaussian component (BBH excess in the mass distribution) and the higher end of the source mass distribution.

The other parameter that correlates with the estimation of H_0 is the rate evolution parameter γ. This parameter models a power-law-increasing merger rate with the redshift. We find that higher values of γ support lower values of H_0, which is due to the fact that lowering H_0 will place events at lower redshifts that are incompatible with the observed mass distribution; therefore γ tries to correct this by supporting higher redshifts. However, the posterior on the rate evolution is well within the statistical uncertainties given in Abbott et al. (2021f).

We run additional systematic studies using different S/N cuts for the selection of the BBHs to include in our analysis. We explore a higher S/N cut of 12 (more pure) that selects a sample of 35 events. We also explore a lower S/N cut of 10, allowing 60 events with a IFAR > 0.5 yr and no plausible instrumental origin. For this set of events, GW190426_152155 and GW190531_023648 are excluded as their secondary mass extends to lower masses in the NS region.

The marginal H_0 posterior for all the mass models is shown in Figure 14, where we show that including more events always produces a posterior on the H_0 within the statistical uncertainties of other selection criteria. In all of these cases, the excess of BBHs around $35M_\odot$ is present for all the S/N
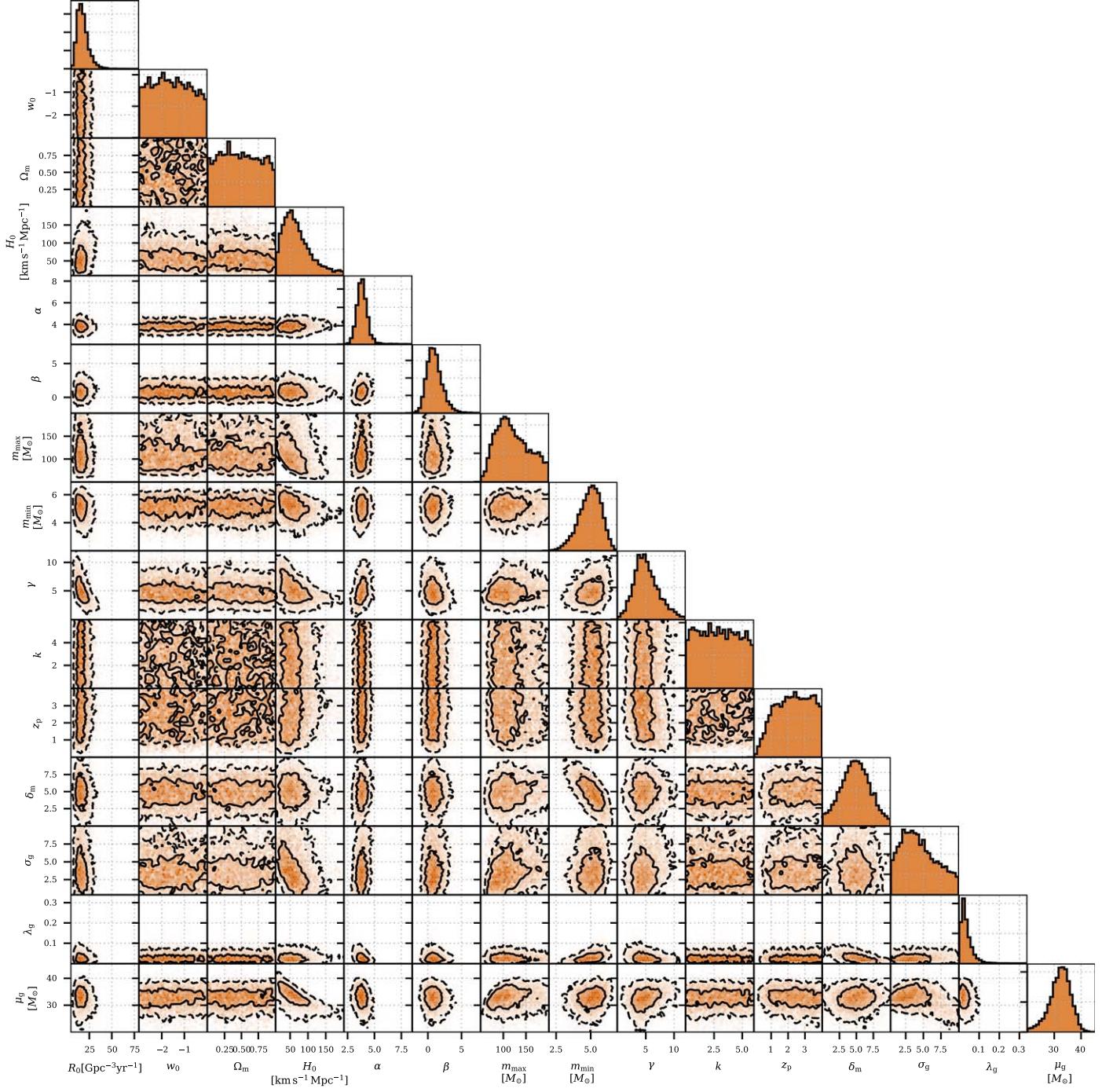
Figure 13. Corner plots for the preferred POWER LAW + PEAK model parameters and cosmological parameters, fitted to BBHs with S/N > 11.
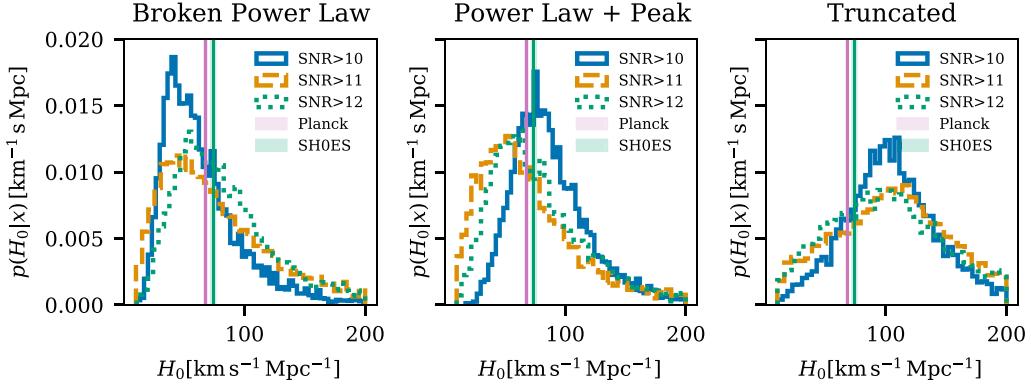
Figure 14. Marginal posterior probability distributions for H_0 with using BBH events with three different S/N cuts and the three mass models.

cuts, and it is responsible for the preference observed in the H_0 posterior.

Appendix C
Schechter Luminosity Function Studies

In this appendix we show comparisons of the Schechter luminosity function (LF) for K- and B_J-band galaxies reported in GLADE+. Wrong assumptions on the LF, or incorrect description of the selection biases, could potentially introduce a bias in the inferred H_0. Indeed, one of the key assumptions that we have made to construct our completeness corrections is that the galaxy catalog is *magnitude limited*, i.e., galaxies are not detected only because they are too faint. This cannot be the case if another selection bias (based on, e.g., colors or spectral features) were present, or if color and evolution corrections are not implemented properly.

In Figure 15 we show a comparison of the assumed LF and the number density of galaxies per comoving volume present in GLADE+. In the case that the galaxy catalog can be correctly described as magnitude-limited, we expect that the distribution of the GLADE+ galaxies distribution will match the assumed LF at its bright end, and then will start to decrease when we reach (and exceed) the corresponding absolute magnitude threshold. Galaxies in the K band are well described by this behavior and missing galaxies can be explained by the impact of the apparent magnitude threshold, while for the B_J band there seems to be some additional missing galaxies at low redshift. This observed behavior motivated our decision to present our main results using the K-band magnitudes compiled in the GLADE+ catalog.
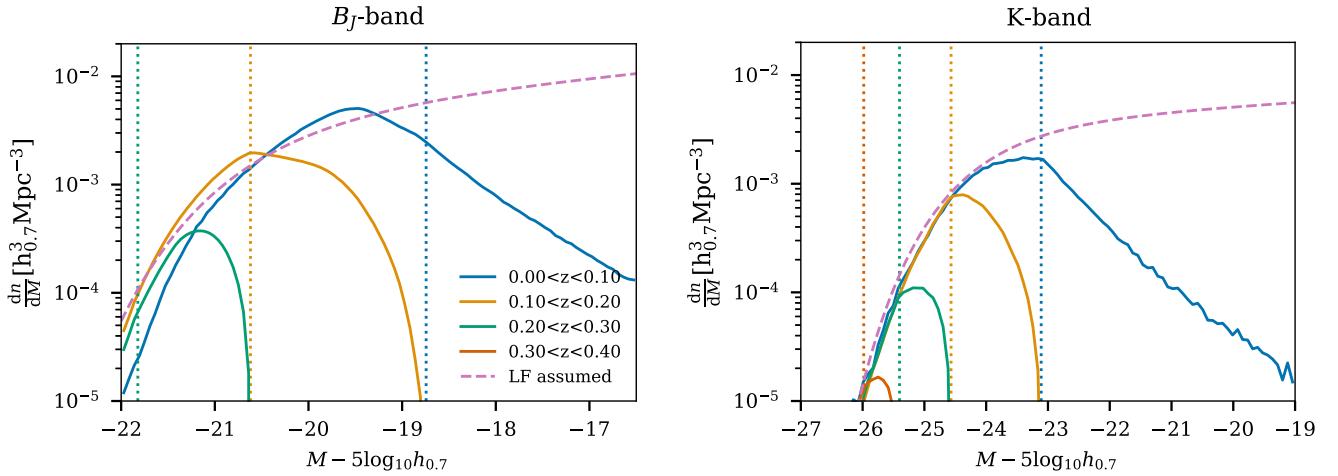
Figure 15. Left: comparison of the assumed B_J-band galaxy LF (pink dashed line) and the differential number density of galaxies in different redshift bins (solid colored lines). The vertical dashed line indicates the median absolute magnitude threshold for galaxy detection, as computed in our code. Right: same comparison, but for the K-band LF. In each panel the solid lines are calculated based on the median apparent magnitude threshold, computed over all sky directions, then collecting and making a histogram of all galaxies in the GLADE+ catalog that lie in the appropriate redshift bin and are brighter than the apparent magnitude threshold.

ORCID iDs

K. Ackley https://orcid.org/0000-0002-8648-0767
N. Adhikari https://orcid.org/0000-0002-4559-8427
R. X. Adhikari https://orcid.org/0000-0002-5731-5076
M. Agathos https://orcid.org/0000-0002-9072-1121
K. Agatsuma https://orcid.org/0000-0002-3952-5985
L. Aiello https://orcid.org/0000-0003-2771-8816
P. Ajith https://orcid.org/0000-0001-7519-2439
T. Akutsu https://orcid.org/0000-0003-0733-7530
A. Allocca https://orcid.org/0000-0002-5288-1351
P. A. Altin https://orcid.org/0000-0001-8193-5825
A. Amato https://orcid.org/0000-0001-9557-651X
S. Anand https://orcid.org/0000-0003-3768-7515
S. B. Anderson https://orcid.org/0000-0003-2219-9383
W. G. Anderson https://orcid.org/0000-0003-0482-5942
N. Andres https://orcid.org/0000-0002-5360-943X
M. Andrés-Carcasona https://orcid.org/0000-0002-8738-1672
T. Andrić https://orcid.org/0000-0002-9277-9773
J. M. Antelis https://orcid.org/0000-0003-3377-0813
S. Antier https://orcid.org/0000-0002-7686-3334
K. Arai https://orcid.org/0000-0001-8916-8915
A. Araya https://orcid.org/0000-0002-6884-2875
M. C. Araya https://orcid.org/0000-0002-6018-6447
J. S. Areeda https://orcid.org/0000-0003-0266-7936
N. Aritomi https://orcid.org/0000-0003-4424-7657
N. Arnaud https://orcid.org/0000-0001-6589-8673
K. G. Arun https://orcid.org/0000-0002-6960-8538
H. Asada https://orcid.org/0000-0001-9442-6050
G. Ashton https://orcid.org/0000-0001-7288-2231
Y. Aso https://orcid.org/0000-0002-1902-6695
P. Astone https://orcid.org/0000-0003-4981-4120
F. Aubin https://orcid.org/0000-0003-1613-3142
K. AultONeal https://orcid.org/0000-0002-6645-4473
S. Babak https://orcid.org/0000-0001-7469-4250
F. Badaracco https://orcid.org/0000-0001-8553-7904
S. Bae https://orcid.org/0000-0003-2429-3357
S. Bagnasco https://orcid.org/0000-0001-6062-6505
R. Bajpai https://orcid.org/0000-0003-0495-5720
G. Baltus https://orcid.org/0000-0002-0304-8152
S. Banagiri https://orcid.org/0000-0001-7852-7484
B. Banerjee https://orcid.org/0000-0002-8008-2485
D. Bankar https://orcid.org/0000-0002-6068-2993
P. Barneo https://orcid.org/0000-0002-8883-7280
F. Barone https://orcid.org/0000-0002-8069-8490
B. Barr https://orcid.org/0000-0002-5232-2736
L. Barsotti https://orcid.org/0000-0001-9819-2562
M. Barsuglia https://orcid.org/0000-0002-1180-4050
D. Barta https://orcid.org/0000-0001-6841-550X
M. A. Barton https://orcid.org/0000-0002-9948-306X
I. Bartos https://orcid.org/0000-0001-5607-3637
R. Bassiri https://orcid.org/0000-0001-8171-6833
M. Bawaj https://orcid.org/0000-0003-3611-3042
J. C. Bayley https://orcid.org/0000-0003-0909-5563
F. Beirnaert https://orcid.org/0000-0002-4003-7233
M. Bejger https://orcid.org/0000-0002-4991-8213
J. D. Bentley https://orcid.org/0000-0002-4736-7403
M. Berbel https://orcid.org/0000-0001-6345-1798
B. K. Berger https://orcid.org/0000-0002-4845-8737
S. Bernuzzi https://orcid.org/0000-0002-2334-0935
C. P. L. Berry https://orcid.org/0000-0003-3870-7215
D. Bersanetti https://orcid.org/0000-0002-7377-415X

J. Betzwieser https://orcid.org/0000-0003-1533-9229
D. Beveridge https://orcid.org/0000-0002-1481-1993
U. Bhardwaj https://orcid.org/0000-0003-1233-4174
D. Bhattacharjee https://orcid.org/0000-0001-6623-9506
S. Bhaumik https://orcid.org/0000-0001-8492-2202
G. Billingsley https://orcid.org/0000-0002-4141-2744
M. Bilicki https://orcid.org/0000-0002-3910-5809
O. Birnholtz https://orcid.org/0000-0002-7562-9263
S. Biscoveanu https://orcid.org/0000-0001-7616-7366
B. Biswas https://orcid.org/0000-0003-2131-1476
M.-A. Bizouard https://orcid.org/0000-0002-4618-1674
J. K. Blackburn https://orcid.org/0000-0002-3838-2986
G. N. Bolingbroke https://orcid.org/0000-0002-7350-5291
E. Bonilla https://orcid.org/0000-0002-6284-9769
R. Bonnand https://orcid.org/0000-0001-5013-5913
V. Boschi https://orcid.org/0000-0001-8665-2293
V. Boudart https://orcid.org/0000-0001-9923-4154
P. R. Brady https://orcid.org/0000-0002-4611-9387
M. Branchesi https://orcid.org/0000-0003-1643-0526
J. E. Brau https://orcid.org/0000-0003-1292-9725
M. Breschi https://orcid.org/0000-0002-3327-3676
T. Briant https://orcid.org/0000-0002-6013-1729
A. F. Brooks https://orcid.org/0000-0003-4295-792X
R. Bruntz https://orcid.org/0000-0002-0840-8567
A. Buonanno https://orcid.org/0000-0002-5433-1409
R. Buscicchio https://orcid.org/0000-0002-7387-6754
C. Buy https://orcid.org/0000-0003-2872-8186
G. S. Cabourn Davies https://orcid.org/0000-0002-4289-3439
G. Cabras https://orcid.org/0000-0002-6852-6856
R. Cabrita https://orcid.org/0000-0003-0133-1306
L. Cadonati https://orcid.org/0000-0002-9846-166X
G. Cagnoli https://orcid.org/0000-0002-7086-6550
T. A. Callister https://orcid.org/0000-0001-9892-177X
K. C. Cannon https://orcid.org/0000-0003-4068-6572
Z. Cao https://orcid.org/0000-0002-1932-7295
E. Capocasa https://orcid.org/0000-0003-3762-6958
J. B. Carlin https://orcid.org/0000-0001-5694-0809
G. Carullo https://orcid.org/0000-0001-9090-1862
T. L. Carver https://orcid.org/0000-0002-3835-6729
F. Cavalier https://orcid.org/0000-0002-3658-7240
R. Cavalieri https://orcid.org/0000-0001-6064-0569
G. Cella https://orcid.org/0000-0002-0752-0338
E. Cesarini https://orcid.org/0000-0001-9127-3167
S. Chalathadka Subrahmanya https://orcid.org/0000-0002-9207-4669
E. Champion https://orcid.org/0000-0002-7901-4100
C.-H. Chan https://orcid.org/0000-0002-3377-4737
P. Chanial https://orcid.org/0000-0003-1753-524X
P. Charlton https://orcid.org/0000-0002-4263-2706
E. A. Chase https://orcid.org/0000-0003-1005-0792
E. Chassande-Mottin https://orcid.org/0000-0003-3768-9908
C. Chatterjee https://orcid.org/0000-0001-8700-3455
Debarati Chatterjee https://orcid.org/0000-0002-0995-2329
Deep Chatterjee https://orcid.org/0000-0003-0038-5468
S. Chaty https://orcid.org/0000-0002-5769-8601
K. Chatziioannou https://orcid.org/0000-0002-5833-413X
C. Chen https://orcid.org/0000-0002-3354-0105
D. Chen https://orcid.org/0000-0003-1433-0716
H. Y. Chen https://orcid.org/0000-0001-5403-3762
F. Chiadini https://orcid.org/0000-0002-9339-8622

A. Chincarini https://orcid.org/0000-0003-4094-9942
A. Chiummo https://orcid.org/0000-0003-2165-2967
R. K. Choudhary https://orcid.org/0000-0003-0949-7298
N. Christensen https://orcid.org/0000-0002-6870-4202
S. S. Y. Chua https://orcid.org/0000-0001-8026-7597
G. Ciani https://orcid.org/0000-0003-4258-9338
M. Cieślar https://orcid.org/0000-0001-8912-5587
R. Ciolfi https://orcid.org/0000-0003-3140-8933
J. A. Clark https://orcid.org/0000-0003-3243-1393
E. Codazzo https://orcid.org/0000-0001-7170-8733
P.-F. Cohadon https://orcid.org/0000-0003-3452-9415
D. E. Cohen https://orcid.org/0000-0002-0583-9919
M. Colleoni https://orcid.org/0000-0002-7214-9088
A. Colombo https://orcid.org/0000-0002-7439-4773
L. Conti https://orcid.org/0000-0003-2731-2656
T. R. Corbitt https://orcid.org/0000-0002-5520-8541
I. Cordero-Carrión https://orcid.org/0000-0002-1985-1361
N. J. Cornish https://orcid.org/0000-0002-7435-0869
A. Corsi https://orcid.org/0000-0001-8104-3536
S. Cortese https://orcid.org/0000-0002-6504-0973
M. W. Coughlin https://orcid.org/0000-0002-8262-2924
B. Cousins https://orcid.org/0000-0002-7026-1340
P. Couvares https://orcid.org/0000-0002-2823-3127
D. C. Coyne https://orcid.org/0000-0002-6427-3222
R. Coyne https://orcid.org/0000-0002-5243-5917
J. D. E. Creighton https://orcid.org/0000-0003-3600-2406
A. W. Criswell https://orcid.org/0000-0002-9225-7756
M. Croquette https://orcid.org/0000-0002-8581-5393
J. R. Cudell https://orcid.org/0000-0002-2003-4238
R. Cummings https://orcid.org/0000-0002-8042-9047
T. Dal Canton https://orcid.org/0000-0001-5078-9044
S. Dall'Osso https://orcid.org/0000-0003-4366-8265
G. Dálya https://orcid.org/0000-0003-3258-5763
B. D'Angelo https://orcid.org/0000-0001-9143-8427
S. Danilishin https://orcid.org/0000-0001-7758-7493
C. Darsow-Fromm https://orcid.org/0000-0001-9602-0388
Sayak Datta https://orcid.org/0000-0001-9200-8867
D. Davis https://orcid.org/0000-0001-5620-6751
M. C. Davis https://orcid.org/0000-0001-7663-0808
E. J. Daw https://orcid.org/0000-0002-3780-5430
J. Degallaix https://orcid.org/0000-0002-1019-6911
S. Deléglise https://orcid.org/0000-0002-8680-5170
F. De Lillo https://orcid.org/0000-0003-4977-0789
D. Dell'Aquila https://orcid.org/0000-0001-5895-0664
T. Dent https://orcid.org/0000-0003-1354-7809
A. Depasse https://orcid.org/0000-0003-1014-8394
R. De Pietri https://orcid.org/0000-0003-1556-8304
R. De Rosa https://orcid.org/0000-0002-4004-947X
R. DeSalvo https://orcid.org/0000-0002-4818-0296
R. De Simone https://orcid.org/0000-0002-7555-8856
T. Dietrich https://orcid.org/0000-0003-2374-307X
C. Di Giorgio https://orcid.org/0000-0003-2127-3991
F. Di Giovanni https://orcid.org/0000-0001-8568-9334
T. Di Girolamo https://orcid.org/0000-0003-2339-4471
A. Di Lieto https://orcid.org/0000-0002-4787-0754
A. Di Michele https://orcid.org/0000-0002-0357-2608
S. Di Pace https://orcid.org/0000-0001-6759-5676
I. Di Palma https://orcid.org/0000-0003-1544-8943
F. Di Renzo https://orcid.org/0000-0002-5447-3810
A. Dmitriev https://orcid.org/0000-0002-0314-956X
Z. Doctor https://orcid.org/0000-0002-2077-4914
L. D'Onofrio https://orcid.org/0000-0001-9546-5959

S. Doravari https://orcid.org/0000-0001-8750-8330
M. Drago https://orcid.org/0000-0002-3738-2431
J. C. Driggers https://orcid.org/0000-0002-6134-7628
D. D'Urso https://orcid.org/0000-0002-8215-4542
T. Eckhardt https://orcid.org/0000-0002-1224-4681
G. Eddolls https://orcid.org/0000-0002-5895-4523
B. Edelman https://orcid.org/0000-0001-7648-1689
O. Edy https://orcid.org/0000-0001-9617-8724
A. Effler https://orcid.org/0000-0001-8242-3944
S. Eguchi https://orcid.org/0000-0003-2814-9336
J. Eichholz https://orcid.org/0000-0002-2643-163X
A. Ejlli https://orcid.org/0000-0002-4149-4532
Y. Enomoto https://orcid.org/0000-0001-6426-7079
R. C. Essick https://orcid.org/0000-0001-8196-9267
D. Estevez https://orcid.org/0000-0002-3021-5964
M. Evans https://orcid.org/0000-0001-8459-4499
F. Fabrizi https://orcid.org/0000-0002-3809-065X
V. Fafone https://orcid.org/0000-0003-1314-1622
P. C. Fan https://orcid.org/0000-0003-3988-9022
A. M. Farah https://orcid.org/0000-0002-6121-0285
B. Farr https://orcid.org/0000-0002-2916-9200
W. M. Farr https://orcid.org/0000-0003-1540-8562
G. Favaro https://orcid.org/0000-0002-0351-6833
M. Favata https://orcid.org/0000-0001-8270-9512
M. Fays https://orcid.org/0000-0002-4390-9746
E. Fenyvesi https://orcid.org/0000-0003-2777-3719
D. L. Ferguson https://orcid.org/0000-0002-4406-591X
A. Fernandez-Galiana https://orcid.org/0000-0002-8940-9261
I. Ferrante https://orcid.org/0000-0002-0083-7228
F. Fidecaro https://orcid.org/0000-0002-6189-3311
P. Figura https://orcid.org/0000-0002-8925-0393
A. Fiori https://orcid.org/0000-0003-3174-0688
I. Fiori https://orcid.org/0000-0002-0210-516X
M. Fishbach https://orcid.org/0000-0002-1980-5293
J. A. Font https://orcid.org/0000-0001-6650-2634
B. Fornal https://orcid.org/0000-0003-3271-2080
F. Frasconi https://orcid.org/0000-0003-4204-6587
Z. Frei https://orcid.org/0000-0002-0181-8491
A. Freise https://orcid.org/0000-0001-6586-9901
R. Frey https://orcid.org/0000-0003-0341-2636
P. Fritschel https://orcid.org/0000-0003-0966-4279
B. U. Gadre https://orcid.org/0000-0002-1534-9761
J. R. Gair https://orcid.org/0000-0002-1671-3668
S. Galaudage https://orcid.org/0000-0002-1819-0215
D. Ganapathy https://orcid.org/0000-0003-3028-4174
A. Ganguly https://orcid.org/0000-0001-7394-0755
D. Gao https://orcid.org/0000-0002-1697-7153
B. Garaventa https://orcid.org/0000-0003-2490-404X
F. Garufi https://orcid.org/0000-0003-1391-6168
G.-G. Ge https://orcid.org/0000-0003-2601-6484
G. Gemme https://orcid.org/0000-0002-1127-7406
A. Gennai https://orcid.org/0000-0003-0149-2089
O. Gerberding https://orcid.org/0000-0001-7740-2698
L. Gergely https://orcid.org/0000-0003-3146-6201
S. Ghonge https://orcid.org/0000-0002-5476-938X
Abhirup Ghosh https://orcid.org/0000-0002-2112-8578
Archisman Ghosh https://orcid.org/0000-0003-0423-3533
Shaon Ghosh https://orcid.org/0000-0001-9848-9905
B. Giacomazzo https://orcid.org/0000-0002-6947-4023
J. A. Giaime https://orcid.org/0000-0002-3531-817X
M. Giesler https://orcid.org/0000-0003-2300-893X

P. Giri https://orcid.org/0000-0002-4628-2432
S. Gkaitatzis https://orcid.org/0000-0001-9420-7499
E. Goetz https://orcid.org/0000-0003-2666-721X
R. Goetz https://orcid.org/0000-0002-9617-5520
B. Goncharov https://orcid.org/0000-0003-3189-5807
G. González https://orcid.org/0000-0003-0199-3158
A. Grado https://orcid.org/0000-0002-0501-8256
M. Granata https://orcid.org/0000-0003-3275-1186
V. Granata https://orcid.org/0000-0002-1425-4541
C. Gray https://orcid.org/0000-0002-5556-9873
A. C. Green https://orcid.org/0000-0002-6287-8746
W. L. Griffiths https://orcid.org/0000-0001-8366-0108
H. L. Griggs https://orcid.org/0000-0001-5018-7908
A. Grimaldi https://orcid.org/0000-0002-6956-4301
H. Grote https://orcid.org/0000-0002-0797-3943
D. Guerra https://orcid.org/0000-0003-0029-5390
G. M. Guidi https://orcid.org/0000-0002-3061-9870
H.-K. Guo https://orcid.org/0000-0002-3777-3117
Anuradha Gupta https://orcid.org/0000-0002-5441-9013
F. Guzman https://orcid.org/0000-0001-9136-929X
L. Haegel https://orcid.org/0000-0002-3680-5519
O. Halim https://orcid.org/0000-0003-1326-5481
E. D. Hall https://orcid.org/0000-0001-9018-666X
W.-B. Han https://orcid.org/0000-0002-2039-0726
M. Haney https://orcid.org/0000-0001-7554-3665
J. Harms https://orcid.org/0000-0002-7332-9806
G. M. Harry https://orcid.org/0000-0002-8905-7622
I. W. Harry https://orcid.org/0000-0002-5304-9372
D. Hartwig https://orcid.org/0000-0002-9742-0794
C.-J. Haster https://orcid.org/0000-0001-8040-9807
K. Hattori https://orcid.org/0000-0001-9933-0023
H. Hayakawa https://orcid.org/0000-0001-5370-3365
J. Healy https://orcid.org/0000-0002-5233-3320
A. Heidmann https://orcid.org/0000-0002-0784-5175
J. Heinze https://orcid.org/0000-0001-8692-2724
H. Heitmann https://orcid.org/0000-0003-0625-5461
F. Hellman https://orcid.org/0000-0002-9135-6330
A. F. Helmling-Cornell https://orcid.org/0000-0002-7709-8638
G. Hemming https://orcid.org/0000-0001-5268-4465
M. Hendry https://orcid.org/0000-0001-8322-5405
E. Hennes https://orcid.org/0000-0002-2246-5496
J. Hennig https://orcid.org/0000-0003-1531-8460
M. Heurs https://orcid.org/0000-0002-5577-2273
A. L. Hewitt https://orcid.org/0000-0002-1255-3492
D. G. Holcomb https://orcid.org/0000-0001-5987-769X
I. J. Hollows https://orcid.org/0000-0002-3404-6459
Z. J. Holmes https://orcid.org/0000-0003-1311-4691
D. E. Holz https://orcid.org/0000-0002-0175-5064
E. J. Howell https://orcid.org/0000-0001-7891-2817
C. G. Hoy https://orcid.org/0000-0002-8843-6719
B-H. Hsieh https://orcid.org/0000-0002-8947-723X
H-Y. Huang https://orcid.org/0000-0002-1665-2383
P. Huang https://orcid.org/0000-0002-3812-2180
Y-C. Huang https://orcid.org/0000-0001-8786-7026
Y.-J. Huang https://orcid.org/0000-0002-2952-8429
M. T. Hübner https://orcid.org/0000-0002-9642-3029
D. C. Y. Hui https://orcid.org/0000-0003-1753-1660
V. Hui https://orcid.org/0000-0002-0233-2346
B. Idzkowski https://orcid.org/0000-0001-5869-2714
K. Inayoshi https://orcid.org/0000-0001-9840-4959
P. Iosif https://orcid.org/0000-0003-1621-7709

M. Isi https://orcid.org/0000-0001-8830-8672
Y. Itoh https://orcid.org/0000-0003-2694-8935
B. R. Iyer https://orcid.org/0000-0002-4141-5179
V. JaberianHamedan https://orcid.org/0000-0003-3605-4169
T. Jacqmin https://orcid.org/0000-0002-0693-4838
P.-E. Jacquet https://orcid.org/0000-0001-9552-0057
S. J. Jadhav https://orcid.org/0000-0003-0554-0084
A. L. James https://orcid.org/0000-0001-9165-0807
A. Z. Jan https://orcid.org/0000-0003-2050-7231
K. Janssens https://orcid.org/0000-0001-8760-4429
P. Jaranowski https://orcid.org/0000-0001-8085-3414
R. Jaume https://orcid.org/0000-0001-8691-3166
A. C. Jenkins https://orcid.org/0000-0003-1785-5841
J. Jiang https://orcid.org/0000-0002-0154-3854
H.-B. Jin https://orcid.org/0000-0002-6217-2428
A. W. Jones https://orcid.org/0000-0002-0395-0680
L. Ju https://orcid.org/0000-0002-7951-4295
P. Jung https://orcid.org/0000-0003-2974-4604
J. Junker https://orcid.org/0000-0002-3051-4374
T. Kajita https://orcid.org/0000-0003-1207-6638
M. Kakizaki https://orcid.org/0000-0003-1430-3339
V. Kalogera https://orcid.org/0000-0001-9236-5469
M. Kamiizumi https://orcid.org/0000-0001-7216-1784
N. Kanda https://orcid.org/0000-0001-6291-0227
S. Kandhasamy https://orcid.org/0000-0002-4825-6764
G. Kang https://orcid.org/0000-0002-6072-8189
D. P. Kapasi https://orcid.org/0000-0001-8189-4920
C. Karathanasis https://orcid.org/0000-0002-0642-5507
M. Kasprzack https://orcid.org/0000-0003-4618-5939
S. Katsanevas https://orcid.org/0000-0003-0324-0758
K. Kawaguchi https://orcid.org/0000-0003-4443-6984
D. Keitel https://orcid.org/0000-0002-2824-626X
J. S. Key https://orcid.org/0000-0003-0123-7600
F. Y. Khalili https://orcid.org/0000-0001-7068-2332
S. Khan https://orcid.org/0000-0003-4953-5754
N. Kijbunchoo https://orcid.org/0000-0002-2874-1228
A. Kim https://orcid.org/0000-0003-3040-8456
C. Kim https://orcid.org/0000-0001-9145-0530
J. C. Kim https://orcid.org/0000-0003-1653-3795
J. Kim https://orcid.org/0000-0001-8720-6113
M. Kinley-Hanlon https://orcid.org/0000-0002-7367-8002
R. Kirchhoff https://orcid.org/0000-0003-0224-8600
J. S. Kissel https://orcid.org/0000-0002-1702-9577
A. M. Knee https://orcid.org/0000-0003-0703-947X
P. Koch https://orcid.org/0000-0003-2777-5861
K. Kokeyama https://orcid.org/0000-0002-2896-1992
S. Koley https://orcid.org/0000-0002-5793-6665
P. Kolitsidou https://orcid.org/0000-0002-6719-8686
M. Kolstein https://orcid.org/0000-0002-5482-6743
A. K. H. Kong https://orcid.org/0000-0002-5105-344X
A. Kontos https://orcid.org/0000-0002-1347-0680
M. Korobko https://orcid.org/0000-0002-3839-3909
C. Kozakai https://orcid.org/0000-0003-2853-869X
A. Królak https://orcid.org/0000-0003-4514-7690
P. Kuijer https://orcid.org/0000-0002-6987-2048
S. Kulkarni https://orcid.org/0000-0001-5390-8563
A. Kumar https://orcid.org/0000-0001-5523-4603
K. Kuns https://orcid.org/0000-0003-0630-3902
S. Kuroyanagi https://orcid.org/0000-0001-6538-1447
K. Kwak https://orcid.org/0000-0002-2304-7798
D. Laghi https://orcid.org/0000-0001-7462-3794

R. N. Lang ⓘ https://orcid.org/0000-0002-4804-5537
B. Lantz ⓘ https://orcid.org/0000-0002-7404-4845
P. D. Lasky ⓘ https://orcid.org/0000-0003-3763-1386
M. Laxen ⓘ https://orcid.org/0000-0001-7515-9639
A. Lazzarini ⓘ https://orcid.org/0000-0002-5993-8808
P. Leaci ⓘ https://orcid.org/0000-0002-3997-5046
S. Leavey ⓘ https://orcid.org/0000-0001-8253-0272
Y. K. Lecoeuche ⓘ https://orcid.org/0000-0002-9186-7034
E. Lee ⓘ https://orcid.org/0000-0003-4412-7161
H. M. Lee ⓘ https://orcid.org/0000-0002-1998-3209
H. W. Lee ⓘ https://orcid.org/0000-0003-0470-3718
K. Lee ⓘ https://orcid.org/0000-0002-7171-7274
M. Lenti ⓘ https://orcid.org/0000-0002-2765-3955
M. Leonardi ⓘ https://orcid.org/0000-0002-7641-0060
N. Leroy ⓘ https://orcid.org/0000-0002-2321-1017
B. Li ⓘ https://orcid.org/0000-0002-3780-7735
K. L. Li ⓘ https://orcid.org/0000-0001-8229-2024
C-Y. Lin ⓘ https://orcid.org/0000-0002-7489-7418
E. T. Lin ⓘ https://orcid.org/0000-0002-0030-8051
F-K. Lin ⓘ https://orcid.org/0000-0002-4277-7219
F-L. Lin ⓘ https://orcid.org/0000-0002-3528-5726
H. L. Lin ⓘ https://orcid.org/0000-0003-4083-9567
G. C. Liu ⓘ https://orcid.org/0000-0001-5663-3016
J. Liu ⓘ https://orcid.org/0000-0001-6726-3268
R. K. L. Lo ⓘ https://orcid.org/0000-0003-1561-6716
A. Longo ⓘ https://orcid.org/0000-0003-4254-8579
M. Lorenzini ⓘ https://orcid.org/0000-0002-2765-7905
G. Losurdo ⓘ https://orcid.org/0000-0003-0452-746X
J. D. Lough ⓘ https://orcid.org/0000-0002-5160-0239
C. O. Lousto ⓘ https://orcid.org/0000-0002-6400-9640
D. Lumaca ⓘ https://orcid.org/0000-0002-3628-1591
L.-W. Luo ⓘ https://orcid.org/0000-0002-2761-8877
R. Macas ⓘ https://orcid.org/0000-0002-6096-8297
D. M. Macleod ⓘ https://orcid.org/0000-0002-1395-8694
I. A. O. MacMillan ⓘ https://orcid.org/0000-0002-6927-1031
A. Macquet ⓘ https://orcid.org/0000-0002-9913-381X
R. M. Magee ⓘ https://orcid.org/0000-0001-9769-531X
R. Maggiore ⓘ https://orcid.org/0000-0001-5140-779X
M. Magnozzi ⓘ https://orcid.org/0000-0003-4512-8430
E. Majorana ⓘ https://orcid.org/0000-0002-2383-3692
V. Mandic ⓘ https://orcid.org/0000-0001-6333-8621
V. Mangano ⓘ https://orcid.org/0000-0001-7902-8505
M. Manske ⓘ https://orcid.org/0000-0002-7778-1189
M. Mantovani ⓘ https://orcid.org/0000-0002-4424-5726
M. Mapelli ⓘ https://orcid.org/0000-0001-8799-2548
D. Marín Pina ⓘ https://orcid.org/0000-0001-6482-1842
S. Márka ⓘ https://orcid.org/0000-0002-3957-1324
Z. Márka ⓘ https://orcid.org/0000-0003-1306-5260
S. Marsat ⓘ https://orcid.org/0000-0001-9449-1071
I. W. Martin ⓘ https://orcid.org/0000-0001-7300-9151
H. Masalehdan ⓘ https://orcid.org/0000-0002-4589-0815
M. Masso-Reid ⓘ https://orcid.org/0000-0001-6177-8105
S. Mastrogiovanni ⓘ https://orcid.org/0000-0003-1606-4183
M. Mateu-Lucena ⓘ https://orcid.org/0000-0003-4817-6913
M. Matiushechkina ⓘ https://orcid.org/0000-0002-9957-8720
N. Mavalvala ⓘ https://orcid.org/0000-0003-0219-9706
D. E. McClelland ⓘ https://orcid.org/0000-0001-6210-5842
J. McIver ⓘ https://orcid.org/0000-0003-0316-1355
D. Meacher ⓘ https://orcid.org/0000-0001-5882-0368
M. Mehmet ⓘ https://orcid.org/0000-0001-9432-7108
C. S. Menoni ⓘ https://orcid.org/0000-0001-9185-2572
C. Messenger ⓘ https://orcid.org/0000-0001-7488-5022

P. M. Meyers ⓘ https://orcid.org/0000-0002-2689-0190
F. Meylahn ⓘ https://orcid.org/0000-0002-9556-142X
A. Miani ⓘ https://orcid.org/0000-0001-7737-3129
I. Michaloliakos ⓘ https://orcid.org/0000-0003-2980-358X
C. Michel ⓘ https://orcid.org/0000-0003-0606-725X
Y. Michimura ⓘ https://orcid.org/0000-0002-2218-4002
H. Middleton ⓘ https://orcid.org/0000-0001-5532-3622
D. P. Mihaylov ⓘ https://orcid.org/0000-0002-8820-407X
M. Miravet-Tenés ⓘ https://orcid.org/0000-0002-8766-1156
C. Mishra ⓘ https://orcid.org/0000-0002-7881-1677
S. Mitra ⓘ https://orcid.org/0000-0002-0800-4626
V. P. Mitrofanov ⓘ https://orcid.org/0000-0002-6983-4981
G. Mitselmakher ⓘ https://orcid.org/0000-0001-5745-3658
O. Miyakawa ⓘ https://orcid.org/0000-0002-9085-7600
K. Miyo ⓘ https://orcid.org/0000-0001-6976-1252
S. Miyoki ⓘ https://orcid.org/0000-0002-1213-8416
Geoffrey Mo ⓘ https://orcid.org/0000-0001-6331-112X
L. M. Modafferi ⓘ https://orcid.org/0000-0002-3422-6986
S. R. Mohite ⓘ https://orcid.org/0000-0003-1356-7156
M. Molina-Ruiz ⓘ https://orcid.org/0000-0003-4892-3042
A. More ⓘ https://orcid.org/0000-0001-7714-7076
S. More ⓘ https://orcid.org/0000-0002-2986-2371
C. Moreno ⓘ https://orcid.org/0000-0002-0496-032X
S. Morisaki ⓘ https://orcid.org/0000-0002-8445-6747
B. Mours ⓘ https://orcid.org/0000-0002-6444-6402
C. M. Mow-Lowry ⓘ https://orcid.org/0000-0002-0351-4555
S. Mozzon ⓘ https://orcid.org/0000-0002-8855-2509
Arunava Mukherjee ⓘ https://orcid.org/0000-0001-7335-9418
D. Mukherjee ⓘ https://orcid.org/0000-0002-3373-5236
N. Mukund ⓘ https://orcid.org/0000-0002-8666-9156
E. A. Muñiz ⓘ https://orcid.org/0000-0001-8844-421X
P. G. Murray ⓘ https://orcid.org/0000-0002-8218-2404
R. Musenich ⓘ https://orcid.org/0000-0002-2168-5462
K. Nagano ⓘ https://orcid.org/0000-0001-6686-1637
K. Nakamura ⓘ https://orcid.org/0000-0001-6148-4289
H. Nakano ⓘ https://orcid.org/0000-0001-7665-0796
I. Nardecchia ⓘ https://orcid.org/0000-0001-5558-2595
L. Naticchioni ⓘ https://orcid.org/0000-0003-2918-0730
B. Nayak ⓘ https://orcid.org/0000-0002-6814-7792
K. Y. Ng ⓘ https://orcid.org/0000-0001-5843-1434
C. Nguyen ⓘ https://orcid.org/0000-0001-8623-0306
L. Nguyen Quynh ⓘ https://orcid.org/0000-0002-1828-3702
J. Ni ⓘ https://orcid.org/0000-0001-6792-4708
A. Nishizawa ⓘ https://orcid.org/0000-0003-3562-0990
E. Nitoglia ⓘ https://orcid.org/0000-0001-8906-9159
L. K. Nuttall ⓘ https://orcid.org/0000-0002-8599-8791
Y. Obayashi ⓘ https://orcid.org/0000-0001-8791-2608
E. Oelker ⓘ https://orcid.org/0000-0002-3916-1595
G. Oganesyan ⓘ https://orcid.org/0000-0001-9765-1552
J. J. Oh ⓘ https://orcid.org/0000-0001-5417-862X
K. Oh ⓘ https://orcid.org/0000-0002-9672-3742
S. H. Oh ⓘ https://orcid.org/0000-0003-1184-7453
M. Ohashi ⓘ https://orcid.org/0000-0001-8072-0304
M. Ohkawa ⓘ https://orcid.org/0000-0002-1380-1419
F. Ohme ⓘ https://orcid.org/0000-0003-0493-5607
K. Oohara ⓘ https://orcid.org/0000-0002-7518-6677
B. O'Reilly ⓘ https://orcid.org/0000-0002-3874-8335
R. O'Shaughnessy ⓘ https://orcid.org/0000-0001-5832-8517
E. O'Shea ⓘ https://orcid.org/0000-0002-0230-9533
S. Oshino ⓘ https://orcid.org/0000-0002-2794-6029
S. Ossokine ⓘ https://orcid.org/0000-0002-2579-1246
D. J. Ottaway ⓘ https://orcid.org/0000-0001-6794-1591

C. Palomba https://orcid.org/0000-0002-4450-9883
H. Pan https://orcid.org/0000-0002-1473-9880
F. Pannarale https://orcid.org/0000-0002-7537-3210
F. Paoletti https://orcid.org/0000-0001-8898-1963
A. Parisi https://orcid.org/0000-0003-0251-8914
H. Park https://orcid.org/0000-0002-7510-0079
W. Parker https://orcid.org/0000-0002-7711-4423
D. Pascucci https://orcid.org/0000-0003-1907-0175
R. Passaquieti https://orcid.org/0000-0003-4753-9428
B. Patricelli https://orcid.org/0000-0001-6709-0969
S. Paul https://orcid.org/0000-0002-4449-1732
F. E. Peña Arellano https://orcid.org/0000-0002-8516-5159
S. Penn https://orcid.org/0000-0003-4956-0853
A. Pereira https://orcid.org/0000-0003-1856-6881
A. Perreca https://orcid.org/0000-0002-6269-2490
J. Petermann https://orcid.org/0000-0002-8949-3803
H. P. Pfeiffer https://orcid.org/0000-0001-9288-519X
H. Pham https://orcid.org/0000-0002-7650-1034
K. S. Phukon https://orcid.org/0000-0003-1561-0760
O. J. Piccinni https://orcid.org/0000-0001-5478-3950
M. Pichot https://orcid.org/0000-0002-4439-8968
L. Pierini https://orcid.org/0000-0003-0945-2196
V. Pierro https://orcid.org/0000-0002-6020-5521
M. D. Pitkin https://orcid.org/0000-0003-4548-526X
A. Placidi https://orcid.org/0000-0001-8032-4416
M. L. Planas https://orcid.org/0000-0001-8278-7406
W. Plastino https://orcid.org/0000-0002-5737-6346
R. Poggiani https://orcid.org/0000-0002-9968-2464
E. Polini https://orcid.org/0000-0003-4059-0765
R. Poulton https://orcid.org/0000-0003-2049-520X
G. Pratten https://orcid.org/0000-0003-4984-0775
G. A. Prodi https://orcid.org/0000-0001-5256-915X
M. Punturo https://orcid.org/0000-0001-8722-4485
M. Pürrer https://orcid.org/0000-0002-3329-9788
H. Qi https://orcid.org/0000-0001-6339-1537
P. Raffai https://orcid.org/0000-0001-7576-0141
K. E. Ramirez https://orcid.org/0000-0003-2194-7669
A. Ramos-Buades https://orcid.org/0000-0002-6874-7421
V. Raymond https://orcid.org/0000-0003-0066-0095
N. Raza https://orcid.org/0000-0002-8549-9124
M. Razzano https://orcid.org/0000-0003-4825-1629
L. Rei https://orcid.org/0000-0002-8690-9180
P. Relton https://orcid.org/0000-0003-2756-3391
P. Rettegno https://orcid.org/0000-0001-8088-3517
B. Revenu https://orcid.org/0000-0002-7629-4805
F. Ricci https://orcid.org/0000-0001-5742-5980
J. W. Richardson https://orcid.org/0000-0002-1472-4806
K. Riles https://orcid.org/0000-0002-6418-5812
S. Rinaldi https://orcid.org/0000-0001-5799-4155
K. Rink https://orcid.org/0000-0002-1494-3494
A. Rocchi https://orcid.org/0000-0002-1382-9016
L. Rolland https://orcid.org/0000-0003-0589-9687
J. G. Rollins https://orcid.org/0000-0002-9388-2799
A. Romero https://orcid.org/0000-0003-2275-4164
S. Ronchini https://orcid.org/0000-0003-0020-687X
M. P. Ross https://orcid.org/0000-0002-8955-5269
D. Rozza https://orcid.org/0000-0002-7378-6353
J. Sadiq https://orcid.org/0000-0001-5931-3624
S. Saha https://orcid.org/0000-0002-3333-8070
M. Sakellariadou https://orcid.org/0000-0002-2715-1517
O. S. Salafia https://orcid.org/0000-0003-4924-7322
F. Salces-Carcoba https://orcid.org/0000-0001-7049-4438
M. Saleem https://orcid.org/0000-0002-3836-7751
F. Salemi https://orcid.org/0000-0002-9511-3846
A. Samajdar https://orcid.org/0000-0002-0857-6018
N. Sanchis-Gual https://orcid.org/0000-0001-5375-7494
A. Sanuy https://orcid.org/0000-0002-5767-3623
N. Sarin https://orcid.org/0000-0003-2700-1030
B. S. Sathyaprakash https://orcid.org/0000-0003-3845-7586
O. Sauter https://orcid.org/0000-0003-2293-1554
R. L. Savage https://orcid.org/0000-0003-3317-1036
T. Sawada https://orcid.org/0000-0001-5726-7150
M. G. Schiworski https://orcid.org/0000-0001-9298-004X
P. Schmidt https://orcid.org/0000-0003-1542-1791
R. Schnabel https://orcid.org/0000-0003-2896-4218
E. Schwartz https://orcid.org/0000-0001-8922-7794
J. Scott https://orcid.org/0000-0001-6701-6515
S. M. Scott https://orcid.org/0000-0002-9875-7700
M. Seglar-Arroyo https://orcid.org/0000-0001-8654-409X
Y. Sekiguchi https://orcid.org/0000-0002-2648-3835
Y. Setyawati https://orcid.org/0000-0003-3718-4491
M. S. Shahriar https://orcid.org/0000-0002-7981-954X
M. A. Shaikh https://orcid.org/0000-0003-0826-6164
L. Shao https://orcid.org/0000-0002-1334-8853
P. Shawhan https://orcid.org/0000-0002-8249-8070
N. S. Shcheblanov https://orcid.org/0000-0001-8696-2435
Y. Shikano https://orcid.org/0000-0003-2107-7536
M. Shikauchi https://orcid.org/0000-0002-3561-8658
H. Shimizu https://orcid.org/0000-0002-4221-0300
K. Shimode https://orcid.org/0000-0002-5682-8750
H. Shinkai https://orcid.org/0000-0003-1082-2844
A. Shoda https://orcid.org/0000-0002-0236-4735
D. H. Shoemaker https://orcid.org/0000-0002-4147-2560
D. M. Shoemaker https://orcid.org/0000-0002-9899-6357
D. Sigg https://orcid.org/0000-0003-4606-6526
L. Silenzi https://orcid.org/0000-0001-7316-3239
L. P. Singer https://orcid.org/0000-0001-9898-5597
D. Singh https://orcid.org/0000-0001-9675-4584
M. K. Singh https://orcid.org/0000-0001-8081-4888
N. Singh https://orcid.org/0000-0002-1135-3456
A. Singha https://orcid.org/0000-0002-9944-5573
A. M. Sintes https://orcid.org/0000-0001-9050-7515
B. J. J. Slagmolen https://orcid.org/0000-0002-2471-3828
J. R. Smith https://orcid.org/0000-0003-0638-9670
L. Smith https://orcid.org/0000-0001-8516-3324
J. Soldateschi https://orcid.org/0000-0002-5458-5206
S. N. Somala https://orcid.org/0000-0003-2663-3351
K. Somiya https://orcid.org/0000-0003-2601-2264
I. Song https://orcid.org/0000-0002-4301-8281
K. Soni https://orcid.org/0000-0001-8051-7883
F. Sorrentino https://orcid.org/0000-0002-1855-5966
A. P. Spencer https://orcid.org/0000-0003-4418-3366
M. Spera https://orcid.org/0000-0003-0930-6930
D. A. Steer https://orcid.org/0000-0002-8781-1273
J. Steinlechner https://orcid.org/0000-0003-4710-8548
K. A. Strain https://orcid.org/0000-0002-2066-5355
G. Stratta https://orcid.org/0000-0003-1055-7980
A. L. Stuver https://orcid.org/0000-0003-0324-5735
S. Sudhagar https://orcid.org/0000-0001-8578-4665
V. Sudhir https://orcid.org/0000-0002-5397-6950
R. Sugimoto https://orcid.org/0000-0001-6705-3658
H. G. Suh https://orcid.org/0000-0003-2662-3903
A. G. Sullivan https://orcid.org/0000-0002-9545-7286

T. Z. Summerscales https://orcid.org/0000-0002-4522-5591
L. Sun https://orcid.org/0000-0001-7959-892X
A. Sur https://orcid.org/0000-0001-6635-5080
J. Suresh https://orcid.org/0000-0003-2389-6666
P. J. Sutton https://orcid.org/0000-0003-1614-3922
Takamasa Suzuki https://orcid.org/0000-0003-3030-6599
B. L. Swinkels https://orcid.org/0000-0002-3066-3601
M. J. Szczepańczyk https://orcid.org/0000-0002-6167-6149
S. C. Tait https://orcid.org/0000-0003-0327-953X
H. Takahashi https://orcid.org/0000-0003-0596-4397
R. Takahashi https://orcid.org/0000-0003-1367-5149
H. Takeda https://orcid.org/0000-0001-9937-2557
C. Talbot https://orcid.org/0000-0003-2053-5582
N. Tamanini https://orcid.org/0000-0001-8760-5421
K. Tanaka https://orcid.org/0000-0001-8406-5183
S. Tanioka https://orcid.org/0000-0003-3321-1018
D. Tao https://orcid.org/0000-0003-4382-5507
E. N. Tapia San Martín https://orcid.org/0000-0002-4817-5606
A. Taruya https://orcid.org/0000-0002-4016-1955
J. D. Tasson https://orcid.org/0000-0002-4777-5087
R. Tenorio https://orcid.org/0000-0002-3582-2587
J. E. S. Terhune https://orcid.org/0000-0001-9078-4993
L. Terkowski https://orcid.org/0000-0003-4622-1215
E. E. Thompson https://orcid.org/0000-0002-0419-5517
Shubhanshu Tiwari https://orcid.org/0000-0003-1611-6625
Srishti Tiwari https://orcid.org/0000-0002-1602-4176
A. E. Tolley https://orcid.org/0000-0001-9841-943X
T. Tomaru https://orcid.org/0000-0002-8927-9014
T. Tomura https://orcid.org/0000-0002-7504-8258
A. Torres-Forné https://orcid.org/0000-0001-8709-5118
I. Tosta e Melo https://orcid.org/0000-0001-5833-4052
A. Trapananti https://orcid.org/0000-0001-7763-5758
F. Travasso https://orcid.org/0000-0002-4653-6156
M. C. Tringali https://orcid.org/0000-0001-5087-189X
A. Tripathee https://orcid.org/0000-0002-6976-5576
A. Trovato https://orcid.org/0000-0002-9714-1904
L. Trozzo https://orcid.org/0000-0002-8803-6715
K. W. Tsang https://orcid.org/0000-0003-3666-686X
T. Tsutsui https://orcid.org/0000-0002-2909-0471
K. Turbang https://orcid.org/0000-0002-9296-8603
D. Tuyenbayev https://orcid.org/0000-0002-4378-5835
A. S. Ubhi https://orcid.org/0000-0002-3240-6000
N. Uchikata https://orcid.org/0000-0003-0030-3653
T. Uchiyama https://orcid.org/0000-0003-2148-1694
T. Uehara https://orcid.org/0000-0003-4375-098X
K. Ueno https://orcid.org/0000-0003-3227-6055
T. Ushiba https://orcid.org/0000-0002-5059-4033
A. Utina https://orcid.org/0000-0003-2975-9208
G. Vajente https://orcid.org/0000-0002-7656-6882
A. Vajpeyi https://orcid.org/0000-0002-4146-1132
G. Valdes https://orcid.org/0000-0001-5411-380X
M. Valentini https://orcid.org/0000-0003-1215-4552
M. van Beuzekom https://orcid.org/0000-0002-0500-1286
J. F. J. van den Brand https://orcid.org/0000-0003-4434-5353
H. van Haevermaet https://orcid.org/0000-0003-2386-957X
J. V. van Heijningen https://orcid.org/0000-0002-8391-7513
N. van Remortel https://orcid.org/0000-0003-4180-8199
V. Varma https://orcid.org/0000-0002-9994-1761
M. Vasúth https://orcid.org/0000-0003-4573-8781

A. Vecchio https://orcid.org/0000-0002-6254-1617
J. Veitch https://orcid.org/0000-0002-6508-0713
P. J. Veitch https://orcid.org/0000-0002-2597-435X
J. Venneberg https://orcid.org/0000-0002-2508-2044
G. Venugopalan https://orcid.org/0000-0003-4414-9918
D. Verkindt https://orcid.org/0000-0003-4344-7227
P. Verma https://orcid.org/0000-0003-4147-3173
S. M. Vermeulen https://orcid.org/0000-0003-4227-8214
D. Veske https://orcid.org/0000-0003-4225-0895
A. Viceré https://orcid.org/0000-0003-0624-6231
A. D. Viets https://orcid.org/0000-0002-4241-1428
A. Vijaykumar https://orcid.org/0000-0002-4103-0666
V. Villa-Ortega https://orcid.org/0000-0001-7983-1963
S. Vitale https://orcid.org/0000-0003-2700-0767
C. Vorvick https://orcid.org/0000-0003-1591-3358
S. P. Vyatchanin https://orcid.org/0000-0002-6823-911X
L. E. Wade https://orcid.org/0000-0002-5703-4469
K. J. Wagner https://orcid.org/0000-0002-7255-4251
J. Wang https://orcid.org/0000-0002-1830-8527
M. Was https://orcid.org/0000-0002-1890-1128
T. Washimi https://orcid.org/0000-0001-5792-4907
J. Watchi https://orcid.org/0000-0002-9154-6433
A. J. Weinstein https://orcid.org/0000-0002-0928-6784
C. M. Weller https://orcid.org/0000-0002-2280-219X
K. Wette https://orcid.org/0000-0002-4394-7179
J. T. Whelan https://orcid.org/0000-0001-5710-6576
B. F. Whiting https://orcid.org/0000-0002-8501-8669
C. Whittle https://orcid.org/0000-0002-8833-7438
D. Williams https://orcid.org/0000-0003-3772-198X
M. J. Williams https://orcid.org/0000-0003-2198-2974
A. R. Williamson https://orcid.org/0000-0002-7627-8688
J. L. Willis https://orcid.org/0000-0002-9929-0225
B. Willke https://orcid.org/0000-0003-0524-2925
G. Woan https://orcid.org/0000-0003-0381-0394
J. K. Wofford https://orcid.org/0000-0002-4301-2859
D. Wong https://orcid.org/0000-0003-2166-0027
C. Wu https://orcid.org/0000-0003-3191-8845
D. S. Wu https://orcid.org/0000-0003-2849-3751
L. Xiao https://orcid.org/0000-0003-2703-449X
H. Yamamoto https://orcid.org/0000-0001-6919-9570
K. Yamamoto https://orcid.org/0000-0002-3033-2845
T. Yamamoto https://orcid.org/0000-0002-0808-4822
F. W. Yang https://orcid.org/0000-0001-9873-6259
K. Z. Yang https://orcid.org/0000-0001-8083-4037
L. Yang https://orcid.org/0000-0002-8868-5977
Y.-C. Yang https://orcid.org/0000-0002-3780-1413
A. B. Yelikar https://orcid.org/0000-0002-8065-1174
J. Yokoyama https://orcid.org/0000-0001-7127-4808
Hang Yu https://orcid.org/0000-0002-6011-6190
Haocun Yu https://orcid.org/0000-0002-7597-098X
S. Zeidler https://orcid.org/0000-0001-7949-1292
M. Zevin https://orcid.org/0000-0002-0147-0835
H. Zhang https://orcid.org/0000-0002-3931-3851
J. Zhang https://orcid.org/0000-0001-8095-483X
C. Zhao https://orcid.org/0000-0001-5825-2401
G. Zhao https://orcid.org/0000-0003-2542-4734
X. J. Zhu https://orcid.org/0000-0001-7049-6468
Z.-H. Zhu https://orcid.org/0000-0002-3567-6743
A. B. Zimmerman https://orcid.org/0000-0002-7453-6372
J. Zweizig https://orcid.org/0000-0002-1521-3397

References

Abbott, B. P., Abbott, R., Abbott, T. D., et al. 2017a, PhRvL, 119, 161101
Abbott, B. P., Abbott, R., Abbott, T. D., et al. 2017b, ApJL, 848, L12
Abbott, B. P., Abbott, R., Abbott, T. D., et al. 2017c, Natur, 551, 85
Abbott, B. P., Abbott, R., Abbott, T. D., et al. 2019a, ApJL, 882, L24
Abbott, B. P., Abbott, R., Abbott, T. D., et al. 2019b, PhRvX, 9, 011001
Abbott, B. P., Abbott, R., Abbott, T. D., et al. 2019c, PhRvX, 9, 031040
Abbott, B. P., Abbott, R., Abbott, T. D., et al. 2020a, ApJL, 892, L3
Abbott, B. P., Abbott, R., Abbott, T. D., et al. 2021a, ApJ, 909, 218
Abbott, R., Abbott, T. D., Abraham, S., et al. 2020b, ApJL, 896, L44
Abbott, R., Abbott, T. D., Abraham, S., et al. 2021b, ApJL, 913, L7
Abbott, R., Abbott, T. D., Abraham, S., et al. 2021c, PhRvX, 11, 021053
Abbott, R., Abbott, T. D., Abraham, S., et al. 2021d, ApJL, 915, L5
Abbott, R., Abbott, T. D., Acernese, F., et al. 2021e, arXiv:2111.03606
Abbott, R., Abbott, T. D., Acernese, F., et al. 2021f, arXiv:2111.03634
Ade, P. A. R., Aghanim, N., Armitage-Caplan, C., et al. 2014, A&A, 571, A16
Ade, P. A. R., Aghanim, N., Arnaud, M., et al. 2016, A&A, 594, A13
Aghanim, N., Akrami, Y., Ashdown, M., et al. 2020, A&A, 641, A6
Alam, S., Ata, M., Bailey, S., et al. 2017, MNRAS, 470, 2617
Ashton, G., Ackley, K., Hernandez, I. M., & Piotrzkowski, B. 2021, CQGra, 38, 235004
Bartelmann, M. 2010, CQGra, 27, 233001
Belczynski, K., Dominik, M., Bulik, T., et al. 2010, ApJL, 715, L138
Bera, S., Rana, D., More, S., & Bose, S. 2020, ApJ, 902, 79
Bilicki, M., Jarrett, T. H., Peacock, J. A., Cluver, M. E., & Steward, L. 2014, ApJS, 210, 9
Bilicki, M., Peacock, J. A., Jarrett, T. H., et al. 2016, ApJS, 225, 5
Borhanian, S., Dhani, A., Gupta, A., Arun, K. G., & Sathyaprakash, B. S. 2020, ApJL, 905, L28
Broadhurst, T., Diego, J. M., & Smoot, G. 2018, arXiv:1802.05273
Buscicchio, R., Moore, C. J., Pratten, G., et al. 2020, PhRvL, 125, 141102
Callister, T., Fishbach, M., Holz, D., & Farr, W. 2020, ApJL, 896, L32
Chatterjee, D., Abhishek, H. K. R., Holder, G., et al. 2021, PhRvD, 104, 083528
Chen, H.-Y., Fishbach, M., & Holz, D. E. 2018, Natur, 562, 545
Chernoff, D. F., & Finn, L. S. 1993, ApJL, 411, L5
Chevallier, M., & Polarski, D. 2001, IJMPD, 10, 213
Collister, A. A., & Lahav, O. 2004, PASP, 116, 345
Coulter, D. A., Foley, R. J., Kilpatrick, C. D., et al. 2017, Sci, 358, 1556
Cutler, C., & Holz, D. E. 2009, PhRvD, 80, 104009
Dai, L., Venumadhav, T., & Sigurdson, K. 2017, PhRvD, 95, 044011
Dalal, N., Holz, D. E., Hughes, S. A., & Jain, B. 2006, PhRvD, 74, 063006
Dálya, G., Galgóczi, G., Dobos, L., et al. 2018, MNRAS, 479, 2374
Dálya, G., Díaz, R., Bouchet, F. R., et al. 2022, MNRAS, 514, 1403
Dawson, K. S., Schlegel, D. J., Ahn, C. P., et al. 2013, AJ, 145, 10
De Paolis, F., Nucita, A. A., Strafella, F., Licchelli, D., & Ingrosso, G. 2020, MNRAS Lett., 499, L87
Del Pozzo, W. 2012, PhRvD, 86, 043011
Diaz, C. C., & Mukherjee, S. 2022, MNRAS, 511, 2782
Diego, J. M. 2019, A&A, 625, A84
Ding, X., Biesiada, M., Zheng, X., et al. 2019, JCAP, 2019, 033
Drlica-Wagner, A., Sevilla-Noarbe, I., Rykoff, E. S., et al. 2018, ApJS, 235, 33
Eisenstein, D. J., & Hu, W. 1997, ApJ, 511, 5
Eisenstein, D. J., & Hu, W. 1998, ApJ, 496, 605
Ezquiaga, J. M., & Holz, D. E. 2021, ApJL, 909, L23
Farmer, R., Renzo, M., de Mink, S. E., Marchant, P., & Justham, S. 2019, ApJ, 887, 53
Farr, W. M., Fishbach, M., Ye, J., & Holz, D. 2019, ApJL, 883, L42
Feeney, S. M., Peiris, H. V., Williamson, A. R., et al. 2019, PhRvL, 122, 061105
Finke, A., Foffa, S., Iacovelli, F., Maggiore, M., & Mancarella, M. 2021, JCAP, 2021, 026
Fishbach, M., & Holz, D. E. 2017, ApJL, 851, L25
Fishbach, M., Holz, D. E., & Farr, W. M. 2018, ApJL, 863, L41
Fishbach, M., & Kalogera, V. 2021, ApJL, 914, L30
Fishbach, M., Gray, R., Magaña Hernandez, I., et al. 2019, ApJL, 871, L13
Fishbach, M., Doctor, Z., Callister, T., et al. 2021, ApJ, 912, 98
Freedman, W. L. 2017, NatAs, 1, 0121
Fryer, C. L., Woosley, S. E., & Heger, A. 2001, ApJ, 550, 372
Gallegos-Garcia, M., Berry, C. P. L., Marchant, P., & Kalogera, V. 2021, ApJ, 922, 110
Górski, K. M., Hivon, E., Banday, A. J., et al. 2005, ApJ, 622, 759
Graham, M. J., Ford, K. E. S., McKernan, B., et al. 2020, PhRvL, 124, 251102
Gray, R., Hernandez, I. R., Qi, H., et al. 2020, PhRvD, 101, 122001
Gray, R., Messenger, C., & Veitch, J. 2022, MNRAS, 512, 1127

Hannuksela, O. A., Haris, K., Ng, K. K. Y., et al. 2019, ApJL, 874, L2
Heger, A., & Woosley, S. E. 2002, ApJ, 567, 532
Hirata, C. M., Holz, D. E., & Cutler, C. 2010, PhRvD, 81, 124046
Holz, D. E., & Hughes, S. A. 2005, ApJ, 629, 15
Holz, D. E., & Wald, R. M. 1998, PhRvD, 58, 063501
Jimenez, R., Cimatti, A., Verde, L., Moresco, M., & Wandelt, B. 2019, JCAP, 2019, 043
Kochanek, C. S., Pahre, M. A., Falco, E. E., et al. 2001, ApJ, 560, 566
Komatsu, E., Smith, K. M., Dunkley, J., et al. 2011, ApJS, 192, 18
Kudritzki, R.-P., & Puls, J. 2000, ARA&A, 38, 613
Kushnir, D., Zaldarriaga, M., Kollmeier, J. A., & Waldman, R. 2016, MNRAS, 462, 844
LIGO Scientific Collaboration, Virgo Collaboration, KAGRA Collaboration 2021, GWTC-3: Compact Binary Coalescences Observed by LIGO and Virgo During the Second Part of the Third Observing Run — Parameter estimation data release, v.1.0, Zenodo, doi:10.5281/zenodo.5546663
Linder, E. V. 2003, PhRvL, 90, 091301
Lyke, B. W., Higley, A. N., McLane, J. N., et al. 2020, ApJS, 250, 8
MacLeod, C. L., & Hogan, C. J. 2008, PhRvD, 77, 043512
Madau, P., & Dickinson, M. 2014, ARA&A, 52, 415
Makarov, D., Prugniel, P., Terekhova, N., Courtois, H., & Vauglin, I. 2014, A&A, 570, A13
Mandel, I., Farr, W. M., & Gair, J. R. 2019, MNRAS, 486, 1086
Mapelli, M. 2021, Handbook of Gravitational Wave Astronomy (Singapore: Springer), 4
Mapelli, M., Bouffanais, Y., Santoliquido, F., Arca Sedda, M., & Artale, M. C. 2022, MNRAS, 511, 5797
Mapelli, M., Giacobbo, N., Santoliquido, F., & Artale, M. C. 2019, MNRAS, 487, 2
Mastrogiovanni, S., Haegel, L., Karathanasis, C., Hernandez, I. M. n., & Steer, D. A. 2021, JCAP, 2021, 043
Mastrogiovanni, S., Leyde, K., Karathanasis, C., et al. 2021, PhRvD, 104, 062009
Matas, A., Dietrich, T., Buonanno, A., et al. 2020, PhRvD, 102, 043023
Messenger, C., & Read, J. 2012, PhRvL, 108, 091101
Moresco, M., Pozzetti, L., Cimatti, A., et al. 2016, JCAP, 2016, 014
Mukherjee, S., Broadhurst, T., Diego, J. M., Silk, J., & Smoot, G. F. 2021a, MNRAS, 501, 2451
Mukherjee, S., Broadhurst, T., Diego, J. M., Silk, J., & Smoot, G. F. 2021b, MNRAS, 506, 3751
Mukherjee, S., Lavaux, G., Bouchet, F. R., et al. 2021c, A&A, 646, A65
Mukherjee, S., Wandelt, B. D., Nissanke, S. M., & Silvestri, A. 2021, PhRvD, 103, 043520
Mukherjee, S., Wandelt, B. D., & Silk, J. 2020, MNRAS, 494, 1956
Nair, R., Bose, S., & Saini, T. D. 2018, PhRvD, 98, 023502
Nakamura, T. T. 1998, PhRvL, 80, 1138
Namikawa, T., Nishizawa, A., & Taruya, A. 2016, PhRvL, 116, 121302
Ng, K. K., Wong, K. W., Broadhurst, T., & Li, T. G. 2018a, PhRvD, 97, 023012
Ng, K. K. Y., Vitale, S., Zimmerman, A., et al. 2018b, PhRvD, 98, 083007
Nishizawa, A. 2017, PhRvD, 96, 101303
Nissanke, S., Holz, D. E., Hughes, S. A., Dalal, N., & Sievers, J. L. 2010, ApJ, 725, 496
Norberg, P., Cole, S., Baugh, C. M., et al. 2002, MNRAS, 336, 907
Oguri, M. 2016, PhRvD, 93, 083511
Oguri, M. 2018, MNRAS, 480, 3842
Ossokine, S., Buonanno, A., Marsat, S., et al. 2020, PhRvD, 102, 044055
Palmese, A., deVicente, J., Pereira, M. E. S., et al. 2020, ApJL, 900, L33
Palmese, A., Fishbach, M., Burke, C. J., Annis, J. T., & Liu, X. 2021, ApJL, 914, L34
Perlmutter, S., Aldering, G., Goldhaber, G., et al. 1999, ApJ, 517, 565
Pratten, G., García-Quirós, C., Colleoni, M., et al. 2021, PhRvD, 103, 104056
Renzo, M., Farmer, R., Justham, S., et al. 2020, A&A, 640, A56
Riess, A. G., Casertano, S., Yuan, W., Macri, L. M., & Scolnic, D. 2019, ApJ, 876, 85
Riess, A. G., Macri, L. M., Hoffmann, S. L., et al. 2016, ApJ, 826, 56
Riess, A. G., Press, W. H., & Kirshner, R. P. 1996, ApJ, 473, 88
Schneider, P., Ehlers, J., & Falco, E. E. 1992, Gravitational Lenses (Berlin: Springer)
Schutz, B. F. 1986, Natur, 323, 310
Skrutskie, M. F., Cutri, R. M., Stiening, R., et al. 2006, AJ, 131, 1163
Soares-Santos, M., Palmese, A., Hartley, W., et al. 2019, ApJL, 876, L7
Spergel, D. N., Bean, R., Doré, O., et al. 2007, ApJS, 170, 377
Spergel, D. N., Verde, L., Peiris, H. V., et al. 2003, ApJS, 148, 175
Suyu, S. H., Marshall, P. J., Auger, M. W., et al. 2010, ApJ, 711, 201
Takahashi, R., & Nakamura, T. 2003, ApJ, 595, 1039

Talbot, C., & Thrane, E. 2018, ApJ, 856, 173

Taylor, S. R., & Gair, J. R. 2012, PhRvD, 86, 023502

Taylor, S. R., Gair, J. R., & Mandel, I. 2012, PhRvD, 85, 023535

Thompson, J. E., Fauchon-Jones, E., Khan, S., et al. 2020, PhRvD, 101, 124059

Thrane, E., & Talbot, C. 2019, PASA, 36, e010

Umeda, H., Yoshida, T., Nagele, C., & Takahashi, K. 2020, ApJL, 905, L21

van Son, L. A. C., de Mink, S. E., Callister, T., et al. 2022, ApJ, 931, 17

Vitale, S., Gerosa, D., Farr, W. M., & Taylor, S. R. 2021, Inferring the Properties of a Population of Compact Binaries in Presence of Selection Effects, ed. C. Bambi, S. Katsanevas, & K. D. Kokkotas (Singapore: Springer), doi:10.1007/978-981-15-4702-7_45-1

Wang, Y., Stebbins, A., & Turner, E. L. 1996, PhRvL, 77, 2875

Weatherford, N. C., Fragione, G., Kremer, K., et al. 2021, ApJL, 907, L25

White, D. J., Daw, E. J., & Dhillon, V. S. 2011, CQGra, 28, 085016

Wong, K. C., Suyu, S. H., Chen, G. C.-F., et al. 2020, MNRAS, 498, 1420

Ye, C., & Fishbach, M. 2021, PhRvD, 104, 043507

You, Z.-Q., Zhu, X.-J., Ashton, G., Thrane, E., & Zhu, Z.-H. 2021, ApJ, 908, 215

Yu, J., Wang, Y., Zhao, W., & Lu, Y. 2020, MNRAS, 498, 1786

Zonca, A., Singer, L., Lenz, D., et al. 2019, JOSS, 4, 1298

Zou, H., Gao, J., Zhou, X., & Kong, X. 2019, ApJS, 242, 8